

Primordial spectra from sudden turning trajectory

Toshifumi Noumi¹ and Masahide Yamaguchi²

¹*Mathematical Physics Laboratory, RIKEN Nishina Center, Saitama 351-0198, JAPAN*

²*Department of Physics, Tokyo Institute of Technology, Tokyo 152-8551, Japan*

toshifumi.noumi“at”riken.jp, gucci“at”phys.titech.ac.jp

Abstract

Effects of heavy fields on primordial spectra of curvature perturbations are discussed in inflationary models with a sudden turning trajectory. When heavy fields are excited after the sudden turn and oscillate around the bottom of the potential, the following two effects are generically induced: deformation of the inflationary background spacetime and conversion interactions between adiabatic and isocurvature perturbations, both of which can affect the primordial density perturbations. In this paper, we calculate primordial spectra in inflationary models with sudden turning potentials taking into account both of the two effects appropriately. We find that there are some non-trivial correlations between the two effects in the power spectrum and, as a consequence, the primordial scalar power spectrum has a peak around the scale exiting the horizon at the turn. Though both effects can induce parametric resonance amplifications, they are shown to be canceled out for the case with the canonical kinetic terms. The peak feature and the scale dependence of bispectra are also discussed.

1 Introduction

Inflation is strongly supported by recent observations of cosmic microwave background (CMB) anisotropies [1, 2]. In particular, single field slow-roll inflation predicts almost adiabatic, Gaussian, and scale invariant primordial curvature perturbations, and these predictions well fit the observational results. On the other hand, high energy theories such as supergravity and superstring theory generically predict additional scalar fields other than inflaton. To reconcile such a generic prediction of theories with recent observations, it may be suggested that only one light field plays a role of inflaton while the others are heavy and their effects are negligible. In fact, propagations of such heavy fields are generically suppressed by their mass and completely negligible in the heavy mass limit: heavy fields can affect inflationary dynamics only via their background energy and their effects can be absorbed into the inflaton potential [3].

However, heavy field propagations can lead to non-negligible effects if their interactions with inflaton are comparable to their mass. In particular, it was pointed out in [4] that heavy fields can reduce the effective sound speed of adiabatic perturbations significantly. Then, a lot of works are devoted to the investigation on the effects of heavy fields [5–29]. As discussed in [12, 13, 20], even if heavy field propagations have non-negligible effects, they can be integrated out simply and inflationary dynamics can be described by effective single-field models [30] as long as time-dependence of interactions are negligible compared to the mass of heavy fields.¹ On the other hand, when time-dependence of interactions are non-negligible, it is necessary to follow the full dynamics of heavy fields in general.

One typical example for the latter is the case when heavy fields are excited for example by the sudden turn of the potential or the phase transition and oscillates with high frequency. Such oscillations of heavy fields can affect inflationary dynamics and can be a probe of high energy physics [8–11, 17, 18, 21, 24, 25, 29, 31, 32]. In general, oscillations of heavy fields generate the following two significant effects: the modification of the Hubble parameter and the conversion effect, that is, the mixing between adiabatic and isocurvature (heavy field) modes. These effects can leave an imprint on the primordial curvature perturbations. In particular, the parametric amplification of the curvature perturbations [8, 9, 18, 24, 25] and the peak at the scale exiting the horizon during the heavy field oscillations may be observable [10, 11, 17, 21, 29].

In this paper, we investigate these effects in detail and evaluate the power spectra and bispectra of the primordial curvature perturbations in inflationary models with sudden turning potentials. For simplicity, we concentrate on the case with the canonical kinetic terms in this paper.² In our calculations, we take the kinetic basis of primordial perturbations, where

¹See also Appendix A in Ref. [22] for the condition of integrating out heavy fields.

² Although some results depend on this setting, it is straightforward to extend our discussions to more

scalar perturbations are described in terms of adiabatic perturbations (which are along the background trajectory) and massive isocurvature perturbations (which are orthogonal to the trajectory). As explained before, the deviation from the single-field slow-roll inflation caused by the presence of heavy field oscillations is characterized by the following two effects: the deformation effect of the Hubble parameter and the conversion effect between the adiabatic and the isocurvature modes. We first evaluate the primordial power spectrum and show that the parametric resonance amplification occurs from both of the two effects and the peak at the turning scale arises from the conversion effect. It is, however, explicitly shown that resonance effects from the two effects accidentally cancel each other out for the case with the canonical kinetic terms.³ As a consequence, the peak at the turning scale becomes clear and this feature characterizes this class of models with heavy field oscillations.

We also evaluate primordial bispectra induced by the sudden turning potentials. The main source of the bispectra comes again from the deformation of the Hubble parameter and the conversion effect. The shape and the scale dependence of the bispectrum for each effect is investigated. We find resonance and peak features in the bispectra as in the case of power spectra.⁴ Although the size of bispectra is not necessarily large, our results may be useful for probing these effects observationally.

The organization of this paper is as follows: In the next section we give our setup to characterize the sudden turning trajectory, in which there are a slow-roll direction and a heavy field direction. We then investigate the background trajectory and discuss the deformation effect of the Hubble parameter caused by the oscillation of the heavy field. By employing the kinetic basis and introducing the Goldstone boson based on the effective field theory approach to inflation [30,34,22], we write down the action for the adiabatic and the isocurvature (heavy field) modes. In Sec. 3, the power spectrum of the primordial curvature perturbations is evaluated using the in-in formalism. The effects of the deformation of the Hubble parameter and the conversion interaction between the adiabatic and isocurvature perturbations are discussed in detail. In particular, it is explicitly shown that resonance effects from the two effects cancel each other out in the case with canonical kinetic terms and an analytic expression for the

general setups such as those with non-canonical kinetic terms or derivative interactions. The results will be given elsewhere [33].

³ Very recently in [29], the effects of sudden turning trajectory on the primordial power spectrum were discussed in the potential basis taking into account both of the deformation of the Hubble parameter and the conversion effect. It was shown there that the parametric resonance effects are significantly suppressed for the models with the canonical kinetic terms. Although the potential basis is useful to discuss the absence of resonance effects, we would like to point out that the potential basis calculation suffers from spurious singularities associated with the suddenness of the turning potential. In this paper we take the kinetic basis to avoid this kind of spurious singularities and explicitly show that the resonance cancellation appears for the canonical kinetic term case. See also footnote 7 in Sec 2.3.2 and footnote 10 in Sec 3.3 for related comments.

⁴ Resonance features from the Hubble deformation effects were discussed in [25] using the potential basis.

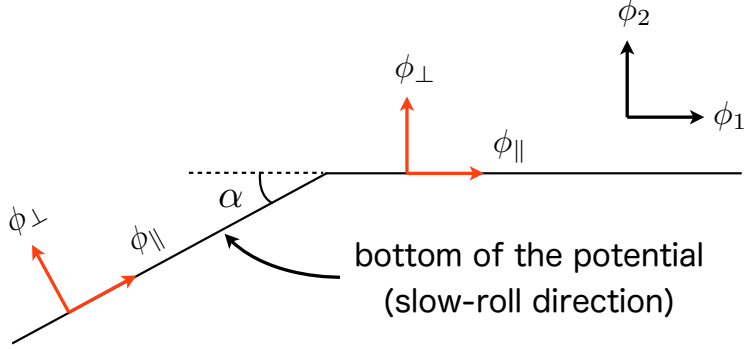


Figure 1: Sudden turning potential with turning angle α .

power spectrum in the heavy mass approximation is also given. In Sec. 4, the bispectrum of the primordial curvature perturbations is evaluated and its shape and scale dependence is investigated. Final section is devoted to the summary and discussion. Some technical details are summarized in Appendices.

2 Setup

2.1 Modeling the potential

In this paper we consider a class of two-field models with the Einstein-Hilbert term, the canonical kinetic terms of scalar fields, and a sudden turning potential:

$$S = \int d^4x \sqrt{-g} \left[\frac{1}{2} M_{\text{Pl}}^2 R - \sum_{i=1,2} \frac{1}{2} \partial_{\mu} \phi_i \partial^{\mu} \phi_i - V(\phi_i) \right]. \quad (2.1)$$

As depicted in Fig. 1, the potential $V(\phi_i)$ is decomposed into the slow-roll direction ϕ_{\parallel} and the massive direction ϕ_{\perp} as

$$V(\phi_i) = V_{\text{sr}}(\phi_{\parallel}) + V_{\perp}(\phi_{\perp}). \quad (2.2)$$

Here $V_{\text{sr}}(\phi_{\parallel})$ is a slow-roll potential and the massive potential V_{\perp} takes its minimum value at $\phi_{\perp} = 0$. The slow-roll direction turns at $(\phi_{\parallel}, \phi_{\perp}) = (0, 0)$ and we identify this point with $(\phi_1, \phi_2) = (0, 0)$ in the ϕ_i basis. Before and after the turn, the slow-roll direction is expressed in the ϕ_i basis as $(\cos \alpha, \sin \alpha)$ and $(1, 0)$, respectively. The relations between the potential basis labeled by $(\phi_{\parallel}, \phi_{\perp})$ and the ϕ_i basis are given by

$$(\phi_{\parallel}, \phi_{\perp}) = (\cos \alpha \phi_1 + \sin \alpha \phi_2, -\sin \alpha \phi_1 + \cos \alpha \phi_2) \quad \text{before the turn,} \quad (2.3)$$

$$(\phi_{\parallel}, \phi_{\perp}) = (\phi_1, \phi_2) \quad \text{after the turn.} \quad (2.4)$$

Then, the potential $V(\phi_i)$ takes the following form in the ϕ_i basis:⁵

$$V(\phi_i) = \theta(-\phi_1) \left[V_{\text{sr}}(\cos \alpha \phi_1 + \sin \alpha \phi_2) + V_{\perp}(-\sin \alpha \phi_1 + \cos \alpha \phi_2) \right] + \theta(\phi_1) \left[V_{\text{sr}}(\phi_1) + V_{\perp}(\phi_2) \right]. \quad (2.5)$$

In the following, we assume the following form of the massive potential V_{\perp} :

$$V_{\perp}(\phi_{\perp}) = \frac{m^2}{2} \phi_{\perp}^2 + \frac{\lambda}{4!} \phi_{\perp}^4, \quad (2.6)$$

which preserves a Z_2 symmetry $\phi_{\perp} \rightarrow -\phi_{\perp}$ and seems to be a natural choice.

2.2 Background evolutions

Let us then summarize the classical dynamics of this class of models. Suppose that the background trajectory is along the slow-roll direction before arriving at the turning point:

$$\bar{\phi}_1(t) = \cos \alpha \bar{\phi}_{\text{sr}}(t), \quad \bar{\phi}_2(t) = \sin \alpha \bar{\phi}_{\text{sr}}(t) \quad \text{for } t < t_*. \quad (2.7)$$

Here $\bar{\phi}_{\text{sr}}$ is the background evolution in single field slow-roll inflation and t_* is the time when the background trajectory passes the turning point: $\bar{\phi}_1(t_*) = \bar{\phi}_2(t_*) = \bar{\phi}_{\text{sr}}(t_*) = 0$. We also introduce the Hubble parameter H_{sr} corresponding to $\bar{\phi}_{\text{sr}}$ as

$$\ddot{\bar{\phi}}_{\text{sr}} + 3H_{\text{sr}} \dot{\bar{\phi}}_{\text{sr}} + V'(\bar{\phi}_{\text{sr}}) = 0, \quad \frac{1}{2} \dot{\bar{\phi}}_{\text{sr}}^2 + V_{\text{sr}}(\bar{\phi}_{\text{sr}}) = 3M_{\text{Pl}}^2 H_{\text{sr}}^2, \quad \dot{\bar{\phi}}_{\text{sr}}^2 = -2M_{\text{Pl}}^2 \dot{H}_{\text{sr}}, \quad (2.8)$$

and assume that H_{sr} satisfies the slow-roll conditions: $\epsilon_{\text{sr}} = -\frac{\dot{H}_{\text{sr}}}{H_{\text{sr}}^2} \ll 1$ and $\eta_{\text{sr}} = \frac{\dot{\epsilon}_{\text{sr}}}{H_{\text{sr}} \epsilon_{\text{sr}}} \ll 1$. After passing the turning point, the background trajectory first deviates from the slow-roll direction and then would be getting to approach that direction because of the cosmic expansion:

$$\bar{\phi}_1(t) \sim \bar{\phi}_{\text{sr}}(t), \quad \bar{\phi}_2(t) \sim 0 \quad \text{for } t \gg t_*. \quad (2.9)$$

We therefore decompose the background trajectory as

$$\bar{\phi}_1(t) = \theta(t_* - t) \cos \alpha \bar{\phi}_{\text{sr}}(t) + \theta(t - t_*) (\bar{\phi}_{\text{sr}}(t) + \varphi_1(t)), \quad (2.10)$$

$$\bar{\phi}_2(t) = \theta(t_* - t) \sin \alpha \bar{\phi}_{\text{sr}}(t) + \theta(t - t_*) \varphi_2(t). \quad (2.11)$$

Here φ_i 's describe the deviation of the background trajectory from the slow-roll direction of the potential and characterize the turning background trajectory. In the following discussions, we assume that α and φ_i 's can be treated as perturbations.

⁵ The coordinate system $(\phi_{\parallel}, \phi_{\perp})$ is not continuously connected before and after the turn so that the expression (2.5) may not seem to be well-defined around the turning point. However, as discussed in Appendix A, the potential (2.5) can be regularized and defined appropriately by introducing a one-parameter family of turning potentials and taking its sudden turning limit.

Background evolution of ϕ_i 's We then solve the background equations of motion after passing the turning point ($t > t_*$). In terms of $\bar{\phi}_i$'s, they are given by

$$\ddot{\bar{\phi}}_1 + 3H\dot{\bar{\phi}}_1 + V'_{\text{sr}}(\bar{\phi}_1) = 0, \quad \ddot{\bar{\phi}}_2 + 3H\dot{\bar{\phi}}_2 + V'_\perp(\bar{\phi}_2) = 0, \quad (2.12)$$

$$\frac{1}{2}(\dot{\bar{\phi}}_1^2 + \dot{\bar{\phi}}_2^2) + V_{\text{sr}}(\bar{\phi}_1) + V_\perp(\bar{\phi}_2) = 3M_{\text{Pl}}^2 H^2, \quad \dot{\bar{\phi}}_1^2 + \dot{\bar{\phi}}_2^2 = -2M_{\text{Pl}}^2 \dot{H}. \quad (2.13)$$

Using the equations of motion (2.8) in single field inflation, we can rewrite (2.12) and (2.13) in terms of φ_i 's as

$$\ddot{\varphi}_1 + 3H_{\text{sr}}\dot{\varphi}_1 = 0, \quad \ddot{\varphi}_2 + 3H_{\text{sr}}\dot{\varphi}_2 + m^2\varphi_2 = 0, \quad (2.14)$$

$$\dot{\bar{\phi}}_{\text{sr}}\dot{\varphi}_1 + V'_{\text{sr}}(\bar{\phi}_{\text{sr}})\varphi_1 + \frac{1}{2}\dot{\varphi}_2^2 + \frac{1}{2}V''_\perp(0)\varphi_2^2 = 6M_{\text{Pl}}^2 H_{\text{sr}}\delta H, \quad (2.15)$$

$$2\dot{\bar{\phi}}_{\text{sr}}\dot{\varphi}_1 + \dot{\varphi}_2^2 = -2M_{\text{Pl}}^2\delta\dot{H}, \quad (2.16)$$

where δH is defined by $\delta H = H - H_{\text{sr}}$. The initial conditions on φ_i 's at $t = t_*$ are given by

$$\varphi_1(t_*) = \varphi_2(t_*) = 0, \quad \dot{\varphi}_1(t_*) = -\frac{\alpha^2}{2}\dot{\bar{\phi}}_{\text{sr}}(t_*), \quad \dot{\varphi}_2(t_*) = \alpha\dot{\bar{\phi}}_{\text{sr}}(t_*). \quad (2.17)$$

Here and in what follows, we drop higher order terms in ϵ_{sr} , η_{sr} , φ_i 's, and α . The equations of motion (2.14) can be then solved as follows:

$$\varphi_1(t) = \frac{\alpha^2\dot{\bar{\phi}}_{\text{sr}}}{6H_{\text{sr}}}(e^{-3H_{\text{sr}}(t-t_*)} - 1), \quad (2.18)$$

$$\varphi_2(t) = \begin{cases} \frac{\alpha\dot{\bar{\phi}}_{\text{sr}}}{\mu H_{\text{sr}}} e^{-\frac{3}{2}H_{\text{sr}}(t-t_*)} \sin[\mu H_{\text{sr}}(t-t_*)] & \text{for } m > \frac{3}{2}H_{\text{sr}}, \\ \frac{\alpha\dot{\bar{\phi}}_{\text{sr}}}{\nu H_{\text{sr}}} e^{-\frac{3}{2}H_{\text{sr}}(t-t_*)} \sinh[\nu H_{\text{sr}}(t-t_*)] & \text{for } m < \frac{3}{2}H_{\text{sr}}, \end{cases} \quad (2.19)$$

where $\mu = \sqrt{\frac{m^2}{H_{\text{sr}}^2} - \frac{9}{4}}$ for $m > \frac{3}{2}H_{\text{sr}}$ and $\nu = \sqrt{\frac{9}{4} - \frac{m^2}{H_{\text{sr}}^2}}$ for $m < \frac{3}{2}H_{\text{sr}}$. As is clear from (2.19), the expression for $m < \frac{3}{2}H_{\text{sr}}$ can be obtained by the replacement $\mu \rightarrow -i\nu$ in that for $m > \frac{3}{2}H_{\text{sr}}$. Therefore, we do not write the expression for $m < \frac{3}{2}H_{\text{sr}}$ explicitly in the following discussions. Using $\dot{\bar{\phi}}_{\text{sr}} = \sqrt{2}\epsilon_{\text{sr}}^{1/2} M_{\text{Pl}} H_{\text{sr}}$, φ_i 's can be rewritten as

$$\varphi_1(t) = \frac{\sqrt{2}\alpha^2}{6}\epsilon_{\text{sr}}^{1/2} M_{\text{Pl}}(e^{-3H_{\text{sr}}(t-t_*)} - 1), \quad (2.20)$$

$$\varphi_2(t) = \frac{\sqrt{2}\alpha}{\mu}\epsilon_{\text{sr}}^{1/2} M_{\text{Pl}} e^{-\frac{3}{2}H_{\text{sr}}(t-t_*)} \sin[\mu H_{\text{sr}}(t-t_*)]. \quad (2.21)$$

Notice that φ_1 and φ_2 are second and first order in α , respectively. Time-derivatives of φ_i 's are given by

$$\begin{aligned}\dot{\varphi}_1(t) &= -\frac{1}{2}\alpha^2\dot{\phi}_{\text{sr}}e^{-3H_{\text{sr}}(t-t_*)} \\ &= -\frac{\sqrt{2}}{2}\alpha^2\epsilon_{\text{sr}}^{1/2}M_{\text{Pl}}H_{\text{sr}}e^{-3H_{\text{sr}}(t-t_*)},\end{aligned}\quad (2.22)$$

$$\begin{aligned}\dot{\varphi}_2(t) &= \alpha\dot{\phi}_{\text{sr}}e^{-\frac{3}{2}H_{\text{sr}}(t-t_*)}\left(-\frac{3}{2\mu}\sin[\mu H_{\text{sr}}(t-t_*)] + \cos[\mu H_{\text{sr}}(t-t_*)]\right) \\ &= \sqrt{2}\alpha\epsilon_{\text{sr}}^{1/2}M_{\text{Pl}}H_{\text{sr}}e^{-\frac{3}{2}H_{\text{sr}}(t-t_*)}\left(-\frac{3}{2\mu}\sin[\mu H_{\text{sr}}(t-t_*)] + \cos[\mu H_{\text{sr}}(t-t_*)]\right).\end{aligned}\quad (2.23)$$

Background spacetime We next discuss the background spacetime and the deviation $\delta H(t)$ of the Hubble parameter from single field slow-roll inflation. First, it follows from the equation of motion (2.16) that $\delta\dot{H}$ for $t \geq t_*$ is given by

$$\begin{aligned}\delta\dot{H} &= -\frac{1}{2M_{\text{Pl}}^2}(2\dot{\phi}_{\text{sr}}\dot{\varphi}_1 + \dot{\varphi}_2^2) \\ &= \alpha^2\frac{\dot{\phi}_{\text{sr}}^2}{M_{\text{Pl}}^2}e^{-3H_{\text{sr}}(t-t_*)}\left[\left(\frac{1}{4} - \frac{9}{16\mu^2}\right)(1 - \cos[2\mu H_{\text{sr}}(t-t_*)]) + \frac{3}{4\mu}\sin[2\mu H_{\text{sr}}(t-t_*)]\right] \\ &= \alpha^2\epsilon_{\text{sr}}H_{\text{sr}}^2e^{-3H_{\text{sr}}(t-t_*)}\left[\left(\frac{1}{2} - \frac{9}{8\mu^2}\right)(1 - \cos[2\mu H_{\text{sr}}(t-t_*)]) + \frac{3}{2\mu}\sin[2\mu H_{\text{sr}}(t-t_*)]\right],\end{aligned}\quad (2.24)$$

which is second order in α . It is convenient to introduce a function $\kappa(t)$ defined by

$$\begin{aligned}\kappa(t) &= 2\frac{\dot{\varphi}_1}{\dot{\phi}_{\text{sr}}} + \left(\frac{\dot{\varphi}_2}{\dot{\phi}_{\text{sr}}}\right)^2 \\ &= -\alpha^2e^{-3H_{\text{sr}}(t-t_*)}\left[\left(\frac{1}{2} - \frac{9}{8\mu^2}\right)(1 - \cos[2\mu H_{\text{sr}}(t-t_*)]) + \frac{3}{2\mu}\sin[2\mu H_{\text{sr}}(t-t_*)]\right].\end{aligned}\quad (2.25)$$

Then, $\delta\dot{H}$ can be expressed in terms of κ as

$$\delta\dot{H} = \theta(t-t_*)\kappa\dot{H}_{\text{sr}}. \quad (2.26)$$

It is also straightforward to evaluate the deviation $\delta H(t)$ of the Hubble parameter as

$$\delta H(t) = \int_{-\infty}^t dt' \delta\dot{H}(t') = \dot{H}_{\text{sr}} \int_{t_*}^t dt' \kappa(t') = -\epsilon_{\text{sr}}H_{\text{sr}}^2 \int_{t_*}^t dt' \kappa(t'), \quad (2.27)$$

where higher order terms in the slow-roll expansion are dropped. More explicitly, it is given by

$$\begin{aligned}\delta H(t) &= \alpha^2\epsilon_{\text{sr}}H_{\text{sr}}\left[\frac{1}{6}\left(1 - e^{-3H_{\text{sr}}(t-t_*)}\right) - \frac{1}{4\mu}e^{-3H_{\text{sr}}(t-t_*)}\sin[2H_{\text{sr}}\mu(t-t_*)]\right. \\ &\quad \left. + \frac{3}{8\mu^2}e^{-3H_{\text{sr}}(t-t_*)}\left(1 - \cos[2H_{\text{sr}}\mu(t-t_*)]\right)\right].\end{aligned}\quad (2.28)$$

Notice that $\delta H(t)$ is first order in ϵ_{sr} as well as second order in α .

2.3 Perturbations in the unitary gauge

Let us next consider perturbations around the background discussed in the previous subsection. We first construct the action in the unitary gauge in this subsection and then introduce that for the Nambu-Goldstone boson in the next subsection.

2.3.1 Generalities

In the unitary gauge, the adiabatic mode is eaten by graviton so that the physical degrees of freedom are three physical modes of graviton and one massive isocurvature mode. Corresponding to the degrees of freedom to change bases of the field space, there are some ambiguities in the description of the massive isocurvature σ .⁶ In fact, we can introduce the following family of definitions of the isocurvature perturbation σ :

$$\phi_1(x) = \bar{\phi}_1(t) - \sin \beta(t)\sigma(x), \quad (2.29)$$

$$\phi_2(x) = \bar{\phi}_2(t) + \cos \beta(t)\sigma(x). \quad (2.30)$$

Here $\beta(t)$ is an arbitrary function of time t and determines the direction of σ perturbations in the field space. We will take one particular choice of $\beta(t)$ later. Before that, however, let us summarize the action in the unitary gauge for general $\beta(t)$. First, derivatives of ϕ_i 's are given by

$$\partial_\mu \phi_1(x) = \delta_\mu^0 \left[\dot{\bar{\phi}}_1(t) - \cos \beta(t) \dot{\beta}(t)\sigma(x) \right] - \sin \beta(t) \partial_\mu \sigma(x), \quad (2.31)$$

$$\partial_\mu \phi_2(x) = \delta_\mu^0 \left[\dot{\bar{\phi}}_2(t) - \sin \beta(t) \dot{\beta}(t)\sigma(x) \right] + \cos \beta(t) \partial_\mu \sigma(x). \quad (2.32)$$

Then, the kinetic term of ϕ_i 's can be written in terms of $\bar{\phi}_i$'s and σ as

$$\begin{aligned} - \sum_{i=1,2} \frac{1}{2} \partial_\mu \phi_i \partial^\mu \phi_i &= -\frac{1}{2} g^{00} \left(\dot{\bar{\phi}}_1^2 + \dot{\bar{\phi}}_2^2 \right) - \frac{1}{2} \partial_\mu \sigma \partial^\mu \sigma - \frac{1}{2} \dot{\beta}^2 g^{00} \sigma^2 \\ &\quad + \left[\sin \beta \dot{\bar{\phi}}_1 - \cos \beta \dot{\bar{\phi}}_2 \right] \partial^0 \sigma + \left[\cos \beta \dot{\bar{\phi}}_1 + \sin \beta \dot{\bar{\phi}}_2 \right] \dot{\beta} g^{00} \sigma \\ &= -\frac{1}{2} g^{00} \left(\dot{\bar{\phi}}_1^2 + \dot{\bar{\phi}}_2^2 \right) - \frac{1}{2} \partial_\mu \sigma \partial^\mu \sigma + \frac{1}{2} \dot{\beta}^2 \sigma^2 \\ &\quad + \left[\cos \beta \dot{\bar{\phi}}_1 + \sin \beta \dot{\bar{\phi}}_2 \right] \dot{\beta} \delta g^{00} \sigma \\ &\quad + \left[\sin \beta \dot{\bar{\phi}}_1 - \cos \beta \dot{\bar{\phi}}_2 \right] \partial^0 \sigma - \left[\cos \beta \dot{\bar{\phi}}_1 + \sin \beta \dot{\bar{\phi}}_2 \right] \dot{\beta} \sigma \\ &\quad - \frac{1}{2} \dot{\beta}^2 \delta g^{00} \sigma^2, \end{aligned} \quad (2.33)$$

⁶ See also [35] for recent discussions on bases of perturbations in multiple-field inflation.

where the linear order fluctuation terms become total derivatives after taking into account the Einstein-Hilbert term and the potential term. In the framework of the effective field theory approach [22], the total action (2.1) can be described in the unitary gauge as

$$S = \int d^4x \sqrt{-g} \left[\frac{1}{2} M_{\text{Pl}}^2 R + M_{\text{Pl}}^2 \dot{H} g^{00} - M_{\text{Pl}}^2 (3H^2 + \dot{H}) - \frac{1}{2} \partial_\mu \sigma \partial^\mu \sigma + \beta_1 \delta g^{00} \sigma + \beta_3(t) \partial^0 \sigma - (\dot{\beta}_3 + 3H\beta_3) \sigma + \bar{\gamma}_1 \delta g^{00} \sigma^2 - V_\sigma(\sigma; t) \right], \quad (2.34)$$

where the parameters H , \dot{H} , β_1 , β_3 , and $\bar{\gamma}_1$ are given by

$$M_{\text{Pl}}^2 H^2 = \frac{1}{3} \left[\frac{1}{2} (\dot{\bar{\phi}}_1^2 + \dot{\bar{\phi}}_2^2) + V(\bar{\phi}_i) \right], \quad M_{\text{Pl}}^2 \dot{H} = -\frac{1}{2} (\dot{\bar{\phi}}_1^2 + \dot{\bar{\phi}}_2^2), \\ \beta_1 = \left[\cos \beta \dot{\bar{\phi}}_1 + \sin \beta \dot{\bar{\phi}}_2 \right] \dot{\beta}, \quad \beta_3 = \sin \beta \dot{\bar{\phi}}_1 - \cos \beta \dot{\bar{\phi}}_2, \quad \bar{\gamma}_1 = -\frac{1}{2} \dot{\beta}^2. \quad (2.35)$$

The time-dependent potential $V_\sigma(\sigma; t)$ of σ takes the form

$$V_\sigma(\sigma; t) = \theta(t_* - t) \left[V_{\text{sr}}(\bar{\phi}_{\text{sr}} - \sin(\beta - \alpha) \sigma) + V_\perp(\cos(\beta - \alpha) \sigma) - \frac{1}{2} \dot{\beta}^2 \sigma^2 \right] \\ + \theta(t - t_*) \left[V_{\text{sr}}(\bar{\phi}_1 - \sin \beta \sigma) + V_\perp(\bar{\phi}_2 + \cos \beta \sigma) - \frac{1}{2} \dot{\beta}^2 \sigma^2 \right] \\ - (\text{zeroth and first order terms in } \sigma), \quad (2.36)$$

where we used $(\bar{\phi}_1, \bar{\phi}_2) = (\bar{\phi}_{\text{sr}}, 0)$ for $t < t_*$. Note that the background value of $V_{\text{sr}} + V_\perp$ contributes to $-M_{\text{Pl}}^2(3H^2 + \dot{H})$ term in (2.34) and the first order fluctuation terms contribute to the $-(\dot{\beta}_3 + 3H\beta_3)\sigma$ term.

2.3.2 Action in the kinetic basis

From the expression (2.35), we notice that the β_3 coupling vanishes when σ perturbations are orthogonal to the background trajectory. We define such a kinetic basis in the following way:

$$\beta(t) = \arctan \frac{\dot{\bar{\phi}}_2}{\dot{\bar{\phi}}_1} = \theta(t_* - t) \alpha + \theta(t - t_*) \gamma(t) \quad \text{with} \quad \gamma(t) = \arctan \frac{\dot{\bar{\phi}}_2}{\dot{\bar{\phi}}_{\text{sr}} + \dot{\bar{\phi}}_1}. \quad (2.37)$$

Note that $\gamma(t) = \frac{\dot{\bar{\phi}}_2}{\dot{\bar{\phi}}_{\text{sr}}}$ at the leading order in α . The time-derivative of β is then given by⁷

$$\dot{\beta}(t) = \delta(t - t_*) (\gamma(t_*) - \alpha) + \theta(t - t_*) \dot{\gamma}(t) = \theta(t - t_*) \dot{\gamma}(t), \quad (2.38)$$

⁷ Here it should be noticed that $\dot{\beta}(t)$ is proportional to a delta function in the bases with $\gamma(t_*) \neq \alpha$. For example, in the potential basis defined by $\gamma(t) = 0$, we have $\dot{\beta}(t) = -\alpha \delta(t - t_*)$. In such bases, the coupling $\bar{\gamma}_1$ in (2.35) and the term $-\frac{1}{2} \dot{\beta}^2 \sigma^2$ in (2.36) are proportional to the delta function squared, which leads to spurious singularities in the calculation of spectra. On the other hand, in the kinetic basis, $\dot{\beta}(t)$ is regular and no spurious singularities appear. This is one of the reasons why we take the kinetic basis in this paper.

and therefore, we have

$$\beta_1 = \theta(t - t_*) |\dot{\phi}_i| \dot{\gamma}, \quad \beta_3 = 0, \quad \bar{\gamma}_1 = -\frac{1}{2}\theta(t - t_*) \dot{\gamma}^2. \quad (2.39)$$

Here $|\dot{\phi}_i|^2 = (\dot{\phi}_1)^2 + (\dot{\phi}_2)^2 = \dot{\phi}_{\text{sr}}^2 + \mathcal{O}(\alpha^2)$. At the leading order in α and ϵ_{sr} , they are given by

$$\beta_1 = \theta(t - t_*) \ddot{\varphi}_2, \quad \beta_3 = 0, \quad \bar{\gamma}_1 = -\frac{1}{2}\theta(t - t_*) \left(\frac{\ddot{\varphi}_2}{\dot{\phi}_{\text{sr}}}\right)^2. \quad (2.40)$$

In this basis, the potential $V(\sigma; t)$ can be expressed as

$$\begin{aligned} V_\sigma(\sigma; t) &= \theta(t_* - t) \left[V_{\text{sr}}(\bar{\phi}_{\text{sr}}) + V_\perp(\sigma) \right] \\ &\quad + \theta(t - t_*) \left[V_{\text{sr}}(\bar{\phi}_1 - \sin \gamma \sigma) + V_\perp(\bar{\phi}_2 + \cos \gamma \sigma) - \frac{1}{2}\dot{\gamma}^2 \sigma^2 \right] \\ &\quad - (\text{zeroth and first order terms in } \sigma). \end{aligned} \quad (2.41)$$

For the potential (2.6), its concrete form is given by

$$\begin{aligned} V_\sigma(\sigma; t) &= \theta(t_* - t) \frac{m^2}{2} \sigma^2 \\ &\quad + \theta(t - t_*) \left[\frac{1}{2} V_{\text{sr}}''(\bar{\phi}_1) \gamma^2 \sigma^2 - \frac{1}{3!} V_{\text{sr}}'''(\bar{\phi}_1) \gamma^3 \sigma^3 + \left(\frac{m^2}{2} + \frac{\lambda}{4} \varphi_2^2 - \frac{1}{2} \dot{\gamma}^2 \right) \sigma^2 + \frac{\lambda}{3!} \varphi_2 \sigma^3 \right] \\ &\quad + \mathcal{O}(\sigma^4). \end{aligned} \quad (2.42)$$

To summarize, in the kinetic basis, the action in the unitary gauge is given by

$$\begin{aligned} S &= \int d^4x \sqrt{-g} \left[\frac{1}{2} M_{\text{Pl}}^2 R + M_{\text{Pl}}^2 \dot{H} g^{00} - M_{\text{Pl}}^2 (3H^2 + \dot{H}) \right. \\ &\quad \left. - \frac{1}{2} \partial_\mu \sigma \partial^\mu \sigma + \beta_1 \delta g^{00} \sigma + \bar{\gamma}_1 \delta g^{00} \sigma^2 - V_\sigma(\sigma; t) \right], \end{aligned} \quad (2.43)$$

where β_1 , $\bar{\gamma}_1$, and $V_\sigma(\sigma; t)$ are given in (2.40) and (2.41). In the rest of this paper, we take the kinetic basis and use (2.43) as the action in the unitary gauge.

2.3.3 Perturbativity

Our models (2.43) contain three free parameters in addition to the Hubble parameter H_{sr} in the single field slow-roll model: the turning angle α , the mass m of the massive potential, and the coupling constant λ for the quartic self-interaction of massive directions ϕ_\perp . In the calculation of primordial spectra, we would like to treat the parameters α and λ as perturbations. From the viewpoint of the action (2.43) for metric perturbations and massive isocurvatures,

the perturbativity of α and λ can be rephrased by that of the following quadratic and cubic interactions:

$$\left(\frac{\lambda}{4}\varphi_2^2 - \frac{1}{2}\dot{\gamma}^2\right)\sigma^2 \quad \text{and} \quad \frac{\lambda}{3!}\varphi_2\sigma^3. \quad (2.44)$$

For the perturbativity of quadratic interactions, we require that they are smaller than the mass term

$$\lambda\varphi_2^2 \lesssim m^2, \quad \dot{\gamma}^2 \lesssim m^2. \quad (2.45)$$

On the other hand, we impose the following condition on the cubic interaction:

$$(\text{cubic coupling}) \times (\text{propagator}) \times (\text{cubic coupling}) \sim \frac{(\lambda\varphi_2)^2}{m^2} \lesssim 1, \quad (2.46)$$

which is essentially the same as the condition that the four-point amplitudes are not large. Using the expression (2.21) of φ_2 , these conditions can be stated as

$$\frac{\lambda\alpha^2}{\mu^4} \frac{2M_{\text{Pl}}^2\epsilon_{\text{sr}}}{H_{\text{sr}}^2} \lesssim 1, \quad \alpha \lesssim 1, \quad \frac{\lambda^2\alpha^2}{\mu^4} \frac{2M_{\text{Pl}}^2\epsilon_{\text{sr}}}{H_{\text{sr}}^2} \lesssim 1. \quad (2.47)$$

If the mass μ and the turning angle α are specified, (2.47) can be thought of as conditions on the coupling λ of the quartic interaction. Using $\frac{H_{\text{sr}}^2}{2M_{\text{Pl}}^2\epsilon_{\text{sr}}} \simeq 4\pi^2 P_\zeta \sim 10^{-8}$, we have for example

$$\lambda \lesssim 0.01 \quad \text{for} \quad (\mu, \alpha) = (10, 0.1) \quad \text{and} \quad \lambda \lesssim 1 \quad \text{for} \quad (\mu, \alpha) = (10, 0.01). \quad (2.48)$$

2.4 Action for the Goldstone boson

For the calculation of primordial perturbations, it is convenient to introduce the Goldstone boson π by the Stückelberg method. In this subsection we construct the action for π and discuss its relevant terms to tree-level two point and three point functions of scalar perturbations ζ . The action for the Goldstone boson π can be obtained by the gauge transformation

$$t \rightarrow \tilde{t}, \quad x^i \rightarrow \tilde{x}^i \quad \text{with} \quad \tilde{t} + \tilde{\pi}(\tilde{t}, \tilde{x}) = t, \quad \tilde{x}^i = x^i, \quad (2.49)$$

which is realized by the following replacement [30]:

$$\begin{aligned} \delta_\mu^0 &\rightarrow \delta_\mu^0 + \partial_\mu \pi, & f(t) &\rightarrow f(t + \pi), & \int d^4x \sqrt{-g} &\rightarrow \int d^4x \sqrt{-g}, \\ \nabla_\mu &\rightarrow \tilde{\nabla}_\mu, & g_{\mu\nu} &\rightarrow g_{\mu\nu}, & g^{\mu\nu} &\rightarrow g^{\mu\nu}, & R_{\mu\nu\rho\sigma} &\rightarrow R_{\mu\nu\rho\sigma}, \end{aligned} \quad (2.50)$$

where we dropped the tilde for simplicity. The action corresponding to (2.43) is then given by [22]

$$\begin{aligned}
S = \int d^4x \sqrt{-g} & \left[\frac{1}{2} M_{\text{Pl}}^2 R + M_{\text{Pl}}^2 \dot{H}(t + \pi)(g^{00} + 2\partial^0\pi + \partial_\mu\pi\partial^\mu\pi) - M_{\text{Pl}}^2(3H^2 + \dot{H})(t + \pi) \right. \\
& - \frac{1}{2} \partial_\mu\sigma\partial^\mu\sigma + \beta_1(t + \pi)(\delta g^{00} + 2\partial^0\pi + \partial_\mu\pi\partial^\mu\pi)\sigma \\
& \left. + \bar{\gamma}_1(t + \pi)(\delta g^{00} + 2\partial^0\pi + \partial_\mu\pi\partial^\mu\pi)\sigma^2 - V_\sigma(\sigma; t + \pi) \right]. \quad (2.51)
\end{aligned}$$

We next discuss which terms are relevant to tree-level three point functions of π . For this purpose, let us take the spatially flat gauge and rewrite the action (2.51) in terms of the ADM decomposition:

$$ds^2 = -(N^2 - N_i N^i) dt^2 + 2N_i dx^i dt + a^2(e^\gamma)_{ij} dx^i dx^j \quad \text{with} \quad \gamma_{ii} = \partial_i \gamma_{ij} = 0. \quad (2.52)$$

Here and in what follows we use the spatial metric $h_{ij} = a^2(e^\gamma)_{ij}$ and its inverse $h^{ij} = a^{-2}(e^{-\gamma})_{ij}$ to raise or lower the indices of N^i . In this gauge, there are no second order mixing terms of π and γ_{ij} because γ_{ij} has two spatial indices and is transverse-traceless. Then, the tensor fluctuation γ_{ij} does not contribute to tree-level three point functions of π . Therefore, possible contributions of metric perturbations come only from the auxiliary fields $\delta N = N - 1$ and N^i . For the calculation of three-point functions, it is sufficient to solve the constraints up to first order [36]. For the action (2.51), it is performed as follows [22]:

$$\delta N = -\frac{\dot{H}}{H}\pi, \quad N^i = a^{-2}\partial_i\psi \quad \text{with} \quad \psi = a^2\partial^{-2}\left(\frac{\dot{H}}{H^2}(\dot{H}\pi + H\dot{\pi}) + \frac{\beta_1}{M_{\text{Pl}}^2 H}\sigma\right). \quad (2.53)$$

In the following discussions, we decompose the kinetic term of π as

$$M_{\text{Pl}}^2 \dot{H} \partial_\mu \pi \partial^\mu \pi = M_{\text{Pl}}^2 \dot{H}_{\text{sr}} \partial_\mu \pi \partial^\mu \pi + M_{\text{Pl}}^2 \delta \dot{H} \partial_\mu \pi \partial^\mu \pi, \quad (2.54)$$

and treat the second term as an interaction term. In such a case, the canonical normalization is given by

$$\pi_c \sim M_{\text{Pl}}(-\dot{H}_{\text{sr}})^{1/2}\pi, \quad \sigma_c = \sigma, \quad \delta N_c \sim M_{\text{Pl}}\delta N, \quad N_c^i \sim M_{\text{Pl}}N^i, \quad (2.55)$$

and we redefine the coupling constants β_1 correspondingly as

$$\beta_1^c \sim \frac{1}{M_{\text{Pl}}(-\dot{H}_{\text{sr}})^{1/2}}\beta_1. \quad (2.56)$$

Then, the constraints (2.53) can be written as

$$\delta N_c \sim \epsilon_{\text{sr}}^{1/2}(1 + \kappa)\pi_c, \quad N_c^i \sim \epsilon_{\text{sr}}^{1/2}\frac{\partial_i}{\partial^2}\left(-\dot{\pi}_c + \beta_1^c\sigma_c\right), \quad (2.57)$$

where higher order terms in ϵ_{sr} and η_{sr} are dropped. It is manifest that δN_c and N_c^i are suppressed by the slow-roll parameter $\epsilon_{\text{sr}}^{1/2}$ and contributions from δN_c and N_c^i are expected to be irrelevant when the slow-roll direction of the potential satisfies the slow-roll conditions. In fact, we can explicitly show that they are irrelevant in our calculations. We then drop these contributions to obtain the following action up to cubic order perturbations:

$$\begin{aligned}
S = \int d^4x a^3 & \left[-M_{\text{Pl}}^2 \dot{H} \left(\dot{\pi}^2 - \frac{(\partial_i \pi)^2}{a^2} \right) - 3M_{\text{Pl}}^2 \dot{H}^2 \pi^2 - M_{\text{Pl}}^2 \ddot{H} \pi \left(\dot{\pi}^2 - \frac{(\partial_i \pi)^2}{a^2} \right) - 3M_{\text{Pl}}^2 \dot{H} \ddot{H} \pi^3 \right. \\
& + \frac{1}{2} \left(\dot{\sigma}^2 - \frac{(\partial_i \sigma)^2}{a^2} \right) - 2\beta_1 \dot{\pi} \sigma - \beta_1 \left(\dot{\pi}^2 - \frac{(\partial_i \pi)^2}{a^2} \right) \sigma - 2\dot{\beta}_1 \pi \dot{\pi} \sigma \\
& \left. - 2\bar{\gamma}_1 \dot{\pi} \sigma^2 - V(\sigma; t + \pi) \right]. \tag{2.58}
\end{aligned}$$

By further dropping the sub-leading terms in the slow-roll expansion, we finally obtain

$$\begin{aligned}
S = \int d^4x a^3 & \left[-M_{\text{Pl}}^2 \dot{H} \left(\dot{\pi}^2 - \frac{(\partial_i \pi)^2}{a^2} \right) - M_{\text{Pl}}^2 \delta \ddot{H} \pi \left(\dot{\pi}^2 - \frac{(\partial_i \pi)^2}{a^2} \right) \right. \\
& + \frac{1}{2} \left(\dot{\sigma}^2 - \frac{(\partial_i \sigma)^2}{a^2} \right) - 2\beta_1 \dot{\pi} \sigma - \beta_1 \left(\dot{\pi}^2 - \frac{(\partial_i \pi)^2}{a^2} \right) \sigma - 2\dot{\beta}_1 \pi \dot{\pi} \sigma \\
& \left. - 2\bar{\gamma}_1 \dot{\pi} \sigma^2 - V(\sigma; t + \pi) \right]. \tag{2.59}
\end{aligned}$$

Note that $\delta \ddot{H}$ and $\dot{\beta}_1$ can be written in terms of κ and γ as

$$\begin{aligned}
\delta \ddot{H} &= \theta(t - t_*) (\ddot{H}_{\text{sr}} \kappa + \dot{H}_{\text{sr}} \dot{\kappa}) + \delta(t - t_*) \dot{H}_{\text{sr}} \kappa \\
&\simeq \theta(t - t_*) \dot{H}_{\text{sr}} \dot{\kappa} + \delta(t - t_*) \dot{H}_{\text{sr}} \kappa \\
&= \theta(t - t_*) \dot{H}_{\text{sr}} \dot{\kappa}, \tag{2.60}
\end{aligned}$$

$$\begin{aligned}
\dot{\beta}_1 &= \theta(t - t_*) (\ddot{\phi}_{\text{sr}} \dot{\gamma} + \dot{\phi}_{\text{sr}} \ddot{\gamma}) + \delta(t - t_*) \dot{\gamma} \\
&\simeq \theta(t - t_*) \dot{\phi}_{\text{sr}} \ddot{\gamma} + \delta(t - t_*) \dot{\gamma}, \tag{2.61}
\end{aligned}$$

where we used $\kappa(t_*) = 0$ and dropped higher order terms in ϵ_{sr} and η_{sr} .

2.5 Hamiltonian in the interaction picture

In the following two sections the primordial power spectrum and bispectrum of scalar perturbations ζ are calculated using the in-in formalism. For this purpose, let us introduce the Hamiltonian in the interaction picture up to the cubic order fluctuations. Since we would like to discuss the deviation from single field slow-roll inflation, we choose the free part and the

interaction part of the Hamiltonian in the following way:

$$H_{\text{free}} = \int d^3x a^3 \left[-M_{\text{Pl}}^2 \dot{H}_{\text{sr}} \left(\dot{\pi}^2 + \frac{(\partial_i \pi)^2}{a^2} \right) + \frac{1}{2} \left(\dot{\sigma}^2 + \frac{(\partial_i \sigma)^2}{a^2} + m^2 \sigma^2 \right) \right], \quad (2.62)$$

$$H_{\text{int}} = H_{\text{int}}^{(2)} + H_{\text{int}}^{(3)}, \quad (2.63)$$

$$H_{\text{int}}^{(2)} = \int d^3x a^3 \left[M_{\text{Pl}}^2 \delta \dot{H} \left(\dot{\pi}^2 - \frac{(\partial_i \pi)^2}{a^2} \right) + 2\beta_1 \dot{\pi} \sigma \right], \quad (2.64)$$

$$H_{\text{int}}^{(3)} = \int d^3x a^3 \left[M_{\text{Pl}}^2 \delta \ddot{H} \pi \left(\dot{\pi}^2 - \frac{(\partial_i \pi)^2}{a^2} \right) + \beta_1 \left(\dot{\pi}^2 - \frac{(\partial_i \pi)^2}{a^2} \right) \sigma + 2\dot{\beta}_1 \pi \dot{\pi} \sigma + \theta(t - t_*) \frac{\lambda \varphi_2}{6} \sigma^3 \right], \quad (2.65)$$

where we dropped terms irrelevant to the spectra up to the leading order in the turning angle α .⁸ The quantum fields π and σ in the interaction picture are expanded in the Fourier space as

$$\pi_{\mathbf{k}} = u_k a_{\mathbf{k}} + u_k^* a_{-\mathbf{k}}^\dagger, \quad \sigma_{\mathbf{k}} = v_k b_{\mathbf{k}} + v_k^* b_{-\mathbf{k}}^\dagger \quad (2.66)$$

with the standard commutation relations

$$[a_{\mathbf{k}}, a_{\mathbf{k}'}^\dagger] = (2\pi)^3 \delta^{(3)}(\mathbf{k} - \mathbf{k}'), \quad [b_{\mathbf{k}}, b_{\mathbf{k}'}^\dagger] = (2\pi)^3 \delta^{(3)}(\mathbf{k} - \mathbf{k}'). \quad (2.67)$$

Here the mode functions u_k and v_k satisfy the equations of motion in the free theory and depend on $k = |\mathbf{k}|$:

$$\ddot{u}_k + 3H_{\text{sr}} \dot{u}_k + \frac{k^2}{a^2} u_k = 0, \quad \ddot{v}_k + 3H_{\text{sr}} \dot{v}_k + \left(m^2 + \frac{k^2}{a^2} \right) v_k = 0, \quad (2.68)$$

where higher order terms in ϵ_{sr} and η_{sr} are dropped. In terms of the conformal time $d\tau = a^{-1} dt$, they can be written as

$$u_k'' - \frac{2}{\tau} u_k' + k^2 u_k = 0, \quad v_k'' - \frac{2}{\tau} v_k' + k^2 v_k + \frac{m^2}{H_{\text{sr}}^2 \tau^2} v_k = 0, \quad (2.69)$$

where the primes denote derivatives with respect to τ and we used $\tau = -1/(aH_{\text{sr}})$ at the leading order in ϵ_{sr} and η_{sr} . The normalizations of the mode functions follow from

$$2M_{\text{Pl}}^2 H_{\text{sr}}^2 \epsilon_{\text{sr}} a^3 (u_k \dot{u}_k^* - \dot{u}_k u_k^*) = i, \quad a^3 (v_k \dot{v}_k^* - \dot{v}_k v_k^*) = i. \quad (2.70)$$

Assuming that π and σ are in the Bunch-Davies vacuum before the turn, the mode functions u_k and v_k are given by

$$u_k = \frac{1}{2M_{\text{Pl}} \epsilon_{\text{sr}}^{1/2} k^{3/2}} (1 + ik\tau) e^{-ik\tau} = \frac{1}{2M_{\text{Pl}} \epsilon_{\text{sr}}^{1/2} k^{3/2}} (1 - ix) e^{ix}, \quad (2.71)$$

$$v_k = -ie^{-\frac{\pi}{2}\mu + \frac{i}{4}\pi} \frac{\sqrt{\pi} H_{\text{sr}}}{2} (-\tau)^{3/2} H_{i\mu}^{(1)}(-k\tau) = -ie^{-\frac{\pi}{2}\mu + \frac{i}{4}\pi} \frac{\sqrt{\pi} H_{\text{sr}}}{2k^{3/2}} x^{3/2} H_{i\mu}^{(1)}(x), \quad (2.72)$$

⁸ Note that contributions from the $2\bar{\gamma}_1 \dot{\pi} \sigma^2$ term are sub-leading in the tree-level three-point functions of π .

where $x = -k\tau$ and $H_\nu^{(1)} = J_\nu + iY_\nu$ is the Hankel function. Note that the time derivative of u_k is given by

$$\dot{u}_k = -H_{\text{sr}}\tau u'_k = -\frac{H_{\text{sr}}}{2M_{\text{Pl}}\epsilon_{\text{sr}}^{1/2}k^{3/2}}x^2e^{ix}. \quad (2.73)$$

It is also convenient to express κ and φ_2 in terms of the conformal time:

$$\begin{aligned} \kappa(t) &= -\alpha^2(\tau/\tau_*)^3 \left[\left(\frac{1}{2} - \frac{9}{8\mu^2} \right) (1 - \cos[2\mu \ln(\tau/\tau_*)]) - \frac{3}{2\mu} \sin[2\mu \ln(\tau/\tau_*)] \right] \\ &= -\alpha^2 \left[\left(\frac{1}{2} - \frac{9}{8\mu^2} \right) (\tau/\tau_*)^3 + \frac{(3+2i\mu)^2}{16\mu^2} (\tau/\tau_*)^{3+2i\mu} + \frac{(3-2i\mu)^2}{16\mu^2} (\tau/\tau_*)^{3-2i\mu} \right], \end{aligned} \quad (2.74)$$

$$\varphi_2(t) = -\frac{\alpha\bar{\phi}_{\text{sr}}}{\mu H_{\text{sr}}} (\tau/\tau_*)^{3/2} \sin[\mu \ln(\tau/\tau_*)] = i\frac{\alpha\bar{\phi}_{\text{sr}}}{2\mu H_{\text{sr}}} \left[(\tau/\tau_*)^{\frac{3}{2}+i\mu} - (\tau/\tau_*)^{\frac{3}{2}-i\mu} \right], \quad (2.75)$$

where τ_* is the conformal time corresponding to the turning time t_* . In the following, we use the above setup for the calculation of primordial spectra.

3 Primordial power spectrum

Let us then calculate the primordial power spectrum. Since the scalar perturbation ζ is given at the linear order by $\zeta = -H\pi$, we calculate the expectation value of $\pi_{\mathbf{k}}(t)\pi_{\mathbf{k}'}(t)$. Using the in-in formalism, it is calculated as

$$\begin{aligned} \langle \pi_{\mathbf{k}}(t)\pi_{\mathbf{k}'}(t) \rangle &= \langle 0 | \left[\bar{T} \exp \left(i \int_{t_0}^t dt' H_{\text{int}}(t') \right) \right] \pi_{\mathbf{k}}(t)\pi_{\mathbf{k}'}(t) \left[T \exp \left(-i \int_{t_0}^t dt' H_{\text{int}}(t') \right) \right] | 0 \rangle \\ &= \langle 0 | \pi_{\mathbf{k}}(t)\pi_{\mathbf{k}'}(t) | 0 \rangle + 2\text{Re} \left[-i \int_{t_0}^t dt_1 \langle 0 | \pi_{\mathbf{k}}(t)\pi_{\mathbf{k}'}(t) H_{\text{int}}(t_1) | 0 \rangle \right] \\ &\quad + \int_{t_0}^t d\tilde{t}_1 \int_{t_0}^{\tilde{t}_1} dt_1 \langle 0 | H_{\text{int}}(\tilde{t}_1) \pi_{\mathbf{k}}(t)\pi_{\mathbf{k}'}(t) H_{\text{int}}(t_1) | 0 \rangle \\ &\quad - 2\text{Re} \left[\int_{t_0}^t dt_1 \int_{t_0}^{t_1} dt_2 \langle 0 | \pi_{\mathbf{k}}(t)\pi_{\mathbf{k}'}(t) H_{\text{int}}(t_1) H_{\text{int}}(t_2) | 0 \rangle \right] + \dots, \end{aligned} \quad (3.1)$$

where the dots stand for higher order terms in the couplings. In the following, we set $t = \infty$ and $t_0 = -\infty$ and drop the indication of the time t in correlators. In terms of the mode functions and couplings, the two point function (3.1) can be expressed up to the leading order corrections from κ and β_1 as

$$\langle \pi_{\mathbf{k}}\pi_{\mathbf{k}'} \rangle = (2\pi)^3 \delta^{(3)}(\mathbf{k} + \mathbf{k}') \frac{1}{4M_{\text{Pl}}^2 \epsilon_{\text{sr}} k^3} \left[1 + \mathcal{C}_{\delta H} + \mathcal{C}_{\text{conv}} \right], \quad (3.2)$$

where $\mathcal{C}_{\delta H}$ and $\mathcal{C}_{\text{conv}}$ are defined by (see Fig. 2 for the corresponding diagrams)

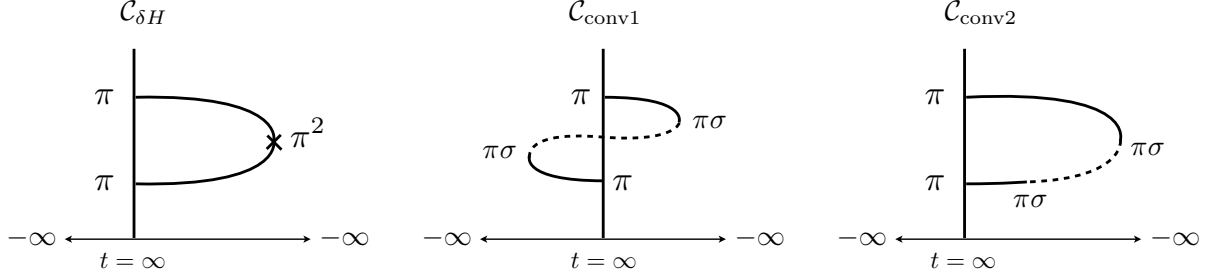


Figure 2: Diagrams corresponding to $\mathcal{C}_{\delta H}$, $\mathcal{C}_{\text{conv1}}$, and $\mathcal{C}_{\text{conv2}}$ (depicted from the left). The solid and dotted lines represent the propagation of π and σ , respectively.

$$\mathcal{C}_{\delta H} = 2\text{Re} \left[i \int_{-\infty}^{\infty} dt_1 a^3 (2M_{\text{Pl}}^2 \dot{H}_{\text{sr}} \kappa(t_1)) \left(\dot{u}_k^2(t_1) - \frac{k^2}{a^2} u_k^2(t_1) \right) \right], \quad (3.3)$$

$$\mathcal{C}_{\text{conv}} = \mathcal{C}_{\text{conv1}} + \mathcal{C}_{\text{conv2}}, \quad (3.4)$$

$$\mathcal{C}_{\text{conv1}} = 8 \left| \int_{-\infty}^{\infty} dt_1 a^3(t_1) \beta_1(t_1) \dot{u}_k(t_1) v_k(t_1) \right|^2, \quad (3.5)$$

$$\mathcal{C}_{\text{conv2}} = -16\text{Re} \left[\int_{-\infty}^{\infty} dt_1 a^3(t_1) \beta_1(t_1) \dot{u}_k^*(t_1) v_k(t_1) \int_{-\infty}^{t_1} dt_2 a^3(t_2) \beta_1(t_2) \dot{u}_k^*(t_2) v_k^*(t_2) \right]. \quad (3.6)$$

Note that $\mathcal{C}_{\delta H}$ describes the effects of the deformation δH of the background Hubble parameter and $\mathcal{C}_{\text{conv}}$ describes the conversion effects between adiabatic and isocurvature perturbations. Also notice that they are second order in the turning angle α because κ and β_1 are second and first order in α , respectively. The two-point functions of scalar perturbations are then given by

$$\langle \zeta_{\mathbf{k}}(t) \zeta_{\mathbf{k}'}(t) \rangle = (2\pi)^3 \delta^{(3)}(\mathbf{k} + \mathbf{k}') \frac{2\pi^2}{k^3} \mathcal{P}_{\zeta}(k), \quad (3.7)$$

where the power spectrum $\mathcal{P}_{\zeta}(k)$ is

$$\mathcal{P}_{\zeta}(k) = \frac{H_{\text{sr}}^2}{8\pi^2 M_{\text{sr}}^2 \epsilon_{\text{sr}}} (1 + \mathcal{C}_{\delta H} + \mathcal{C}_{\text{conv}}). \quad (3.8)$$

In the rest of this section, we evaluate $\mathcal{C}_{\delta H}$ and $\mathcal{C}_{\text{conv}}$, which can be thought of as deviation factors from the single field slow-roll model.

3.1 Hubble deformation effects

Using the expression (2.71) of the mode functions, $\mathcal{C}_{\delta H}$ can be expressed as

$$\mathcal{C}_{\delta H} = -\text{Im} \left[\int_0^{x_*} dx \kappa (2 - 2ix^{-1} - x^{-2}) e^{-2ix} \right], \quad (3.9)$$

where $x = -k\tau$ and $x_* = -k\tau_*$. It is convenient to introduce the mode $k_* = -1/\tau_*$, which crosses the horizon at the time $t = t_*$ of turning. In terms of k_* , the parameter x_* can be expressed as $x_* = k/k_*$. Using x and x_* , the coupling κ can be written as

$$\kappa = -\alpha^2 \left[\left(\frac{1}{2} - \frac{9}{8\mu^2} \right) (x/x_*)^3 + \frac{(3+2i\mu)^2}{16\mu^2} (x/x_*)^{3+2i\mu} + \frac{(3-2i\mu)^2}{16\mu^2} (x/x_*)^{3-2i\mu} \right]. \quad (3.10)$$

Then, the integral (3.9) reduces to integrals of the form

$$\mathcal{I}(\delta, n, x) = \int_0^x d\tilde{x} (\tilde{x}/x)^{3+\delta} \tilde{x}^n e^{-i\tilde{x}}, \quad (3.11)$$

whose analytic expression can be obtained as follows:

$$\mathcal{I}(\delta, n, x) = i^{-1-n} (1/ix)^{3+\delta} \left[\Gamma(4+n+\delta) - \Gamma(4+n+\delta, ix) \right]. \quad (3.12)$$

Here $\Gamma(z)$ and $\Gamma(a, z)$ are the gamma function and the incomplete gamma function, respectively. In terms of $\mathcal{I}(\delta, n, x)$, the integral (3.9) can be expressed as

$$\begin{aligned} \mathcal{C}_{\delta H}(x_*) = \text{Im} & \left[\alpha^2 \left(\frac{1}{2} - \frac{9}{8\mu^2} \right) \left[\mathcal{I}(0, 0, 2x_*) - 2i\mathcal{I}(0, -1, 2x_*) - 2\mathcal{I}(0, -2, 2x_*) \right] \right. \\ & + \alpha^2 \frac{(3+2i\mu)^2}{16\mu^2} \left[\mathcal{I}(2i\mu, 0, 2x_*) - 2i\mathcal{I}(2i\mu, -1, 2x_*) - 2\mathcal{I}(2i\mu, -2, 2x_*) \right] \\ & \left. + \alpha^2 \frac{(3-2i\mu)^2}{16\mu^2} \left[\mathcal{I}(-2i\mu, 0, 2x_*) - 2i\mathcal{I}(-2i\mu, -1, 2x_*) - 2\mathcal{I}(-2i\mu, -2, 2x_*) \right] \right]. \end{aligned} \quad (3.13)$$

As displayed in Fig. 3, a kind of resonance appears in $\mathcal{C}_{\delta H}$ around the scale $k \sim \frac{m}{H_{\text{sr}}} k_* \sim \mu k_*$ [8, 9, 18, 24, 25]. In the rest of this subsection, we discuss qualitative features of this resonance effect.

3.1.1 Mathieu equation and the resonance effect

Following [18], let us introduce the Mathieu equation characterizing the above resonance effects and estimate the scale and size of the resonance. For our purpose, it is convenient to introduce a canonically normalized field u defined by

$$u = z_\pi \pi \quad \text{with} \quad z_\pi = (-2M_{\text{Pl}}^2 \dot{H} a^3)^{1/2} = (2M_{\text{Pl}}^2 \epsilon)^{1/2} H a^{3/2}. \quad (3.14)$$

In terms of u , the second order action of π can be written as

$$S = \int dt d^3x a^3 (-M_{\text{Pl}}^2 \dot{H}) \left(\dot{\pi}^2 - \frac{(\partial_i \pi^2)}{a^2} \right) = \frac{1}{2} \int dt d^3x \left(\dot{u}^2 - \frac{(\partial_i u)^2}{a^2} - \frac{\ddot{z}_\pi}{z_\pi} u^2 \right), \quad (3.15)$$

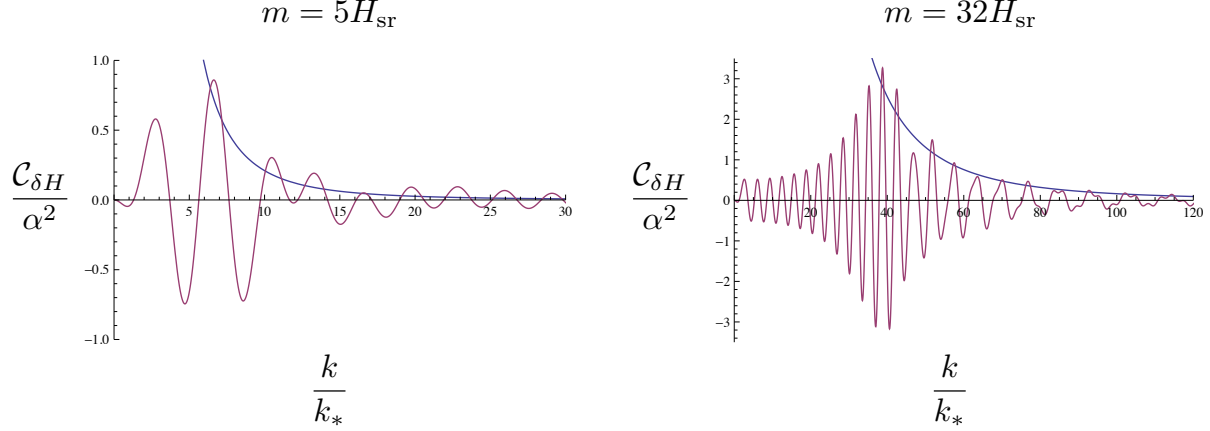


Figure 3: Scale-dependence of $\mathcal{C}_{\delta H}$ for $m = 5H_{\text{sr}}$ (left figure) and $m = 32H_{\text{sr}}$ (right figure). The red curve is the exact expression (3.13) for $\mathcal{C}_{\delta H}$. The blue curve is the resonance size estimated via the parametric resonance arguments: $\mathcal{C}_{\delta H} = \frac{\sqrt{\pi}}{2}\alpha^2\mu^{1/2}(k/(\mu k_*))^{-3}$, where the numerical coefficient $\sqrt{\pi}/2$ is determined by the stationary phase approximation. As shown in the above figures, the parametric resonance arguments well explain and capture our exact results.

and the equation of motion in the momentum space is given by

$$\ddot{u} + \left(\frac{k^2}{a^2} + \frac{\ddot{z}_\pi}{z_\pi} \right) u = 0, \quad (3.16)$$

where the explicit form of \ddot{z}_π/z_π is

$$\frac{\ddot{z}_\pi}{z_\pi} = \frac{9}{4}H_{\text{sr}}^2 + \frac{3}{2}H_{\text{sr}}\dot{\kappa} + \frac{1}{2}\ddot{\kappa} + \mathcal{O}(\epsilon_{\text{sr}}, \eta_{\text{sr}}, \kappa^2) \quad \text{with} \quad \kappa = \frac{\dot{H} - \dot{H}_{\text{sr}}}{\dot{H}_{\text{sr}}} = \frac{\delta\dot{H}}{\dot{H}_{\text{sr}}}. \quad (3.17)$$

To characterize the highly oscillating background, let us rewrite κ as

$$\kappa = A(t) \sin(2\omega t + \theta), \quad (3.18)$$

where we assume that $\omega \gg H_{\text{sr}}$ and the time-dependence of the normalization factor $A(t)$ is negligible compared to ω . At the leading order in H_{sr}/ω , the equation of motion (3.16) can be written as

$$\ddot{u} + \left(\frac{k^2}{a^2} + \frac{9}{4}H_{\text{sr}}^2 - 2\omega^2 A(t) \sin(2\omega t + \theta) \right) u = 0, \quad (3.19)$$

which can be regarded as the Mathieu equation. From this expression, it is obvious that the mode k feels resonance effects around the time t_k given by

$$\frac{k}{a(t_k)} = \omega. \quad (3.20)$$

Here we dropped higher order terms in ω/H_{sr} . From general discussions on the parametric resonance, it follows that $u(t)$ is changed around $t = t_k$ as

$$\left| \frac{u(t) - u(t_k)}{u(t_k)} \right| \sim |A(t_k)| \omega (t - t_k) \quad (3.21)$$

and the duration Δt of the resonance can be estimated as

$$\Delta t \sim (H_{\text{sr}}\omega)^{-1/2}. \quad (3.22)$$

We then conclude that the mode k is changed after experiencing the parametric resonance as

$$\left| \frac{u_{\text{after}} - u_{\text{before}}}{u_{\text{before}}} \right| \sim |A(t_k)| \sqrt{\frac{\omega}{H_{\text{sr}}}}. \quad (3.23)$$

In our models, the parameters $A(t)$ and ω are given by

$$A(t) \sim \frac{\alpha^2}{2} e^{-3H(t-t_*)}, \quad \omega = \mu H_{\text{sr}}, \quad (3.24)$$

and the mode k feels resonance effects around the time t_k given by

$$\frac{k}{a(t_k)} = \mu H_{\text{sr}} \quad \leftrightarrow \quad \frac{a(t_k)}{a(t_*)} = \frac{1}{\mu} \frac{k}{k_*}. \quad (3.25)$$

Since the background oscillation starts at $t = t_*$, the mode $k \lesssim \mu k_*$ does not experience the parametric resonance and the resonance effect appears at the scale $k \gtrsim \mu k_*$. The size of $\mathcal{C}_{\delta H}$ for $k \gtrsim \mu k_*$ can be also estimated as

$$|\mathcal{C}_{\delta H}| \sim \alpha^2 \mu^{1/2} e^{-3H(t_k-t_*)} \sim \alpha^2 \mu^{1/2} \left(\frac{k}{\mu k_*} \right)^{-3}. \quad (3.26)$$

As depicted in Fig. 3, the above estimation well explains our exact results.

It would be also notable that the resonance effects can be also estimated via the stationary phase approximation,⁹ which is useful to evaluate integrals with oscillations. As discussed in Appendix B, the integral $\mathcal{I}(2i\mu, n, x)$ in the heavy mass region $\mu \gg 1$ can be evaluated via the stationary phase approximation as

$$\mathcal{I}(2i\mu, n, x) \simeq \begin{cases} \left(\frac{2\mu}{x} \right)^{3+2i\mu} (2\mu)^{n+\frac{1}{2}} \sqrt{2\pi} e^{-2i\mu - \frac{i}{4}\pi} & \text{for } x \gtrsim 2\mu, \\ 0 & \text{for } x \lesssim 2\mu. \end{cases} \quad (3.27)$$

⁹ See e.g. Refs. [24, 25] for the use of the stationary phase approximation in the context of heavy field oscillations.

Applying this approximation to (3.13), the resonance effect can be again expected to appear at the scale $x_* \gtrsim \mu$ and its size can be again estimated as

$$|\mathcal{C}_{\delta H}| \simeq \left| \text{Im} \left[\frac{\alpha^2}{4} \mathcal{I}(2i\mu, 0, 2x_*) \right] \right| \simeq \left| \alpha^2 \frac{\sqrt{\pi}}{2} \left(\frac{\mu}{x_*} \right)^{3+2i\mu} \mu^{1/2} e^{-2i\mu - \frac{i}{4}\pi} \right| \simeq \frac{\sqrt{\pi}}{2} \alpha^2 \mu^{1/2} \left(\frac{k}{\mu k_*} \right)^{-3}, \quad (3.28)$$

which coincides with Eq. (3.26). Here note that resonance effects do not appear in $\mathcal{I}(0, n, x)$ and $\mathcal{I}(-2i\mu, n, x)$, which are therefore irrelevant in the heavy mass region.

3.2 Conversion effects

Let us next discuss the conversion effects $\mathcal{C}_{\text{conv}}$. Substituting the expressions (2.71) and (2.72) of the mode functions into (3.4)-(3.6), $\mathcal{C}_{\text{conv}}$ can be written as

$$\mathcal{C}_{\text{conv}} = \mathcal{C}_{\text{conv}1} + \mathcal{C}_{\text{conv}2}, \quad (3.29)$$

$$\mathcal{C}_{\text{conv}1} = \pi e^{-\mu\pi} \left| \int_0^{x_*} dx \frac{\dot{\gamma}}{H_{\text{sr}}} x^{-1/2} e^{ix} H_{i\mu}^{(1)}(x) \right|^2, \quad (3.30)$$

$$\mathcal{C}_{\text{conv}2} = -2\pi e^{-\mu\pi} \text{Re} \left[\int_0^{x_*} dx_1 \frac{\dot{\gamma}}{H_{\text{sr}}} x_1^{-1/2} e^{ix_1} H_{-i\mu}^{(2)}(x_1) \int_{x_1}^{x_*} dx_2 \frac{\dot{\gamma}}{H_{\text{sr}}} x_2^{-1/2} e^{ix_2} H_{i\mu}^{(1)}(x_2) \right], \quad (3.31)$$

where $\dot{\gamma}/H_{\text{sr}}$ is given by

$$\frac{\dot{\gamma}}{H_{\text{sr}}} = i\alpha \left[\frac{(\frac{3}{2} + i\mu)^2}{2\mu} (x/x_*)^{3/2+i\mu} - \frac{(\frac{3}{2} - i\mu)^2}{2\mu} (x/x_*)^{3/2-i\mu} \right]. \quad (3.32)$$

It is convenient to introduce the indefinite integral $\mathcal{D}_+(\ell, \mu, x)$ defined by

$$\mathcal{D}_+(\ell, \mu, x) = \int dx x^{-\frac{1}{2}+\ell} e^{ix} H_{i\mu}^{(1)}(x), \quad (3.33)$$

whose analytic expression is [14, 22]

$$\begin{aligned} \mathcal{D}_+(\ell, \mu, x) &= \frac{2^{i\mu} x^{\frac{1}{2}+\ell-i\mu} \Gamma(i\mu)}{i\pi(\frac{1}{2}+\ell-i\mu)} {}_2F_2\left(\frac{1}{2}-i\mu, \frac{1}{2}+\ell-i\mu; \frac{3}{2}+\ell-i\mu, 1-2i\mu; 2ix\right) \\ &+ e^{\pi\mu} \frac{2^{-i\mu} x^{\frac{1}{2}+\ell+i\mu} \Gamma(-i\mu)}{i\pi(\frac{1}{2}+\ell+i\mu)} {}_2F_2\left(\frac{1}{2}+i\mu, \frac{1}{2}+\ell+i\mu; \frac{3}{2}+\ell+i\mu, 1+2i\mu; 2ix\right). \end{aligned} \quad (3.34)$$

Using this function $\mathcal{D}_+(\ell, \mu, x)$, we obtain the following useful relation:

$$\begin{aligned} &\int dx \frac{\dot{\gamma}}{H_{\text{sr}}} x^{-1/2} e^{ix} H_{i\mu}^{(1)}(x) \\ &= i\alpha \left[\frac{(\frac{3}{2} + i\mu)^2}{2\mu} x_*^{-(\frac{3}{2}+i\mu)} \mathcal{D}_+(\frac{3}{2} + i\mu, \mu, x) - \frac{(\frac{3}{2} - i\mu)^2}{2\mu} x_*^{-(\frac{3}{2}-i\mu)} \mathcal{D}_+(\frac{3}{2} - i\mu, \mu, x) \right], \end{aligned} \quad (3.35)$$

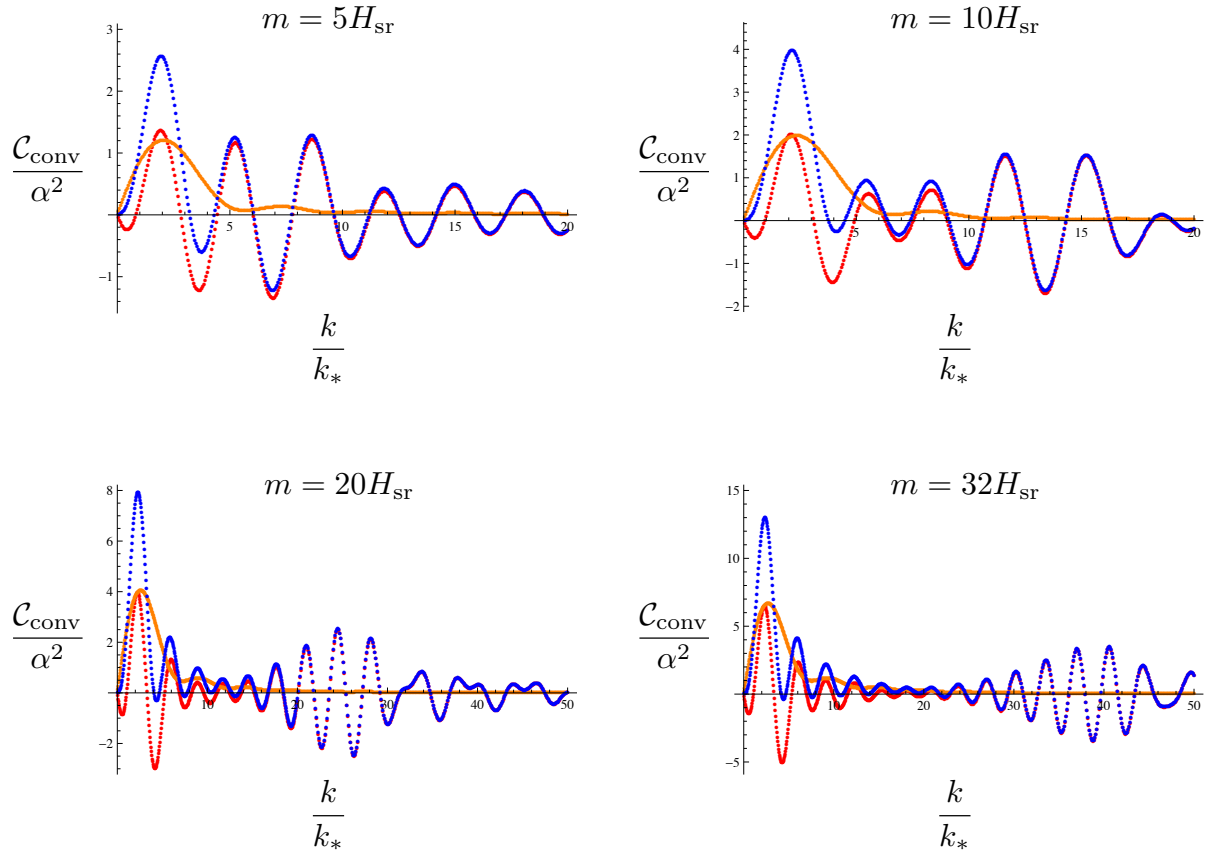


Figure 4: Scale-dependence of $\mathcal{C}_{\text{conv}}$ for $m/H_{\text{sr}} = 5$ (upper left), 10 (upper right), 20 (lower left), and 32 (lower right). The blue/red dots are numerical results for $\mathcal{C}_{\text{conv}}/\mathcal{C}_{\text{conv}2}$ and the orange curve is the analytic result for $\mathcal{C}_{\text{conv}1}$. The total conversion effect has a peak $\mathcal{C}_{\text{conve}} \sim 0.5\mu\alpha^2$ at $k \sim 2k_*$ and the resonance at $k \gtrsim \mu k_*$. It is also observed that the resonance effects arise only from $\mathcal{C}_{\text{conv}2}$.

which enables us to evaluate $\mathcal{C}_{\text{conv}1}$ analytically and reduces the calculation of $\mathcal{C}_{\text{conv}2}$ to one integral over x_1 . Since it seems difficult to perform the x_1 -integral in $\mathcal{C}_{\text{conv}2}$ analytically, we evaluated $\mathcal{C}_{\text{conv}2}$ numerically. The obtained $\mathcal{C}_{\text{conv}}$, $\mathcal{C}_{\text{conv}1}$, and $\mathcal{C}_{\text{conv}2}$ are summarized in Fig. 4. We first notice that there is a peak at $k \sim 2k_*$, which has been discussed in recent literatures [17, 10, 11, 22]. In addition, resonance-like features can be observed at the scale $k \gtrsim \mu k_*$. In the rest of this subsection, we discuss qualitative features of these two effects.

3.2.1 Peak at the turning scale

As depicted in Fig. 4, $\mathcal{C}_{\text{conv}}$ has a peak around the turning scale. In particular, it is notable that its size becomes larger as the massive direction gets heavier. Since effects of highly oscillating interactions and those of heavy fields are suppressed by the high frequency or the heavy mass

in general, this kind of behavior might seem to be curious. In the following, we explain how the conversion effects become relevant around the turning scale and analytically calculate $\mathcal{C}_{\text{conv}}$ in the heavy mass region. Using the heavy mass approximation, $m \gg H_{\text{sr}}$, the mode function for $k \sim k_*$ can be written as

$$v_k(t) \simeq \frac{1}{\sqrt{2ma^3}} e^{-im(t-t_*)} \quad (3.36)$$

up to a phase factor irrelevant to the computation of $\mathcal{C}_{\text{conv}}$. With this expression, $\mathcal{C}_{\text{conv1}}$ can be written for example as

$$\begin{aligned} \mathcal{C}_{\text{conv1}}(k) &= 8 \left| \int_{-\infty}^{\infty} dt_1 a^3(t_1) \beta_1(t_1) \dot{u}_k(t_1) v_k(t_1) \right|^2 \\ &= \frac{8\alpha^2 m^2 \dot{\phi}_{\text{sr}}^2}{2m} \left| \int_{t_*}^{\infty} dt a^{3/2} e^{-\frac{3}{2}H_{\text{sr}}(t-t_*)} \sin[m(t-t_*)] e^{-im(t-t_*)} \dot{u}_k(t) \right|^2. \end{aligned} \quad (3.37)$$

An important observation is that the coupling β_1 and the mode function v_k have the same frequency m so that $\beta_1 v_k$ has a non-oscillating component:

$$\sin[m(t-t_*)] e^{-im(t-t_*)} = \frac{1 - e^{-2im(t-t_*)}}{2i}. \quad (3.38)$$

Then, this non-oscillating component becomes relevant to the integral in (3.37) and $\mathcal{C}_{\text{conv1}}$ can be evaluated as follows:

$$\mathcal{C}_{\text{conv1}}(k) \simeq \alpha^2 m \dot{\phi}_{\text{sr}}^2 \left| \int_{t_*}^{\infty} dt a^{3/2} e^{-\frac{3}{2}H_{\text{sr}}(t-t_*)} \dot{u}_k(t) \right|^2 = \frac{\mu\alpha^2}{2x_*^3} \left| e^{ix_*} (1 - ix_*) - 1 \right|^2, \quad (3.39)$$

where $x_* = k/k_*$. Notice that the contributions from the non-oscillating part are proportional to $\mu \simeq m/H_{\text{sr}}$ while those from oscillating components are suppressed by the factor $1/\mu$. Similarly, $\mathcal{C}_{\text{conv2}}$ is calculated as

$$\mathcal{C}_{\text{conv2}}(k) \simeq -\frac{\mu\alpha^2}{2x_*^3} \text{Re} \left[(e^{-ix_*} (1 + ix_*) - 1)^2 \right],$$

and we have the following analytic expression for $\mathcal{C}_{\text{conv}}$ in the heavy mass approximation:

$$\mathcal{C}_{\text{conv}}(k) \simeq \mu\alpha^2 \frac{(\sin x_* - x_* \cos x_*)^2}{x_*^3}. \quad (3.40)$$

Note that (3.40) takes its maximum value $\mathcal{C}_{\text{conv}} \sim 0.43 \mu\alpha^2$ at $x_* \sim 2.46$. As depicted in Fig. 5, the analytic expression (3.40) well explains the behavior around the turning scale $k \sim k_*$, but the approximation becomes worse in the region $k \gtrsim \mu k_*$ essentially because of resonance effects discussed below. To summarize, the peak around the turning scale arises because of the coincidence between the frequency of the oscillating coupling β_1 and the mass m of massive isocurvature perturbations. Using the heavy mass approximation, the scale of the peak and its size can be estimated as $k \sim 2.46 k_*$ and $\mathcal{C}_{\text{conv}} \sim 0.43 \mu\alpha^2$.

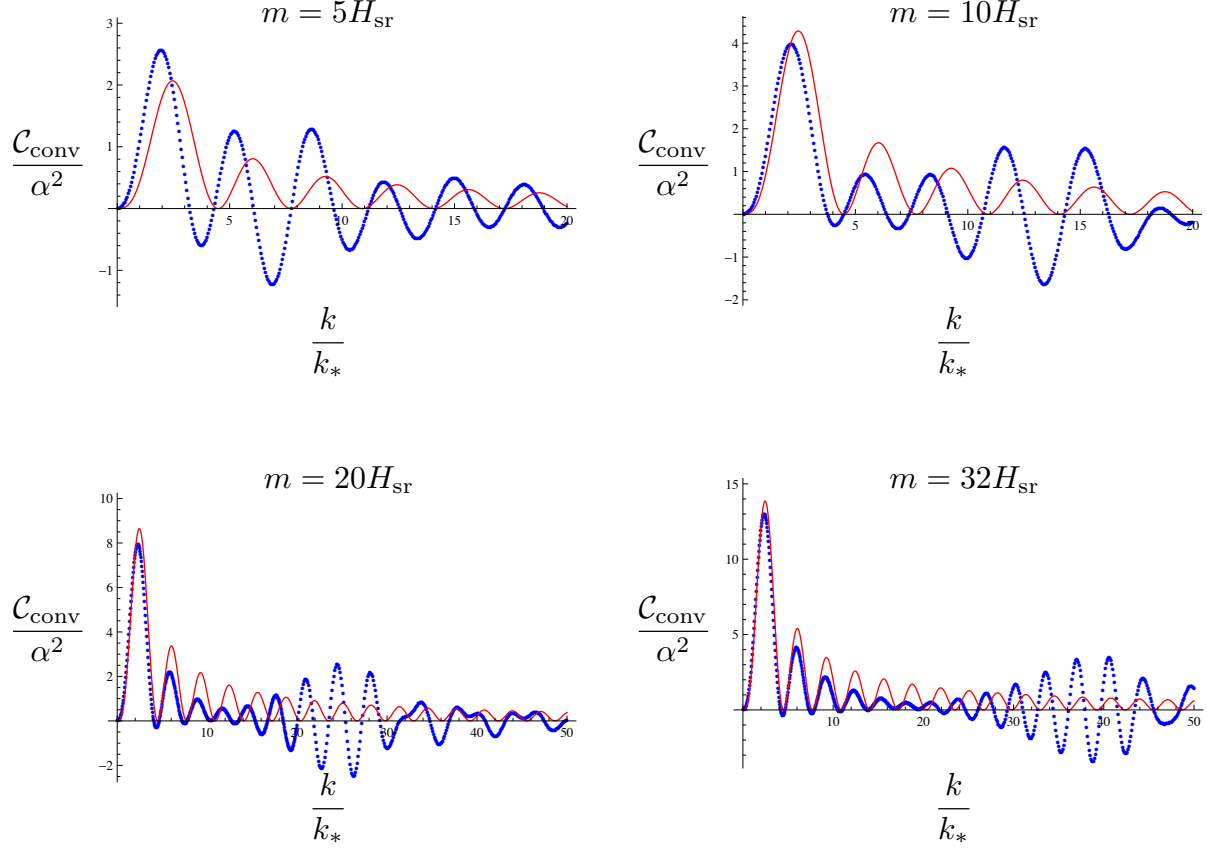


Figure 5: Heavy mass approximation for $\mathcal{C}_{\text{conv}}$ around the turning scale $k \sim k_*$. The red curve is the analytic expression (3.40) in the heavy mass approximation and the blue dots are the numerical results without approximations. While the behavior around $k \sim k_*$ is well explained by the analytic expression, the approximation becomes worth at $k \gtrsim \mu k_*$.

3.2.2 Resonance effects

Let us next discuss the resonance-like effects at the scale $k \gtrsim \mu k_*$ using the heavy mass approximation $m \gg H_{\text{sr}}$. In this approximation, the mode function for $k \sim \mu k_*$ is given up to an irrelevant phase factor as

$$v_k(t) \simeq \frac{1}{\sqrt{2Ea^3}} e^{-iE(t-t_*)} \quad \text{with} \quad E = \sqrt{m^2 + \frac{k^2}{a^2}}. \quad (3.41)$$

Using this expression, we first estimate the size of $\mathcal{C}_{\text{conv}1}$:

$$\begin{aligned} \mathcal{C}_{\text{conv}1}(k) &= 8 \left| \int_{-\infty}^{\infty} dt_1 a^3(t_1) \beta_1(t_1) \dot{u}_k(t_1) v_k(t_1) \right|^2 \\ &\simeq 8\alpha^2 m^2 \dot{\phi}_{\text{sr}}^2 \left| \int_{t_*}^{\infty} dt \frac{a^{3/2}}{\sqrt{2E}} e^{-\frac{3}{2}H_{\text{sr}}(t-t_*)} \sin[m(t-t_*)] e^{-iE(t-t_*)} \dot{u}_k(t) \right|^2. \end{aligned} \quad (3.42)$$

The phase factor of the integrand takes the form

$$\sim \exp \left[i \left(\pm m - E - \frac{k}{a} \right) t \right] = \exp \left[i \left(\pm m - \sqrt{m^2 + \frac{k^2}{a^2}} - \frac{k}{a} \right) t \right], \quad (3.43)$$

which always oscillates with a frequency of the order m . Therefore, the integral in (3.42) is suppressed by $1/(m E^{1/2}) \sim m^{-3/2}$ and it is found that $\mathcal{C}_{\text{conv}1} \sim \alpha^2/\mu$, which is irrelevant in the heavy mass region.

Let us then consider $\mathcal{C}_{\text{conv}2}$ in the heavy mass approximation:

$$\begin{aligned} \mathcal{C}_{\text{conv}2} &= -16 \text{Re} \left[\int_{-\infty}^{\infty} dt_1 a^3(t_1) \beta_1(t_1) \dot{u}_k^*(t_1) v_k(t_1) \int_{-\infty}^{t_1} dt_2 a^3(t_2) \beta_1(t_2) \dot{u}_k^*(t_2) v_k^*(t_2) \right] \\ &= -16 \alpha^2 m^2 \dot{\phi}_{\text{sr}}^2 \text{Re} \left[\int_{t_*}^{\infty} dt_1 \frac{a^{3/2}}{\sqrt{2E}} e^{-\frac{3}{2} H_{\text{sr}}(t_1-t_*)} \sin[m(t_1-t_*)] e^{-iE(t_1-t_*)} \dot{u}_k^*(t_1) \right. \\ &\quad \left. \times \int_{t_*}^{t_1} dt_2 \frac{a^{3/2}}{\sqrt{2E}} e^{-\frac{3}{2} H_{\text{sr}}(t_2-t_*)} \sin[m(t_2-t_*)] e^{iE(t_2-t_*)} \dot{u}_k^*(t_2) \right]. \quad (3.44) \end{aligned}$$

Apparently, (3.44) may seem to be suppressed by the factor $1/\mu$ like $\mathcal{C}_{\text{conv}2}$. However, it turns out that non-trivial contributions arise around the time $t_1 = t_k$ determined by $\frac{k}{a(t_k)} \sim m$, which is the time when resonance effects from the Hubble deformation appear. Around the time $t_2 = t_k$, $\sin[m(t_2-t_*)] \dot{u}_k^*(t_2)$ has non-oscillating components (whose time-dependence is negligible compared to E) so that the t_2 -integral in (3.44) can be performed as

$$\begin{aligned} &\int_{t_*}^{t_1} dt_2 \frac{a^{3/2}}{\sqrt{2E}} e^{-\frac{3}{2} H_{\text{sr}}(t_2-t_*)} \sin[m(t_2-t_*)] e^{iE(t_2-t_*)} \dot{u}_k^*(t_2) \\ &\simeq \frac{1}{iE} \frac{a^{3/2}}{\sqrt{2E}} e^{-\frac{3}{2} H_{\text{sr}}(t_1-t_*)} \sin[m(t_2-t_*)] e^{iE(t_1-t_*)} \dot{u}_k^*(t_1), \quad (3.45) \end{aligned}$$

which implies that adiabatic and isocurvature perturbations around $t \sim t_k$ are converted to each other instantaneously. We therefore obtain the following expression for (3.44):

$$\begin{aligned} \mathcal{C}_{\text{conv}2} &\simeq -16 \alpha^2 m^2 \dot{\phi}_{\text{sr}}^2 \text{Re} \left[\int_{t_*}^{\infty} dt_1 \frac{a^3}{2iE^2} e^{-3H_{\text{sr}}(t_1-t_*)} \sin^2[m(t_1-t_*)] (\dot{u}_k^*(t_1))^2 \right] \\ &= 8 \alpha^2 M_{\text{Pl}}^2 \dot{H}_{\text{sr}} \text{Re} \left[i \int_{t_*}^{\infty} dt_1 a^3 \frac{m^2}{E^2} e^{-3H_{\text{sr}}(t_1-t_*)} (1 - \cos[2m(t_1-t_*)]) \dot{u}_k^2(t_1) \right]. \quad (3.46) \end{aligned}$$

When $t_1 \sim t_k$, non-oscillating components appear in $\cos[2m(t_1-t_*)] \dot{u}_k^2(t_1)$ so that the t_1 -integral has a non-trivial contribution from $t_1 \sim t_k$, which can be observed as the resonance in Fig. 4.

It is also notable that (3.46) can be written up to higher order terms in $1/\mu$ as

$$\mathcal{C}_{\text{conv}2} = -2M_{\text{Pl}}^2 \dot{H}_{\text{sr}} \text{Re} \left[i \int_{t_*}^{\infty} dt_1 a^3 \frac{8m^2}{E^2} \kappa(t_1) \dot{u}_k^2(t_1) \right], \quad (3.47)$$

which takes a similar form as $\mathcal{C}_{\delta H}$. Since the leading contribution in the t_1 -integral arises from $t_1 \sim t_k$, we can further rewrite $\mathcal{C}_{\text{conv}2}$ in the following way:

$$\begin{aligned} \mathcal{C}_{\text{conv}2} &\simeq -2M_{\text{Pl}}^2 \dot{H}_{\text{sr}} \text{Re} \left[i \int_{t_*}^{\infty} dt_1 a^3 \frac{4m^2}{E^2} \kappa(t_1) \left(\dot{u}_k^2(t_1) - \frac{(\partial_i u_k)^2}{a^2} \right) \right] \\ &\simeq -2 \text{Re} \left[i \int_{t_*}^{\infty} dt_1 a^3 (2M_{\text{Pl}}^2 \dot{H}_{\text{sr}} \kappa(t_1)) \left(\dot{u}_k^2(t_1) - \frac{(\partial_i u_k)^2}{a^2} \right) \right], \end{aligned} \quad (3.48)$$

where we used the relation $\dot{u}_k^2 = -\frac{(\partial_i u_k)^2}{a^2}$ in the heavy mass limit and the relation $E^2(t_k) = 2m^2$. Surprisingly, we obtained the relation $\mathcal{C}_{\text{conv}2} = -\mathcal{C}_{\delta H}$ in the heavy mass limit, which suggests that the resonance effects from the Hubble deformation and the conversion interaction cancel each other out.

To summarize, at the scale $k \gtrsim \mu k_*$, the leading contribution from the conversion interaction arises from $t \sim t_k$ and resonance effects are induced. In particular, it is suggested that the resonance in $\mathcal{C}_{\delta H}$ and $\mathcal{C}_{\text{conv}}$ cancels each other out in the heavy mass limit. In the next subsection, we confirm this cancellation by numerical calculations. At the end of this section, it is also discussed from the effective interaction perspective that this kind of cancellation generically occurs in a wider class of models with heavy field oscillations.

3.3 Total power spectrum

Now we combine the results in the previous two subsections and evaluate the total deviation factor $\mathcal{C} = \mathcal{C}_{\delta H} + \mathcal{C}_{\text{conv}}$. As depicted in Fig. 6, we can observe the resonance cancellation discussed in the previous subsection and no resonance appears in the power spectrum after taking into account both of the Hubble deformation effects and the conversion effects appropriately. An important consequence of this cancellation is that the peak at the turning scale becomes clearer and the analytic expression (3.40) describing the peak around the turning scale becomes

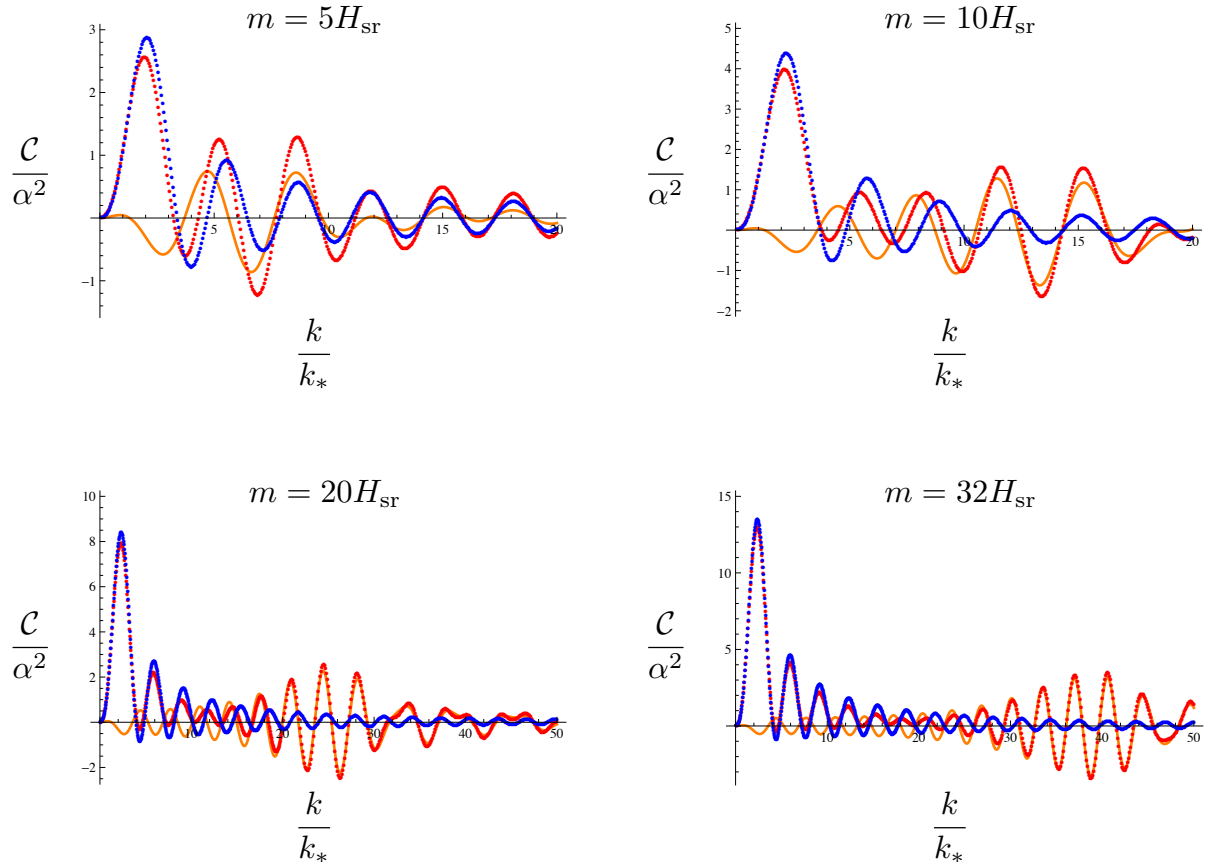


Figure 6: Total deviation factor \mathcal{C} . The blue/red dots are numerical results for $\mathcal{C}/\mathcal{C}_{\text{conv}}$. The orange curve is the analytic result for $-\mathcal{C}_{\delta H}$. It is observed that the resonances in $\mathcal{C}_{\text{conv}}$ and $-\mathcal{C}_{\delta H}$ well coincide in the heavy mass region so that these resonance effects disappear in the total deviation factor \mathcal{C} .

applicable to the total deviation factor \mathcal{C} in the whole scale:¹⁰

$$\mathcal{C} \simeq \mu \alpha^2 \frac{(\sin x_* - x_* \cos x_*)^2}{x_*^3}. \quad (3.49)$$

As shown in Fig. 7, this analytic expression provides a good approximation.

¹⁰ Interestingly, our analytic expression (3.49) for the total deviation factor \mathcal{C} exactly coincides with the sudden turning limit of \mathcal{F}_h in [17], where the power spectra in a wider class of models with turning potentials were investigated via the potential basis. Our deviation factor \mathcal{C} corresponds to $\Delta\mathcal{P}/\mathcal{P}_0 = \mathcal{F}_l + \mathcal{F}_h + \mathcal{F}_{lh}$ there and the sudden turning limit is realized by $\mu \rightarrow \infty$ in their language. As we have mentioned in the introduction and footnote 7 in Sec. 2.3.2, the calculation in the potential basis suffers from spurious singularities. Correspondingly, \mathcal{F}_l and \mathcal{F}_{lh} diverges in the limit $\mu \rightarrow \infty$. Based on our results, we expect that \mathcal{F}_l and \mathcal{F}_{lh} will cancel each other out and the total deviation factor there will reduce to the form $\Delta\mathcal{P}/\mathcal{P}_0 = \mathcal{F}_h$ in the sudden turning limit.

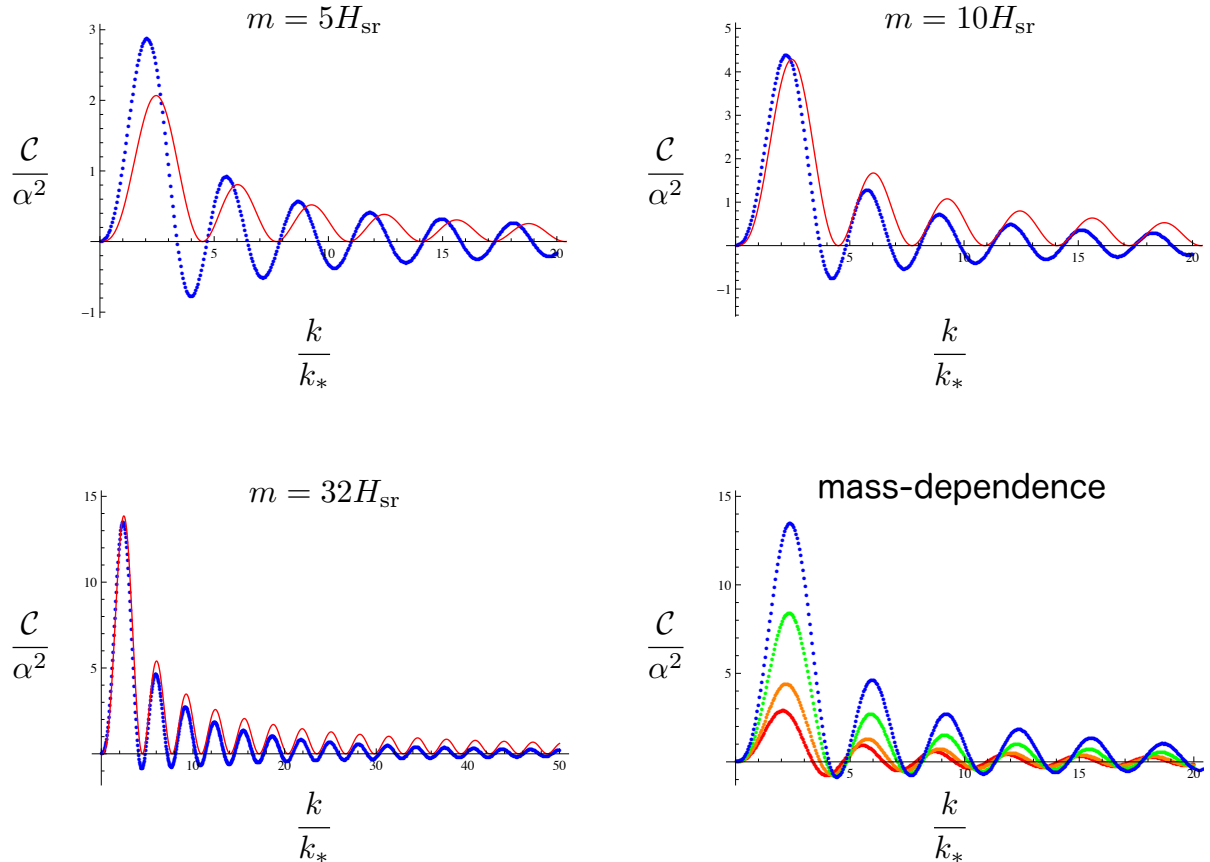


Figure 7: Heavy mass approximation for the total deviation factor \mathcal{C} (upper figures and lower left figure). The analytic expression (3.49) denoted by the red curve provides a good approximation for the full total deviation factor \mathcal{C} (blue dots). As is suggested from the expression (3.49), the shape of \mathcal{C} does not depend on the mass m up to a normalization factor proportional to $\mu\alpha^2$ (lower right figure; the red/orange/green/blue dots are numerical results of \mathcal{C} for $m = 5H_{\text{sr}}/10H_{\text{sr}}/20H_{\text{sr}}/32H_{\text{sr}}$).

3.4 On resonance cancellation for more general settings

In this section we have discussed the effects of sudden turning potentials on the primordial power spectrum. In particular, we found a non-trivial resonance cancellation between the Hubble deformation effects and the conversion effects. Before closing this section, we would like to point out that this kind of resonance cancellation generically occurs in more general two field models with canonical kinetic terms.

With this class of models in mind, let us first consider the following action:

$$S = \int d^4x a^3 \left[-M_{\text{Pl}}^2 \dot{H} \left(\dot{\pi}^2 - \frac{(\partial_i \pi)^2}{a^2} \right) + \frac{1}{2} \left(\dot{\sigma}^2 - \frac{(\partial_i \sigma)^2}{a^2} - m^2 \sigma^2 \right) - 2\beta_1 \dot{\pi} \sigma \right], \quad (3.50)$$

where π and σ correspond to the Goldstone boson and the massive isocurvature perturbation

in the kinetic basis, respectively. Suppose that the Hubble parameter can be decomposed into the slow-roll part H_{sr} and the oscillating part δH ,

$$H = H_{\text{sr}} + \delta H, \quad (3.51)$$

and H_{sr} satisfies the slow-roll conditions $\epsilon_{\text{sr}} = -\dot{H}_{\text{sr}}/H_{\text{sr}}^2 \ll 1$ and $\eta_{\text{sr}} = \dot{\epsilon}_{\text{sr}}/(H_{\text{sr}}\epsilon_{\text{sr}}) \ll 1$. We also assume that δH can be treated as perturbations: $\kappa = \frac{\delta \dot{H}}{H_{\text{sr}}} \ll 1$. As discussed in Sec. 3.1.1, when κ oscillates with a high frequency $2\omega \gg H_{\text{sr}}$, the mode k experiences the parametric resonance around the time t_k determined by $\frac{k}{a(t_k)} = \omega$ due to the Hubble deformations.

We then consider the conversion effects. Suppose that the coupling β_1 oscillates with a high frequency $\tilde{\omega} \gg H_{\text{sr}}$ and the mass m of σ is also heavy $m \gg H_{\text{sr}}$. In this setting, we would like to integrate out the heavy field σ and to construct the effective action for π . In general, when the time-dependence of $\beta_1 \dot{\pi}$ is comparable to the mass of σ , it is not possible to integrate out σ in a simple manner and it is required to consider its full dynamics. As discussed in Sec. 3.2.2, however, the time-dependence of $\beta_1 \dot{\pi}$ becomes negligible when $\frac{k}{a} \sim \tilde{\omega}$. In such a case, σ can be integrated out and the conversion effects around the time $t = \tilde{t}_k$ defined by $\frac{k}{a(\tilde{t}_k)} = \tilde{\omega}$ can be simplified in the following way (see e.g. [22] for a detailed discussion):

$$\begin{aligned} & \int d^4x a^3 \left[\frac{1}{2} \left(\dot{\sigma}^2 - \frac{(\partial_i \sigma)^2}{a^2} - m^2 \sigma^2 \right) - 2\beta_1 \dot{\pi} \sigma \right] \\ & \simeq \int dt \frac{d^3k}{(2\pi)^3} a^3 \left[-\frac{1}{2} \left(\frac{k^2}{a^2} + m^2 \right) \sigma^2 - 2\beta_1 \dot{\pi} \sigma \right] \\ & = \int dt \frac{d^3k}{(2\pi)^3} a^3 \left[-\frac{m^2 + \tilde{\omega}^2}{2} (\sigma + \beta_1 \dot{\pi})^2 + \frac{2\beta_1^2}{m^2 + \tilde{\omega}^2} \dot{\pi}^2 \right] \rightarrow \int d^4x a^3 \frac{2\beta_1^2}{m^2 + \tilde{\omega}^2} \dot{\pi}^2, \end{aligned} \quad (3.52)$$

where we used $\frac{\omega}{a(t_k)} = \tilde{\omega}$ and σ was integrated out at the last arrow. Then, the dynamics of π at $t \sim \tilde{t}_k$ can be described by the effective action

$$S_{\text{eff}} = \int d^4x a^3 \left[-M_{\text{Pl}}^2 \dot{H} \left(\dot{\pi}^2 - \frac{(\partial_i \pi)^2}{a^2} \right) + \frac{2\beta_1^2}{m^2 + \tilde{\omega}^2} \dot{\pi}^2 \right]. \quad (3.53)$$

Here notice that the time t_k of resonances from Hubble deformations and the time \tilde{t}_k of those from conversion interactions coincide if and only if $\omega = \tilde{\omega}$.

Finally, let us apply the above discussions to two-field models with canonical kinetic terms. Suppose that a heavy field ϕ_{\perp} starts oscillating at some time $t = t_*$ and the action for $t > t_*$ is given by

$$S = \int d^4x \sqrt{-g} \left[\frac{1}{2} M_{\text{Pl}}^2 R - \sum_{i=\parallel, \perp} \frac{1}{2} \partial_{\mu} \phi_i \partial^{\mu} \phi_i - V_{\text{sr}}(\phi_{\parallel}) - V_{\perp}(\phi_{\perp}) \right]. \quad (3.54)$$

Here V_{sr} is a slow-roll potential and ϕ_{\perp} is defined such that the massive potential V_{\perp} takes its minimum value at $\phi_{\perp} = 0$. Let us define the deviations φ_i of the background trajectory from the single field slow-roll model as

$$\bar{\phi}_{\parallel}(t) = \bar{\phi}_{\text{sr}}(t) + \varphi_1, \quad \bar{\phi}_{\perp}(t) = \varphi_2. \quad (3.55)$$

Then, applying our general discussions in Sec. 2, the action for the Goldstone boson in the kinetic basis is given by (3.50) with the parameters

$$\kappa = 2 \frac{\dot{\varphi}_1}{\dot{\phi}_{\text{sr}}} + \left(\frac{\dot{\varphi}_2}{\dot{\phi}_{\text{sr}}} \right)^2, \quad \beta_1 = \ddot{\varphi}_2. \quad (3.56)$$

Since the typical time-dependence of φ_1 is of order H_{sr} , φ_1 is irrelevant to the resonance effects. We therefore concentrate on the effects of φ_2 and introduce the frequency ω characterizing the highly oscillating background φ_2 as $\varphi_2 = \alpha \sin(\omega t + \theta)$, where the time-dependence of the normalization factor α and the phase factor θ is negligible compared to ω . Notice that the couplings κ and β_1 oscillate with the frequency 2ω and ω , respectively, so that the resonance effects from the Hubble deformation and the conversion effect appear at the same time. The effective action (3.53) for π at $t \sim t_k$ can be then written as

$$\begin{aligned} S_{\text{eff}} &= \int d^4x a^3 \left[-M_{\text{Pl}}^2 \dot{H}_{\text{sr}} \left(\dot{\pi}^2 - \frac{(\partial_i \pi)^2}{a^2} \right) + \frac{1}{2} \dot{\varphi}_2^2 \left(\dot{\pi}^2 - \frac{(\partial_i \pi)^2}{a^2} \right) + \frac{\ddot{\varphi}_2^2}{m^2 + \omega^2} \dot{\pi}^2 \right] \\ &= \int d^4x a^3 \left[-M_{\text{Pl}}^2 \dot{H}_{\text{sr}} \left(\dot{\pi}^2 - \frac{(\partial_i \pi)^2}{a^2} \right) \right. \\ &\quad \left. + \frac{\alpha^2 \omega^2}{2} \cos^2(\omega t + \theta) \left(\dot{\pi}^2 - \frac{(\partial_i \pi)^2}{a^2} \right) + \frac{\alpha^2 \omega^4}{m^2 + \omega^2} \sin^2(\omega t + \theta) \dot{\pi}^2 \right]. \quad (3.57) \end{aligned}$$

As discussed in Sec. 3.2.2, the $\frac{(\partial_i \pi)^2}{a^2}$ interaction gives the same contribution as $-\dot{\pi}^2$ when $\frac{k}{a} \gg H_{\text{sr}}$. Then, the interaction terms in (3.57) can be written effectively as

$$\dot{\varphi}_2^2 \dot{\pi}^2 + \frac{2\ddot{\varphi}_2^2}{m^2 + \omega^2} \dot{\pi}^2 = \alpha^2 \omega^2 \left(\cos^2(\omega t + \theta) + \frac{2\omega^2}{m^2 + \omega^2} \sin^2(\omega t + \theta) \right) \dot{\pi}^2. \quad (3.58)$$

In particular, when the mass of the heavy isocurvature σ coincides with the frequency of the highly oscillating background φ_2 , $m = \omega$, the oscillating features of the two interactions in the action cancel each other out, which causes no resonance in the power spectrum:

$$\dot{\varphi}_2^2 \dot{\pi}^2 + \frac{2\ddot{\varphi}_2^2}{m^2 + \omega^2} \dot{\pi}^2 = \alpha^2 m^2 \dot{\pi}^2. \quad (3.59)$$

Note that the condition $m = \omega$ is always satisfied at the leading order in φ_i 's in the models described by the action (3.54). We then conclude that no resonance appears in the power

spectrum so that the important signature of this class of models is the peak at the turning scale, whose analytic expression in the heavy mass approximation can be obtained straightforwardly by extending the discussion in Sec. 3.2.1.

4 Primordial bispectrum

Let us next calculate the primordial bispectrum induced by the sudden turning potentials. Using the relation $\zeta = -H\pi$ at the linear order, three-point functions of scalar perturbations ζ can be obtained as

$$\langle \zeta_{\mathbf{k}_1} \zeta_{\mathbf{k}_2} \zeta_{\mathbf{k}_3} \rangle = -H^3 \langle \pi_{\mathbf{k}_1} \pi_{\mathbf{k}_2} \pi_{\mathbf{k}_3} \rangle. \quad (4.1)$$

We define $\mathcal{B}_\zeta(k_1, k_2, k_3)$ and $\mathcal{B}_\pi(k_1, k_2, k_3)$ by the three point functions without the delta function factor:

$$\langle \zeta_{\mathbf{k}_1} \zeta_{\mathbf{k}_2} \zeta_{\mathbf{k}_3} \rangle = (2\pi)^3 \delta^{(3)}(\mathbf{k}_1 + \mathbf{k}_2 + \mathbf{k}_3) \mathcal{B}_\zeta(k_1, k_2, k_3), \quad (4.2)$$

$$\langle \pi_{\mathbf{k}_1} \pi_{\mathbf{k}_2} \pi_{\mathbf{k}_3} \rangle = (2\pi)^3 \delta^{(3)}(\mathbf{k}_1 + \mathbf{k}_2 + \mathbf{k}_3) \mathcal{B}_\pi(k_1, k_2, k_3). \quad (4.3)$$

It is also convenient to introduce the conventional shape function S and f_{NL} parameter:

$$S(k_1, k_2, k_3) = \frac{k_1^2 k_2^2 k_3^2}{(2\pi)^4 \mathcal{P}_\zeta^2} \mathcal{B}_\zeta(k_1, k_2, k_3), \quad (4.4)$$

$$f_{NL}(k_1, k_2, k_3) = \frac{10}{3} \frac{k_1^3 k_2^3 k_3^3}{\sum_i k_i^3} \frac{1}{(2\pi)^4 \mathcal{P}_\zeta^2} \mathcal{B}_\zeta(k_1, k_2, k_3) = \frac{10}{3} \frac{k_1 k_2 k_3}{\sum_i k_i^3} S(k_1, k_2, k_3), \quad (4.5)$$

where \mathcal{P}_ζ is given at the leading order in slow-roll parameters as

$$\mathcal{P}_\zeta = \frac{1}{(2\pi)^2} \frac{H_{\text{sr}}^2}{2M_{\text{Pl}}^2 \epsilon_{\text{sr}}}. \quad (4.6)$$

Using this expression, $S(k_1, k_2, k_3)$ and $f_{NL}(k_1, k_2, k_3)$ can be related to $\mathcal{B}_\pi(k_1, k_2, k_3)$ as

$$S(k_1, k_2, k_3) = -\frac{4M_{\text{Pl}}^4 \epsilon_{\text{sr}}^2}{H_{\text{sr}}} k_1^2 k_2^2 k_3^2 \mathcal{B}_\pi(k_1, k_2, k_3), \quad (4.7)$$

$$f_{NL}(k_1, k_2, k_3) = -\frac{10}{3} \frac{4M_{\text{Pl}}^4 \epsilon_{\text{sr}}^2}{H_{\text{sr}}} \frac{k_1^3 k_2^3 k_3^3}{\sum_i k_i^3} \mathcal{B}_\pi(k_1, k_2, k_3) = \frac{10}{3} \frac{k_1 k_2 k_3}{\sum_i k_i^3} S(k_1, k_2, k_3). \quad (4.8)$$

Let us then calculate the three point functions $\mathcal{B}_\pi(k_1, k_2, k_3)$ of π using the in-in formalism. As we introduced earlier, the interaction Hamiltonian of our model takes the form

$$H_{\text{int}}^{(2)} = \int d^3x a^3 \left[\theta(t - t_*) M_{\text{Pl}}^2 \dot{H}_{\text{sr}} \kappa \left(\dot{\pi}^2 - \frac{(\partial_i \pi)^2}{a^2} \right) + 2\beta_1 \dot{\pi} \sigma \right], \quad (4.9)$$

$$H_{\text{int}}^{(3)} = \int d^3x a^3 \left[\theta(t - t_*) M_{\text{Pl}}^2 \dot{H}_{\text{sr}} \kappa \dot{\pi} \left(\dot{\pi}^2 - \frac{(\partial_i \pi)^2}{a^2} \right) + \beta_1 \left(\dot{\pi}^2 - \frac{(\partial_i \pi)^2}{a^2} \right) \sigma + 2\dot{\beta}_1 \pi \dot{\pi} \sigma + \theta(t - t_*) \frac{\lambda \varphi_2}{6} \sigma^3 \right]. \quad (4.10)$$

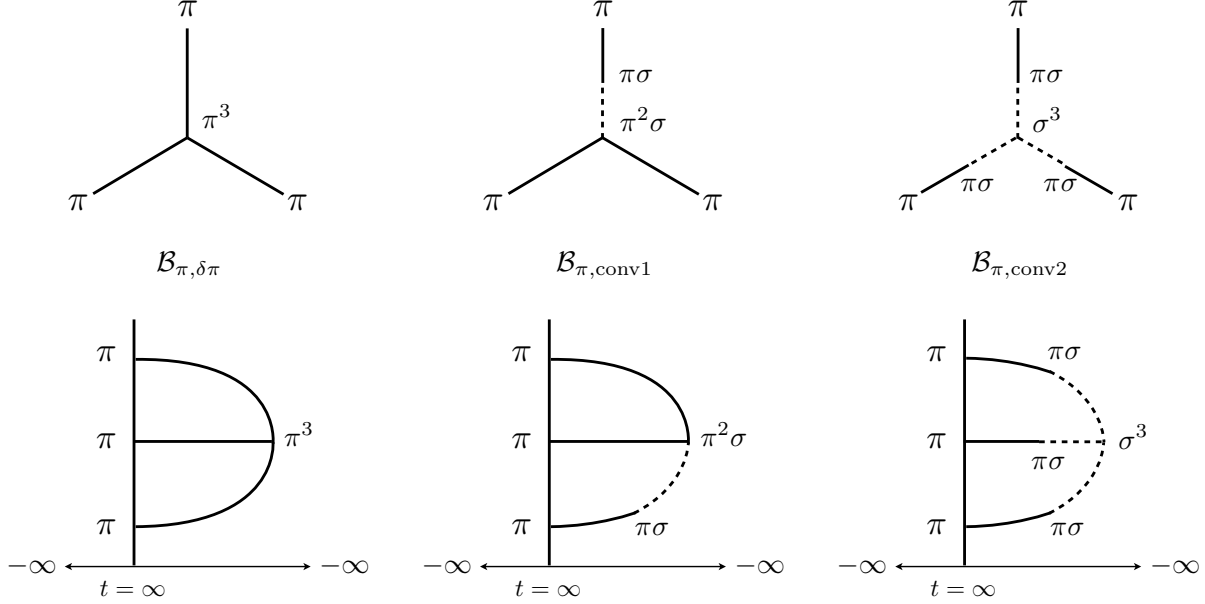


Figure 8: Diagrams for the three-point functions of π are classified into $\mathcal{B}_{\pi, \delta H}$, $\mathcal{B}_{\pi, \delta H}$, and $\mathcal{B}_{\pi, \delta H}$ with respect to the number of conversion interactions (upper figures). Examples of corresponding diagrams for the in-in calculations are given in lower figures.

Corresponding to three types of diagrams depicted in Fig 8, $\mathcal{B}_\pi(k_1, k_2, k_3)$ contains three types of contributions:

$$\mathcal{B}_\pi(k_1, k_2, k_3) = \mathcal{B}_{\pi, \delta H}(k_1, k_2, k_3) + \mathcal{B}_{\pi, \text{conv1}}(k_1, k_2, k_3) + \mathcal{B}_{\pi, \text{conv2}}(k_1, k_2, k_3). \quad (4.11)$$

The first contribution $\mathcal{B}_{\pi, \delta H}(k_1, k_2, k_3)$ originates from the first term in the cubic interaction (4.10) and describes the Hubble deformation effects. It can be expressed in terms of the mode functions and couplings as

$$\mathcal{B}_{\pi, \delta H}(k_1, k_2, k_3) = \frac{1}{2M_{\text{Pl}}^3 \epsilon_{\text{sr}}^{3/2} (k_1 k_2 k_3)^{3/2}} \text{Re} \left[-i \int_{t_*}^{\infty} dt a^3 M_{\text{Pl}}^2 \dot{H}_{\text{sr}} \kappa u_{k_3}^* \left(\dot{u}_{k_1}^* \dot{u}_{k_2}^* + \frac{\mathbf{k}_1 \cdot \mathbf{k}_2}{a^2} u_{k_1}^* u_{k_2}^* \right) \right] + (2 \text{ permutations}). \quad (4.12)$$

The second and the third contributions, $\mathcal{B}_{\pi, \text{conv1}}(k_1, k_2, k_3)$ and $\mathcal{B}_{\pi, \text{conv2}}(k_1, k_2, k_3)$, describe the conversion effects. They originate from the second and third terms and the last term in (4.10), respectively. In terms of the mode functions and couplings, they can be written as

$$\mathcal{B}_{\pi, \text{conv1}}(k_1, k_2, k_3) = \frac{1}{4M_{\text{Pl}}^3 \epsilon_{\text{sr}}^{3/2} (k_1 k_2 k_3)^{3/2}} \text{Re} \left[-i \int_{-\infty}^{\infty} dt a^3 \left\{ 2\beta_1 \left(\dot{u}_{k_1}^* \dot{u}_{k_2}^* + \frac{\mathbf{k}_1 \cdot \mathbf{k}_2}{a^2} u_{k_1}^* u_{k_2}^* \right) \mathcal{F}_3(t) + 2\dot{\beta}_1 (u_{k_1}^* \dot{u}_{k_2}^* + \dot{u}_{k_1}^* u_{k_2}^*) \mathcal{F}_3(t) \right\} \right] + (2 \text{ permutations}), \quad (4.13)$$

$$\mathcal{B}_{\pi, \text{conv}2}(k_1, k_2, k_3) = \frac{1}{4M_{\text{Pl}}^3 \epsilon_{\text{sr}}^{3/2} (k_1 k_2 k_3)^{3/2}} \text{Re} \left[-i \int_{-\infty}^{\infty} dt \theta(t - t_*) a^3 \lambda \varphi_2 \mathcal{F}_1(t) \mathcal{F}_2(t) \mathcal{F}_3(t) \right], \quad (4.14)$$

where $\mathcal{F}_i(t)$ is a deformed propagator defined by

$$\begin{aligned} \mathcal{F}_i(t) = & -iv_{k_i}^*(t) \int_t^{\infty} dt' a^3 2\beta_1 \dot{u}_{k_i}^* v_{k_i}(t') - iv_{k_i}(t) \int_{t_*}^t dt' a^3 2\beta_1 \dot{u}_{k_i}^* v_{k_i}^*(t') \\ & + iv_{k_i}^*(t) \int_{t_*}^{\infty} dt' a^3 2\beta_1 \dot{u}_{k_i} v_{k_i}(t'). \end{aligned} \quad (4.15)$$

In the rest of this section, we calculate each contribution and evaluate non-Gaussianities for our models.

4.1 Hubble deformation effects

Let us start from the Hubble deformation effects $\mathcal{B}_{\pi, \delta H}$:

$$\begin{aligned} \mathcal{B}_{\pi, \delta H}(k_1, k_2, k_3) = & -\frac{H_{\text{sr}}}{16M_{\text{Pl}}^4 \epsilon_{\text{sr}}^2} \frac{k_t^3}{k_1^3 k_2^3 k_3^3} \\ & \times \text{Im} \left[\int_0^{x_*} dx \frac{\dot{\kappa}}{H_{\text{sr}}} (1 + ix_3) \left(\frac{x_1^2 x_2^2}{x^4} + \frac{\mathbf{k}_1 \cdot \mathbf{k}_2}{k_t^2} \frac{(1 + ix_1)(1 + ix_2)}{x^2} \right) e^{-ix} \right] \\ & + (2 \text{ permutations}), \end{aligned} \quad (4.16)$$

where $k_t = k_1 + k_2 + k_3$, $x_i = -k_i \tau$, $x = -k_t \tau$, and $x_* = k_t/k_*$. The corresponding shape function $S_{\delta H}$ is also given by

$$\begin{aligned} S_{\delta H}(k_1, k_2, k_3) = & \frac{1}{4} \frac{k_t^3}{k_1 k_2 k_3} \text{Im} \left[\int_0^{x_*} dx \frac{\dot{\kappa}}{H_{\text{sr}}} (1 + ix_3) \left(\frac{x_1^2 x_2^2}{x^4} + \frac{\mathbf{k}_1 \cdot \mathbf{k}_2}{k_t^2} \frac{(1 + ix_1)(1 + ix_2)}{x^2} \right) e^{-ix} \right] \\ & + (2 \text{ permutations}). \end{aligned} \quad (4.17)$$

After some algebraic calculations, the following expression of $S_{\delta H}$ can be obtained:

$$\begin{aligned} S_{\delta H}(k_1, k_2, k_3) = & \frac{1}{4} \frac{k_t^3}{k_1 k_2 k_3} \text{Im} \left[\int_0^{x_*} dx \frac{\dot{\kappa}}{H_{\text{sr}}} \left(\frac{i}{2} \alpha_1 \alpha_2 \alpha_3 x + \left(\frac{1}{2} \sum_{i>j} \alpha_i \alpha_j - 2\alpha_1 \alpha_2 \alpha_3 \right) \right. \right. \\ & \left. \left. - \frac{i}{2} \sum_i \alpha_i^2 x^{-1} - \frac{1}{2} \sum_i \alpha_i^2 x^{-2} \right) e^{-ix} \right] \\ = & \frac{1}{8} \text{Im} \left[\int_0^{x_*} dx \frac{\dot{\kappa}}{H_{\text{sr}}} \left(ix + \left(\sum_{i>j} \frac{\alpha_i \alpha_j}{\alpha_1 \alpha_2 \alpha_3} - 4 \right) - \frac{\sum_i \alpha_i^2}{\alpha_1 \alpha_2 \alpha_3} (ix^{-1} + x^{-2}) \right) e^{-ix} \right], \end{aligned} \quad (4.18)$$

where $\alpha_i = k_i/k_t$. This integral reduces to the following integral $\tilde{I}(n, \mu, x_*)$ defined by

$$\tilde{I}(n, \mu, x_*) = \int_0^{x_*} dx \frac{\dot{\kappa}}{H_{\text{sr}}} x^n e^{-ix}, \quad (4.19)$$

whose analytic expression can be obtained using the function $\mathcal{I}(\delta, n, x)$ in (3.12) as

$$\tilde{I}(n, \mu, x_*) = \alpha^2 \left[\left(\frac{3}{2} - \frac{27}{8\mu^2} \right) \mathcal{I}(0, n, x_*) + \frac{(3 + 2i\mu)^3}{16\mu^2} \mathcal{I}(2i\mu, n, x_*) + \frac{(3 - 2i\mu)^3}{16\mu^2} \mathcal{I}(-2i\mu, n, x_*) \right]. \quad (4.20)$$

In terms of $\tilde{I}(n; \mu; x_*)$, the shape function $S_{\delta H}(k_1, k_2, k_3)$ is then given by

$$S_{\delta H}(k_1, k_2, k_3) = \frac{1}{8} \text{Im} \left[i \tilde{I}(1, \mu, x_*) + \left(\sum_{i>j} \frac{\alpha_i \alpha_j}{\alpha_1 \alpha_2 \alpha_3} - 4 \right) \tilde{I}(0, \mu, x_*) \right. \\ \left. - \sum_i \frac{\alpha_i^2}{\alpha_1 \alpha_2 \alpha_3} \left(i \tilde{I}(-1, \mu, x_*) + \tilde{I}(-2, \mu, x_*) \right) \right]. \quad (4.21)$$

From this expression, we first notice that there are no contributions of $\mathcal{O}(\mathcal{P}_\zeta^{-1/2})$ and higher order so that large non-Gaussianities do not arise from the Hubble deformation effects unless $\tilde{\mathcal{I}}$ is large. Also notice that the shape function depends on α_i only through the coefficients in front of $\tilde{\mathcal{I}}$. In the rest of this subsection, we discuss the scale-dependence and shape of $S_{\delta H}$.

4.1.1 Scale-dependence of equilateral type non-Gaussianities

Let us first discuss the scale-dependence of the shape function $S_{\delta H}$. As is clear from (4.21), the scale-dependence of $S_{\delta H}$ is determined by that of the function \tilde{I} once the shape of momentum configurations is specified. For the equilateral momentum configurations $\alpha_i = 1/3$, for example, we have

$$S_{\delta H}(k_t/3, k_t/3, k_t/3) = \frac{1}{8} \text{Im} \left[i \tilde{I}(1, \mu, x_*) + 5 \tilde{I}(0, \mu, x_*) - 9i \tilde{I}(-1, \mu, x_*) - 9 \tilde{I}(-2, \mu, x_*) \right]. \quad (4.22)$$

As we discuss in Appendix B, the integral $\mathcal{I}(\delta, n, x)$ for $n = 1, 0$, and therefore, $\tilde{I}(\delta, n, x)$ and $S_{\delta H}$ suffer from singular behaviors in the region $x \gg 1$, where the mode is deep inside the horizon. This kind of singular behaviors deep inside the horizon are common in the interacting theory and they are usually eliminated by assuming that the Bunch-Davies vacuum is realized deep inside the horizon. In the bispectrum calculation of this paper, we subtract these singular behaviors based on a similar assumption (see Appendix B). The scale-dependence of $S_{\delta H}$ before and after the subtraction is displayed in Fig. 9, where resonance-like effects can be observed at the scale $k \gtrsim 2\mu k_*$. As discussed in [25], these resonance effects can be understood by noticing

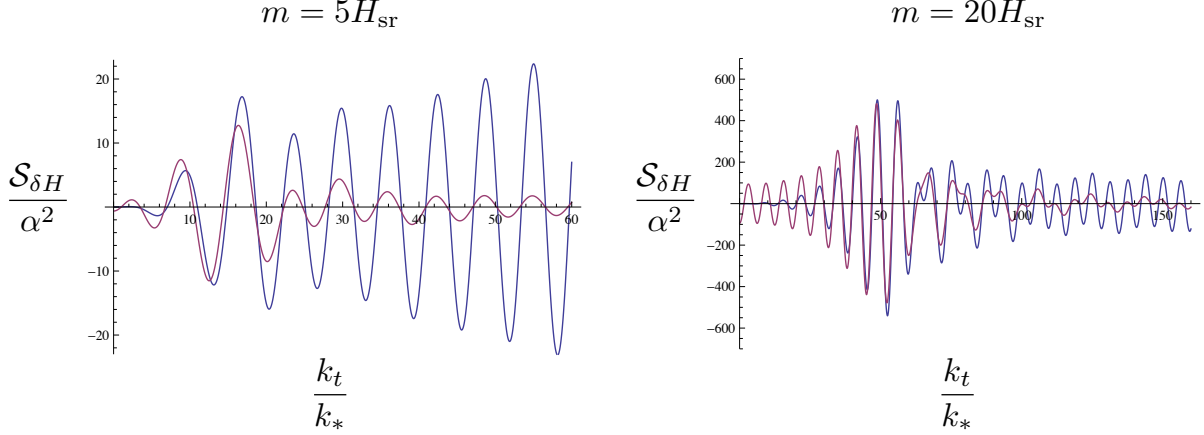


Figure 9: Scale-dependence of $S_{\delta H}$ for the equilateral momentum configurations and singular behaviors deep inside the horizon. The exact results (4.21) for $S_{\delta H}$ (blue curves) oscillate and linearly diverge in the region $k_t \gg k_*$, where the mode k is deep inside the horizon. Based on the assumption that the Bunch-Davies vacuum is realized deep inside the horizon, we eliminate this kind of singular behaviors via the prescription discussed in Appendix B: We interpolate the original function (blue curves) and the regularized function obtained by subtracting singular behaviors (red curves) at the resonance scale $k \simeq \mu k_t$.

that $S_{\delta H}$ contains the same integrals \mathcal{I} as the Hubble deformation effects $\mathcal{C}_{\delta H}$ on power spectra. Using the stationary phase approximation as in Sec. 3.1.1, (4.22) can be estimated in the heavy mass region as

$$|S_{\delta H}(k_t/3, k_t/3, k_t/3)| \simeq \left| \frac{\mu}{16} \alpha^2 \text{Im} [\mathcal{I}(2i\mu, 1, x_*)] \right| \sim \begin{cases} 2\sqrt{\pi} \alpha^2 \mu^{5/2} \left(\frac{k}{\mu k_*} \right)^{-3} & \text{for } x_* \gtrsim 2\mu, \\ 0 & \text{for } x_* \lesssim 2\mu. \end{cases} \quad (4.23)$$

As displayed in Fig. 10, the above estimation well agrees with the exact results. To summarize, resonances in $S_{\delta H}(k_t/3, k_t/3, k_t/3)$ appear at the scale $k_t \gtrsim 2\mu k_*$ and the size is of the order $\alpha^2 \mu^{5/2}$ in the heavy mass approximation.

4.1.2 Shape of $S_{\delta H}$

We next discuss the shape of $S_{\delta H}(k_1, k_2, k_3)$. Although shape functions are scale-invariant $S(k_1, k_2, k_3) = S(\lambda k_1, \lambda k_2, \lambda k_3)$ in inflationary models with scale-invariance, those in our models are not scale-invariant because the sudden turning potentials and associated background oscillations break the scale-invariance. We therefore need to specify both of the shape of momentum configurations and the maximum momentum in order to draw the conventional 3D plot of bispectra. In Fig. 11, we plotted $S_{\delta H}$ around the resonance scale as a function of

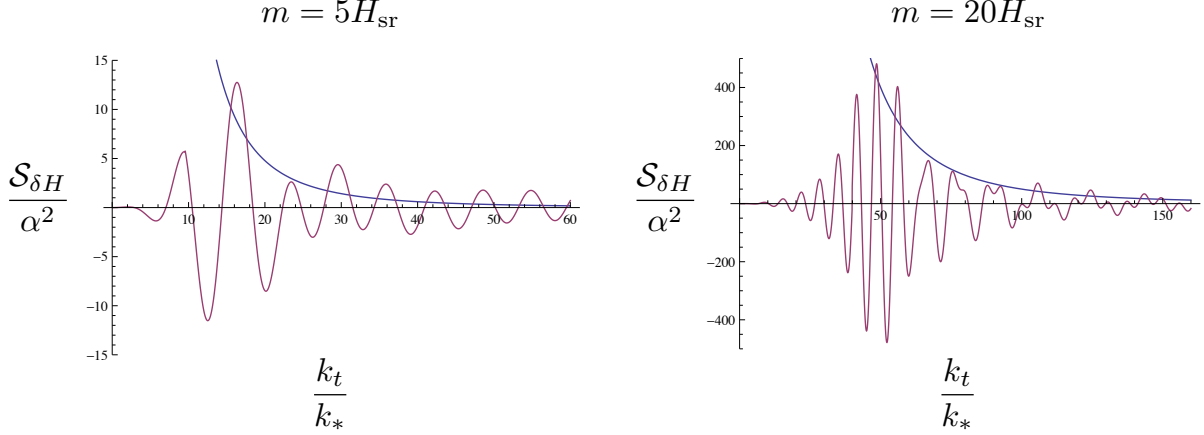


Figure 10: Scale-dependence of $S_{\delta H}$ for the equilateral momentum configurations. The red curve is the exact expression for $S_{\delta H}$ with singular behaviors deep inside the horizon being subtracted. The blue curve is the estimation based on the stationary phase approximation: $S_{\delta H} = 2\sqrt{\pi}\alpha^2\mu^{5/2}(k/(\mu k_*))^{-3}$.

k_2/k_1 and k_3/k_1 , where $k_1 > k_2 > k_3$ and the maximum momentum k_1 is fixed. In this standard 3D plot, the shape function takes a wavy form and it is almost flat along the direction $k_2 + k_3 = \text{constant}$ [25]. We can also find a peak at the squeezed configuration $k_1 = k_2 \gg k_3$. These features can be understood using the analytic expression (4.21) as follows: First, just as discussions in Sec. 4.1.1, the integral \tilde{I} can be estimated via the stationary phase approximation as

$$\tilde{I}(n, \mu, x) \simeq -\frac{i}{2}\alpha^2\mu\mathcal{I}(2i\mu, n, x) \sim 2^{3+n}\sqrt{\pi}\alpha^2\left(\frac{\mu}{x}\right)^3\mu^{n+\frac{3}{2}}. \quad (4.24)$$

Then, the contribution from $\tilde{I}(1, \mu, x)$ dominates in (4.21) unless the prefactors $\sum_{i>j} \frac{\alpha_i\alpha_j}{\alpha_1\alpha_2\alpha_3}$ and/or $\sum_i \frac{\alpha_i^2}{\alpha_1\alpha_2\alpha_3}$ are large. In other words, $\tilde{I}(1, \mu, x)$ dominates unless we take the squeezed limit:

$$S_{\delta H}(k_1, k_2, k_3) \simeq \frac{1}{8}\text{Im}\left[i\tilde{I}(1, \mu, k_t/k_*)\right] \quad \text{for } \alpha_3 \gtrsim \frac{1}{\mu}, \quad (4.25)$$

which depends only on the total momentum $k_t = k_1 + k_2 + k_3$. Because of this property, $S_{\delta H}$ is almost flat along the direction $k_2 + k_3 = \text{constant}$. In the squeezed limit $k_1 = k_2 \gg k_3$, on the other hand, the prefactors $\sum_{i>j} \frac{\alpha_i\alpha_j}{\alpha_1\alpha_2\alpha_3}$ and $\sum_i \frac{\alpha_i^2}{\alpha_1\alpha_2\alpha_3}$ diverge so that a peak appears at the squeezed point. Also notice that the peak becomes sharp for the large mass because $\frac{\tilde{I}(1, \mu, k_t/k_*)}{\tilde{I}(0, \mu, k_t/k_*)} \sim \mu$ and therefore the region in which $\tilde{I}(1, \mu, k_t/k_*)$ dominates becomes wider for larger μ .

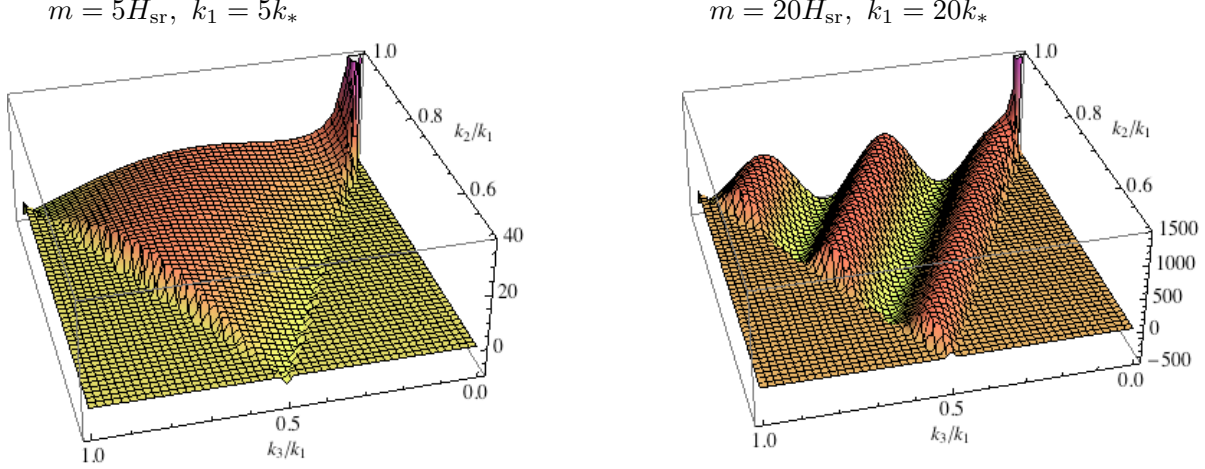


Figure 11: Shape of $S_{\delta H}$ around the resonance scale with fixed maximum momentum. In the left figure, $-S_{\delta H}/\alpha^2$ with $m = 5H_{sr}$ and $k_1 = 5k_*$ is plotted as a function of k_2/k_1 and k_3/k_1 . In the right figure, $S_{\delta H}/\alpha^2$ with $m = 20H_{sr}$ and $k_1 = 20k_*$ is plotted as a function of k_2/k_1 and k_3/k_1 . In this type of conventional 3D plots, $S_{\delta H}$ takes a wavy form and has a peak at the squeezed momentum configuration $k_1 = k_2 \gg k_3$.

In order to make the above properties manifest, it may be convenient to introduce a different type of 3D plots, where the total momentum k_t is fixed instead of the maximum momentum k_1 and the shape function is plotted as a function of $\alpha_2 = k_2/k_t$ and $\alpha_3 = k_3/k_t$. As in the case of the conventional 3D plot, we can take k_i such that $k_1 > k_2 > k_3$ without loss of generality and the momentum conservation implies $k_1 < k_2 + k_3$. In terms of α_2 and α_3 , these conditions can be rephrased as

$$\begin{aligned}
k_1 > k_2 &\leftrightarrow \alpha_1 > \alpha_2 \quad \leftrightarrow \quad 1 > 2\alpha_2 + \alpha_3, \\
k_2 > k_3 &\leftrightarrow \alpha_2 > \alpha_3, \\
k_1 < k_2 + k_3 &\leftrightarrow \alpha_1 < \alpha_2 + \alpha_3 \quad \leftrightarrow \quad \frac{1}{2} < \alpha_2 + \alpha_3,
\end{aligned} \tag{4.26}$$

where we used $\alpha_1 + \alpha_2 + \alpha_3 = 1$. The region satisfying the above three conditions is depicted in Fig. 12 and a close up of this region is given in Fig. 13, where the points corresponding to the squeezed, equilateral, and folded momentum configurations are also described. As described in Fig. 14, in this type of 3D plots, the shape function $S_{\delta H}$ takes a flat form in the region where $\tilde{I}(1, \mu, k_t/k_*)$ dominates and it is clear that the peak at the squeezed configuration becomes sharp for large mass. We will use both types of the 3D plots in the rest of this section.

4.2 Conversion effects

We next consider the conversion effects. After discussing properties of the deformed propagator $\mathcal{F}_i(t)$, shape functions are evaluated.

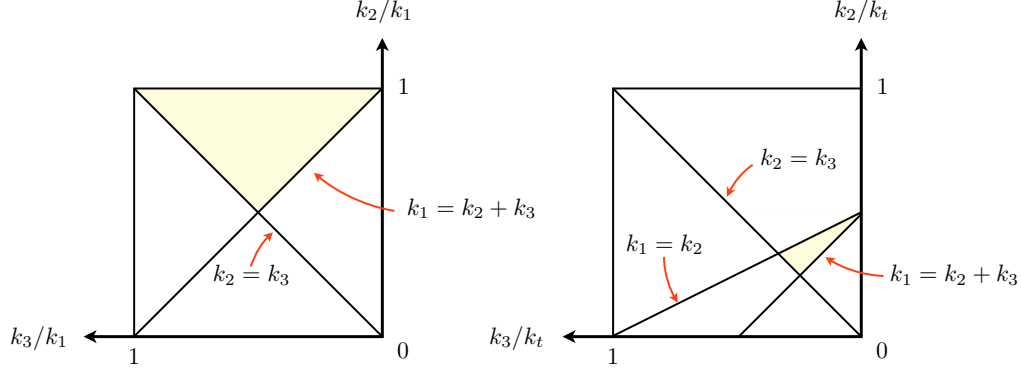


Figure 12: In the conventional 3D plots (the left figure), shape functions are plotted in the region satisfying $1 > k_2/k_1 > k_3/k_1$ and $1 > k_2/k_1 + k_3/k_1$. On the other hand, in the 3D plots with fixed total momenta (the right figure), they are plotted in the region satisfying $k_1/k_t > k_2/k_t > k_3/k_t$ and $k_1/k_t > k_2/k_t + k_3/k_t$, which can be rephrased in terms of α_2 and α_3 as (4.26).

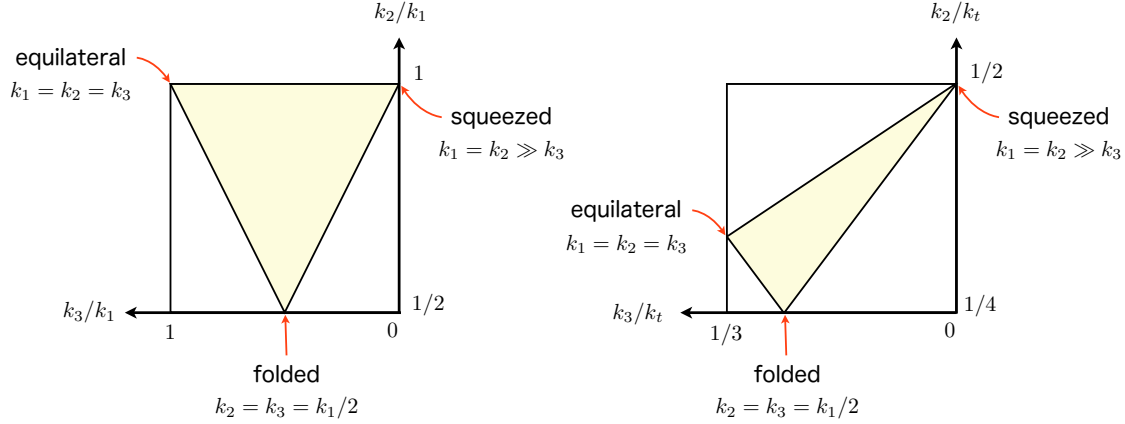


Figure 13: Closeup of Fig. 12 with squeezed/equilateral/folded configurations depicted.

4.2.1 Deformed propagators

Let us first introduce an analytic expression for the deformed propagator $\mathcal{F}_i(t)$:

$$\begin{aligned}
\mathcal{F}_i(t) = \frac{1}{2M_{\text{Pl}}\epsilon_{\text{sr}}^{1/2}k_i^{3/2}} \frac{i\pi e^{-\pi\mu}}{2} & \left[x_i^{3/2} H_{-i\mu}^{(2)}(x_i) \int_0^{x_i} dx'_i \frac{\beta_1}{H_{\text{sr}}} x_i'^{-1/2} e^{-ix'_i} H_{i\mu}^{(1)}(x'_i) \right. \\
& + x_i^{3/2} H_{i\mu}^{(1)}(x_i) \int_{x_i}^{x_i^*} dx'_i \frac{\beta_1}{H_{\text{sr}}} x_i'^{-1/2} e^{-ix'_i} H_{-i\mu}^{(2)}(x'_i) \\
& \left. - x_i^{3/2} H_{-i\mu}^{(2)}(x_i) \int_0^{x_i^*} dx'_i \frac{\beta_1}{H_{\text{sr}}} x_i'^{-1/2} e^{+ix'_i} H_{i\mu}^{(1)}(x'_i) \right], \quad (4.27)
\end{aligned}$$

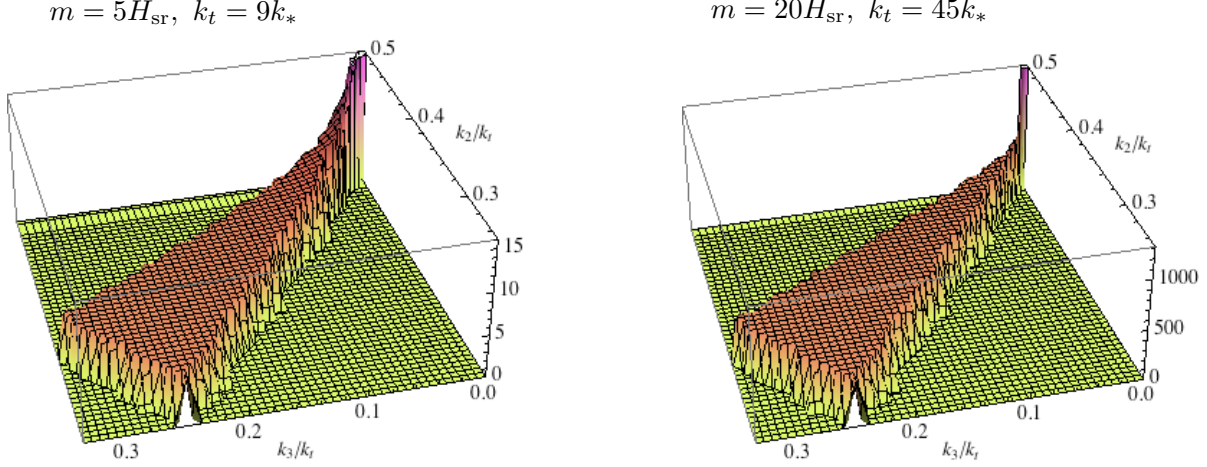


Figure 14: Shape of $S_{\delta H}$ around the resonance scale with fixed total momenta. In the left and right figures, $S_{\delta H}/\alpha^2$ with $m = 5H_{\text{sr}}$ and $-S_{\delta H}/\alpha^2$ with $m = 20H_{\text{sr}}$ are plotted. The total momenta are taken as $k_t = 9k_*$ and $k_t = 45k_*$, respectively. In this type of 3D plots, it is clear that the region where $\tilde{I}(1, \mu, k_t/k_*)$ dominates becomes wide and the peak at the squeezed configurations become sharp for large μ .

where $x_{i*} = \alpha_i x_*$. Using the relation

$$\frac{\beta_1}{H_{\text{sr}}} = \theta(t - t_*) \dot{\phi}_{\text{sr}} \frac{\dot{\gamma}}{H_{\text{sr}}} = \theta(t - t_*) \sqrt{2} \epsilon_{\text{sr}}^{1/2} M_{\text{Pl}} H_{\text{sr}} \frac{\dot{\gamma}}{H_{\text{sr}}}, \quad (4.28)$$

it is rewritten as

$$\begin{aligned} \mathcal{F}_i(t) = \frac{H_{\text{sr}}}{\sqrt{2} k_i^{3/2}} \frac{i\pi e^{-\pi\mu}}{2} \left[x_i^{3/2} H_{-i\mu}^{(2)}(x_i) \int_0^{x_i} dx'_i \frac{\dot{\gamma}}{H_{\text{sr}}} x_i'^{-1/2} e^{-ix'_i} H_{i\mu}^{(1)}(x'_i) \right. \\ \left. + x_i^{3/2} H_{i\mu}^{(1)}(x_i) \int_{x_i}^{x_{i*}} dx'_i \frac{\dot{\gamma}}{H_{\text{sr}}} x_i'^{-1/2} e^{-ix'_i} H_{-i\mu}^{(2)}(x'_i) \right. \\ \left. - x_i^{3/2} H_{-i\mu}^{(2)}(x_i) \int_0^{x_{i*}} dx'_i \frac{\dot{\gamma}}{H_{\text{sr}}} x_i'^{-1/2} e^{+ix'_i} H_{i\mu}^{(1)}(x'_i) \right]. \quad (4.29) \end{aligned}$$

It is useful to introduce the following indefinite integral $\mathcal{D}_-(\ell, \mu, x)$ analogously to $\mathcal{D}_+(\ell, \mu, x)$ in (3.34):

$$\mathcal{D}_-(\ell, \mu, x) = \int dx x^{-\frac{1}{2}+\ell} e^{-ix} H_{i\mu}^{(1)}(x), \quad (4.30)$$

whose analytic expression is given by

$$\begin{aligned} \mathcal{D}_-(\ell, \mu, x) = \frac{2^{i\mu} x^{\frac{1}{2}+\ell-i\mu} \Gamma(i\mu)}{i\pi(\frac{1}{2}+\ell-i\mu)} {}_2F_2\left(\frac{1}{2}-i\mu, \frac{1}{2}+\ell-i\mu; \frac{3}{2}+\ell-i\mu, 1-2i\mu; -2ix\right) \\ + e^{\pi\mu} \frac{2^{-i\mu} x^{\frac{1}{2}+\ell+i\mu} \Gamma(-i\mu)}{i\pi(\frac{1}{2}+\ell+i\mu)} {}_2F_2\left(\frac{1}{2}+i\mu, \frac{1}{2}+\ell+i\mu; \frac{3}{2}+\ell+i\mu, 1+2i\mu; -2ix\right). \quad (4.31) \end{aligned}$$

Then, the deformed propagator \mathcal{F}_i can be written in terms of $\mathcal{D}_\pm(\ell, \mu, x)$ as

$$\mathcal{F}_i(t) = \frac{H_{\text{sr}}}{\sqrt{2}k_i^{3/2}} \tilde{\mathcal{F}}_i(x_i), \quad (4.32)$$

$$\begin{aligned} \tilde{\mathcal{F}}_i(x_i) = & -\alpha \frac{\pi e^{-\pi\mu}}{2} \left[x_i^{3/2} H_{-i\mu}^{(2)}(x_i) \sum_{\pm} (-1)^{\pm} \frac{(\frac{3}{2} \pm i\mu)^2}{2\mu} x_{i*}^{-(\frac{3}{2} \pm i\mu)} \mathcal{D}_- \left(\frac{3}{2} \pm i\mu, \mu, x_i \right) \right. \\ & + x_i^{3/2} H_{i\mu}^{(1)}(x_i) \sum_{\pm} (-1)^{\pm} \frac{(\frac{3}{2} \pm i\mu)^2}{2\mu} x_{i*}^{-(\frac{3}{2} \pm i\mu)} \left(\mathcal{D}_+ \left(\frac{3}{2} \mp i\mu, \mu, x_{i*} \right) - \mathcal{D}_+ \left(\frac{3}{2} \mp i\mu, \mu, x_i \right) \right)^* \\ & \left. - x_i^{3/2} H_{-i\mu}^{(2)}(x_i) \sum_{\pm} (-1)^{\pm} \frac{(\frac{3}{2} \pm i\mu)^2}{2\mu} x_{i*}^{-(\frac{3}{2} \pm i\mu)} \mathcal{D}_+ \left(\frac{3}{2} \pm i\mu, \mu, x_{i*} \right) \right], \end{aligned} \quad (4.33)$$

which reduces the calculation of conversion effects to one integral. In order to clarify qualitative features of the deformed propagators $\mathcal{F}_i(t)$ and $\tilde{\mathcal{F}}_i(x_i)$, let us discuss their behaviors using the heavy mass approximation. In particular, we consider the following two regimes: $\frac{k_i}{a(t)} \sim H_{\text{sr}}$ and $\frac{k_i}{a(t)} \sim m \gg H_{\text{sr}}$, or in other words, $x_i \sim 1$ and $x_i \sim \mu \gg 1$. Here we assume that $t > t_*$, or equally, $x_i < x_{i*}$.

1. $\tilde{\mathcal{F}}_i(x_i)$ in the regime $\frac{k_i}{a(t)} \sim H_{\text{sr}} \leftrightarrow x_i \sim 1$.

In this region, the mode function v_{k_i} of the massive isocurvature can be expressed as

$$v_{k_i} \simeq \frac{H_{\text{sr}}}{\sqrt{2\mu k_*^3}} \left(\frac{x_i}{x_{i*}} \right)^{\frac{3}{2} + i\mu} \quad (4.34)$$

up to a phase factor irrelevant to our discussions. Using this expression, $\tilde{\mathcal{F}}_i$ can be written as

$$\begin{aligned} \tilde{\mathcal{F}}_i(x_i) \simeq & \frac{i}{\mu} \left[x_i^{3/2} \left(\frac{x_i}{x_{i*}} \right)^{-i\mu} \int_0^{x_i} dx'_i \frac{\dot{\gamma}}{H_{\text{sr}}} x_i'^{-1/2} e^{-ix'_i} \left(\frac{x_i}{x_{i*}} \right)^{i\mu} \right. \\ & + x_i^{3/2} \left(\frac{x_i}{x_{i*}} \right)^{i\mu} \int_{x_i}^{x_{i*}} dx'_i \frac{\dot{\gamma}}{H_{\text{sr}}} x_i'^{-1/2} e^{-ix'_i} \left(\frac{x_i}{x_{i*}} \right)^{-i\mu} \\ & \left. - x_i^{3/2} \left(\frac{x_i}{x_{i*}} \right)^{-i\mu} \int_0^{x_{i*}} dx'_i \frac{\dot{\gamma}}{H_{\text{sr}}} x_i'^{-1/2} e^{ix'_i} \left(\frac{x_i}{x_{i*}} \right)^{i\mu} \right]. \end{aligned} \quad (4.35)$$

Just as in the case of power spectra, $\frac{\dot{\gamma}}{H_{\text{sr}}} \left(\frac{x_i}{x_{i*}} \right)^{\pm i\mu}$ contains a non-oscillating component,

$$\frac{\dot{\gamma}}{H_{\text{sr}}} \left(\frac{x_i}{x_{i*}} \right)^{\pm i\mu} \simeq \pm \frac{i}{2} \alpha \mu \left[\left(\frac{x_i}{x_{i*}} \right)^{\frac{3}{2}} - \left(\frac{x_i}{x_{i*}} \right)^{\frac{3}{2} \pm 2i\mu} \right], \quad (4.36)$$

and therefore, the leading contribution to $\tilde{\mathcal{F}}_i$ in the heavy mass approximation is given by

$$\begin{aligned}
\tilde{\mathcal{F}}_i(x_i) &\simeq \frac{\alpha}{2} \left(\frac{x_i}{x_{i*}} \right)^{3/2} \left[- \left(\frac{x_i}{x_{i*}} \right)^{-i\mu} \int_0^{x_i} dx'_i x'_i e^{-ix'_i} \right. \\
&\quad \left. + \left(\frac{x_i}{x_{i*}} \right)^{i\mu} \int_{x_i}^{x_{i*}} dx'_i x'_i e^{-ix'_i} + \left(\frac{x_i}{x_{i*}} \right)^{-i\mu} \int_0^{x_{i*}} dx'_i x'_i e^{ix'_i} \right] \\
&= \frac{\alpha}{2} \left[\left(\frac{x}{x_*} \right)^{\frac{3}{2}+i\mu} \left[(1 + i\alpha_i x_*) e^{-i\alpha_i x_*} - (1 + i\alpha_i x) e^{-i\alpha_i x} \right] \right. \\
&\quad \left. - \left(\frac{x}{x_*} \right)^{\frac{3}{2}-i\mu} \left[(1 - i\alpha_i x_*) e^{i\alpha_i x_*} - (1 + i\alpha_i x) e^{-i\alpha_i x} \right] \right]. \tag{4.37}
\end{aligned}$$

Notice that (4.37) is of the order α and oscillates with a frequency $\sim \mu$. Also note that it is of the order α_i^2 in the limit $\alpha_i = k_i/k_t \rightarrow 0$.

2. $\mathcal{F}_i(t)$ in the regime $\frac{k}{a(t)} \sim m \gg 1 \leftrightarrow \mu \sim x_i \gg 1$.

As we introduced at the beginning of this section, the deformed propagator $\mathcal{F}_i(t)$ is given by

$$\begin{aligned}
\mathcal{F}_i(t) &= -iv_{k_i}^*(t) \int_t^\infty dt' a^3 2\beta_1 \dot{u}_{k_i}^* v_{k_i}(t') - iv_{k_i}(t) \int_{t_*}^t dt' a^3 2\beta_1 \dot{u}_{k_i}^* v_{k_i}^*(t') \\
&\quad + iv_{k_i}^*(t) \int_{t_*}^\infty dt' a^3 2\beta_1 \dot{u}_{k_i} v_{k_i}(t'), \tag{4.38}
\end{aligned}$$

and the phase factor of each integrand takes the form

$$\sim \exp \left[i \left(\pm m \pm E \pm \frac{k}{a} \right) t \right] = \exp \left[i \left(\pm m \pm \sqrt{m^2 + \frac{k^2}{a^2}} \pm \frac{k}{a} \right) t \right]. \tag{4.39}$$

Here $E = \sqrt{m^2 + \frac{k^2}{a^2}}$ and the phase factor always oscillates with a frequency of the order m . Therefore, the integral is suppressed by $1/m$ and $\mathcal{F}_i(t)$ can be roughly order estimated as

$$\mathcal{F}_i(t) \sim \frac{1}{m} a^3 \beta_1 |v_{k_i}|^2 \dot{u}_{k_i}^* \sim \frac{1}{m^2} \beta_1 \dot{u}_{k_i}^*. \tag{4.40}$$

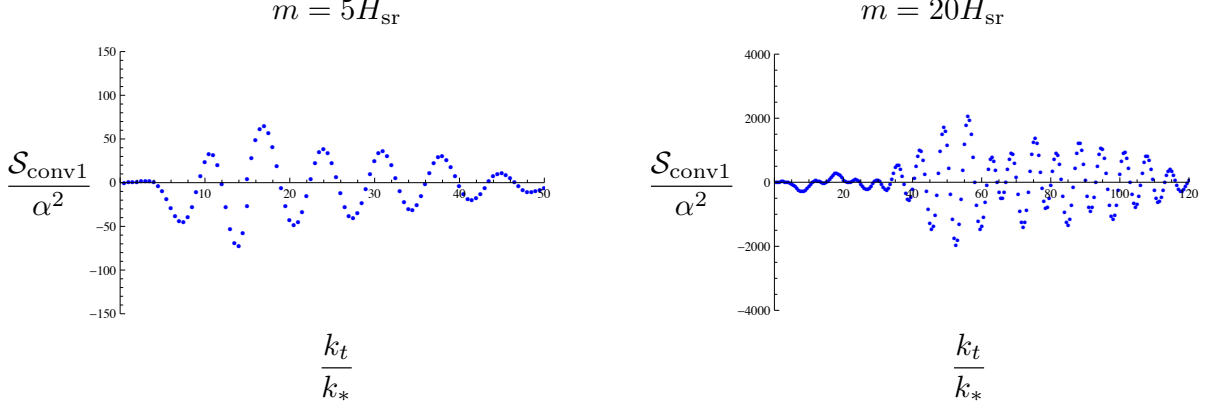


Figure 15: Scale-dependence of S_{conv1} for the equilateral momentum configurations. As in the case of the Hubble deformation effects $S_{\delta H}$, S_{conv1} becomes singular deep inside the horizon. Following the assumption that the Bunch-Davies vacuum is realized deep inside the horizon, we subtracted such singular behaviors and the results after the subtraction are plotted in this figure, where resonances can be observed at the scale $k \gtrsim 2\mu$.

4.2.2 Conversion effect 1

Now we evaluate the shape function $\mathcal{S}_{\text{conv1}}$ for the first type of conversion effects. Using the expressions (2.71) and (2.72) of the mode functions, the three-point function $\mathcal{B}_{\text{conv1}}$ and the corresponding shape function $\mathcal{S}_{\text{conv1}}$ can be written as

$$\begin{aligned}
\mathcal{B}_{\pi,\text{conv1}}(k_1, k_2, k_3) &= \frac{H_{\text{sr}}}{8M_{\text{Pl}}^4 \epsilon_{\text{sr}}^2} \frac{k_t^3}{k_1^3 k_2^3 k_3^3} \\
&\times \text{Im} \left[\int_0^\infty dx \left\{ \theta(x_* - x) \frac{\dot{\gamma}}{H_{\text{sr}}} \left(\frac{x_1^2 x_2^2}{x^4} + \frac{\mathbf{k}_1 \cdot \mathbf{k}_2 (1 + ix_1)(1 + ix_2)}{k_t^2 x^2} \right) \right. \right. \\
&\quad \left. \left. + \left(\theta(x_* - x) \frac{\ddot{\gamma}}{H_{\text{sr}}^2} + \delta(x - x_*) x \frac{\dot{\gamma}}{H_{\text{sr}}} \right) \frac{x_1^2 + x_2^2 + ix_1 x_2 (x_1 + x_2)}{x^4} \right\} \right. \\
&\quad \left. \times e^{-i(x_1 + x_2)} \tilde{\mathcal{F}}_3(x_3) \right] + (2 \text{ permutations}), \quad (4.41)
\end{aligned}$$

$$\begin{aligned}
\mathcal{S}_{\text{conv1}}(k_1, k_2, k_3) &= -\frac{1}{2} \frac{k_t^3}{k_1 k_2 k_3} \\
&\times \text{Im} \left[\int_0^\infty dx \left\{ \theta(x_* - x) \frac{\dot{\gamma}}{H_{\text{sr}}} \left(\frac{x_1^2 x_2^2}{x^4} + \frac{\mathbf{k}_1 \cdot \mathbf{k}_2 (1 + ix_1)(1 + ix_2)}{k_t^2 x^2} \right) \right. \right. \\
&\quad \left. \left. + \left(\theta(x_* - x) \frac{\ddot{\gamma}}{H_{\text{sr}}^2} + \delta(x - x_*) x \frac{\dot{\gamma}}{H_{\text{sr}}} \right) \frac{x_1^2 + x_2^2 + ix_1 x_2 (x_1 + x_2)}{x^4} \right\} \right. \\
&\quad \left. \times e^{-i(x_1 + x_2)} \tilde{\mathcal{F}}_3(x_3) \right] + (2 \text{ permutations}). \quad (4.42)
\end{aligned}$$

From this expression, we can see that there are no contributions of $\mathcal{O}(\mathcal{P}_\zeta^{-1/2})$ and higher order so that large non-Gaussianities do not arise unless the above integral is large. Using the analytic expression (4.33), the calculation of S_{conv1} reduces to one integration over x . We performed this integral numerically and the scale-dependence of the shape function S_{conv1} for the equilateral momentum configurations are for example given in Fig. 15, where we find resonances around the scale $k_t \gtrsim 2\mu k_*$ similarly to the case of Hubble deformation effects $S_{\delta H}$. Let us then order estimate these resonances by using the heavy mass approximation and comparing with the Hubble deformation effects. As an example, we discuss the following contribution to the bispectrum $\mathcal{B}_{\text{conv1}}$:

$$\mathcal{B}_{\text{conv1}} \ni \frac{1}{4M_{\text{Pl}}^3 \epsilon_{\text{sr}}^{3/2} (k_1 k_2 k_3)^{3/2}} \text{Re} \left[-i \int_{-\infty}^{\infty} dt a^3 2\beta_1 \dot{u}_{k_1}^* \dot{u}_{k_2}^* \mathcal{F}_3(t) \right]. \quad (4.43)$$

Using (4.40), it can be roughly estimated as

$$\begin{aligned} &\sim \frac{1}{2M_{\text{Pl}}^3 \epsilon_{\text{sr}}^{3/2} (k_1 k_2 k_3)^{3/2}} \int_{-\infty}^{\infty} dt a^3 \frac{\beta_1^2}{m^2} \dot{u}_{k_1}^* \dot{u}_{k_2}^* \dot{u}_{k_3}^* \\ &\sim \frac{1}{2M_{\text{Pl}}^3 \epsilon_{\text{sr}}^{3/2} (k_1 k_2 k_3)^{3/2}} \int_{t_*}^{\infty} dt a^3 \dot{\varphi}_2^2 m^3 u_{k_1}^* u_{k_2}^* u_{k_3}^*, \end{aligned} \quad (4.44)$$

where we used $\beta_1 \sim \dot{\varphi}_2 \sim m\dot{\varphi}_2$ and $\dot{u}_{k_i} \sim (k_i/a) u_{k_i} \sim \mu u_{k_i}$. It is not difficult to see that the integral (4.44) has a similar structure as the Hubble deformation effects $\mathcal{B}_{\pi, \delta H}$. Let us consider the following contribution for example:

$$\mathcal{B}_{\pi, \delta H}(k_1, k_2, k_3) \ni \frac{1}{2M_{\text{Pl}}^3 \epsilon_{\text{sr}}^{3/2} (k_1 k_2 k_3)^{3/2}} \text{Re} \left[-i \int_{t_*}^{\infty} dt a^3 M_{\text{Pl}}^2 \dot{H}_{\text{sr}} \dot{\kappa} \dot{u}_{k_1}^* \dot{u}_{k_2}^* u_{k_3}^* \right]. \quad (4.45)$$

Picking up the oscillating component $-\frac{\dot{\varphi}_2^2}{2M_{\text{Pl}}^2 \dot{H}_{\text{sr}}} \in \kappa$ relevant to the resonance and using $\dot{\varphi}_2 \sim m\dot{\varphi}_2$ and $\dot{u}_{k_i} \sim \mu u_{k_i}$, (4.45) can be estimated as

$$\begin{aligned} &\sim \frac{1}{4M_{\text{Pl}}^3 \epsilon_{\text{sr}}^{3/2} (k_1 k_2 k_3)^{3/2}} \int_{t_*}^{\infty} dt a^3 (2\dot{\varphi}_2 \dot{\varphi}_2) \dot{u}_{k_1}^* \dot{u}_{k_2}^* u_{k_3}^* \\ &\sim \frac{1}{2M_{\text{Pl}}^3 \epsilon_{\text{sr}}^{3/2} (k_1 k_2 k_3)^{3/2}} \int_{t_*}^{\infty} dt a^3 \dot{\varphi}_2^2 m^3 u_{k_1}^* u_{k_2}^* u_{k_3}^*, \end{aligned} \quad (4.46)$$

which takes a similar form as (4.44). We therefore conclude that resonance effects appear also in the first type of contribution S_{conv1} from the conversion interaction and the size of resonances is the same as those in the Hubble deformation effects: the order $\alpha^2 \mu^{5/2}$ in the heavy mass approximation. As is expected from the above discussions, the shape of non-Gaussianities around the resonance scale $k_t \sim 2\mu k_*$ is also similar to that of the Hubble deformation effects $S_{\delta H}$ (see Fig. 16).

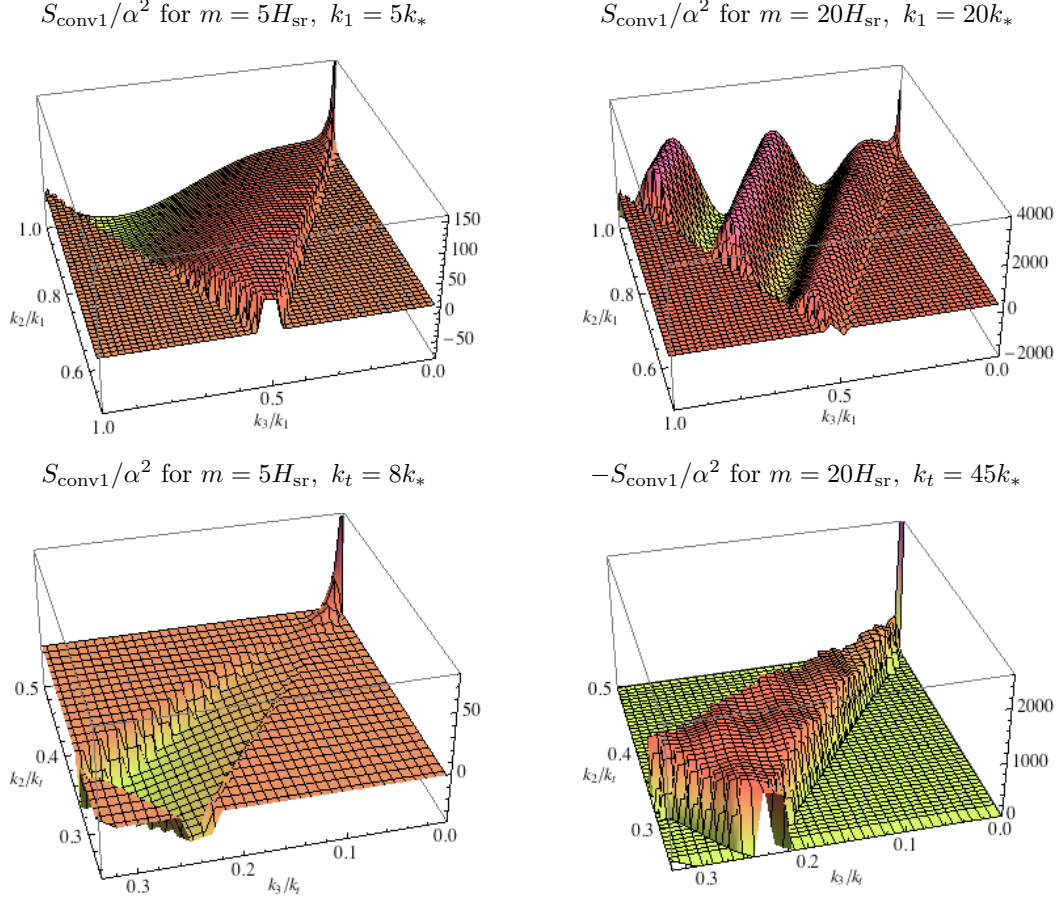


Figure 16: Shape of S_{conv1} around the resonance scale. Similarly to the Hubble deformation effects $S_{\delta H}$, the shape function takes a wavy form when plotted with the maximum momentum k_1 being fixed (upper figures) and has a peak at the squeezed configuration. In 3D plots with fixed total momenta k_t (lower figures), the flat region becomes large and the peak at the squeezed configuration becomes sharp when the mass is heavy.

4.2.3 Conversion effect 2

Let us next evaluate the bispectrum for the second type of conversion effects. In terms of $x = -k_t\tau$, $\mathcal{B}_{\pi,\text{conv2}}$ and $S_{\pi,\text{conv2}}$ can be written as

$$\mathcal{B}_{\pi,\text{conv2}}(k_1, k_2, k_3) = \frac{H_{\text{sr}}}{8M_{\text{Pl}}^4 \epsilon_{\text{sr}}^2} \frac{k_t^3}{k_1^3 k_2^3 k_3^3} \frac{\lambda M_{\text{Pl}}^2 \epsilon_{\text{sr}}}{H_{\text{sr}}^2} \text{Im} \left[\int_0^{x^*} dx \frac{\varphi_2}{\dot{\phi}_{\text{sr}}/H_{\text{sr}}} \frac{1}{x^4} \tilde{\mathcal{F}}_1(x_1) \tilde{\mathcal{F}}_2(x_2) \tilde{\mathcal{F}}_3(x_3) \right], \quad (4.47)$$

$$S_{\text{conv2}}(k_1, k_2, k_3) = -\frac{1}{2} \frac{k_t^3}{k_1 k_2 k_3} \frac{\lambda M_{\text{Pl}}^2 \epsilon_{\text{sr}}}{H_{\text{sr}}^2} \text{Im} \left[\int_0^{x^*} dx \frac{\varphi_2}{\dot{\phi}_{\text{sr}}/H_{\text{sr}}} \frac{1}{x^4} \tilde{\mathcal{F}}_1(x_1) \tilde{\mathcal{F}}_2(x_2) \tilde{\mathcal{F}}_3(x_3) \right]. \quad (4.48)$$

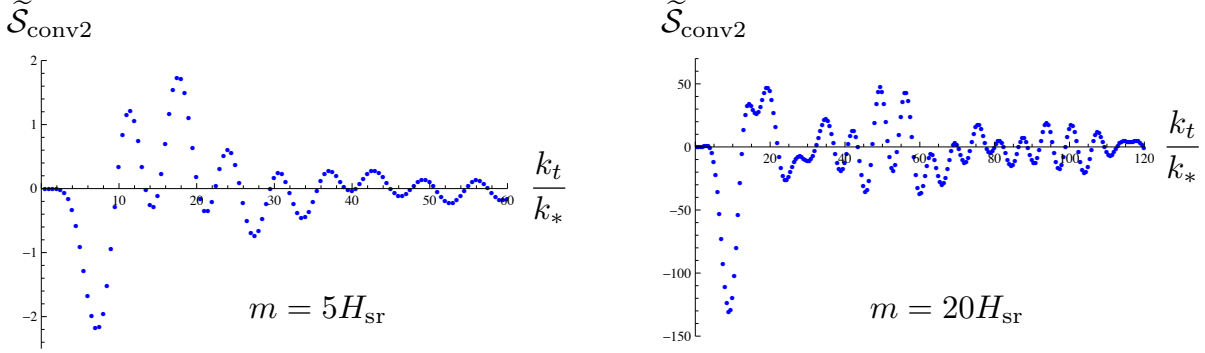


Figure 17: Scale-dependence of $S_{\text{conv}2}$ for the equilateral momentum configurations. Here we plotted $\tilde{S}_{\text{conv}2}$ normalized as $S_{\text{conv}2} = \frac{\lambda\alpha^2}{\mu^4} \frac{2M_{\text{Pl}}^2\epsilon_{\text{sr}}}{H_{\text{sr}}^2} \alpha^2 \tilde{S}_{\text{conv}2}$. The shape function $\tilde{S}_{\text{conv}2}$ has a peak at the scale $k \simeq 9k_*$ as well as the resonances around the scale $k \gtrsim 2\mu k_*$ and $k \gtrsim 4\mu k_*$.

As discussed in Sec. 2.3.3, it is required from the perturbativity that $\frac{\lambda\alpha^2}{\mu^4} \frac{2M_{\text{Pl}}^2\epsilon_{\text{sr}}}{H_{\text{sr}}^2} \lesssim 1$. With this condition in mind, we rewrite the shape function as

$$S_{\text{conv}2}(k_1, k_2, k_3) = -\frac{1}{4} \frac{k_t^3}{k_1 k_2 k_3} \frac{\lambda\alpha^2}{\mu^4} \frac{2M_{\text{Pl}}^2\epsilon_{\text{sr}}}{H_{\text{sr}}^2} \text{Im} \left[\int_0^{x_*} dx \frac{\mu^4}{\alpha^2} \frac{\varphi_2}{\dot{\phi}_{\text{sr}}/H_{\text{sr}}} \frac{1}{x^4} \tilde{\mathcal{F}}_1(x_1) \tilde{\mathcal{F}}_2(x_2) \tilde{\mathcal{F}}_3(x_3) \right], \quad (4.49)$$

from which we can see that large non-Gaussianities do not arise unless the integral is large. Using the analytic expression (4.33), the calculation of $S_{\text{conv}2}$ can be reduced to one integration over x and we evaluated it numerically. The scale-dependence of the shape function $S_{\text{conv}2}$ for the equilateral momentum configurations are for example given by Fig. 17, where we observe a peak around the turning scale $k_t \simeq 9k_*$ as well as resonances around $k_t \gtrsim 2\mu k_*$ and $k_t \gtrsim 4\mu k_*$.

We then estimate the size of the above peak and resonances using the heavy mass approximation. Let us first discuss the resonances around $k_t \gtrsim 2\mu k_*$ and $k_t \gtrsim 4\mu k_*$. Extending discussions for the case of $\mathcal{B}_{\text{conv}1}$, the shape function $\mathcal{B}_{\text{conv}2}$ in this region can be estimated as

$$\begin{aligned} \mathcal{B}_{\text{conv}2}(k_1, k_2, k_3) &= \frac{1}{4M_{\text{Pl}}^3\epsilon_{\text{sr}}^{3/2}(k_1 k_2 k_3)^{3/2}} \text{Re} \left[-i \int_{-\infty}^{\infty} dt a^3 \lambda \varphi_2 \mathcal{F}_1(t) \mathcal{F}_2(t) \mathcal{F}_3(t) \right] \\ &\sim \frac{1}{4M_{\text{Pl}}^3\epsilon_{\text{sr}}^{3/2}(k_1 k_2 k_3)^{3/2}} \int_{-\infty}^{\infty} dt a^3 \lambda \varphi_2 \frac{\beta_1^3}{m^6} \dot{u}_{k_1}^* \dot{u}_{k_2}^* \dot{u}_{k_3}^* \\ &\sim \frac{1}{4M_{\text{Pl}}^3\epsilon_{\text{sr}}^{3/2}(k_1 k_2 k_3)^{3/2}} \int_{t_*}^{\infty} dt a^3 \lambda \frac{\dot{\varphi}_2^4}{m} u_{k_1}^* u_{k_2}^* u_{k_3}^* \end{aligned}$$

$$\begin{aligned} & \sim \frac{1}{4M_{\text{Pl}}^3 \epsilon_{\text{sr}}^{3/2} (k_1 k_2 k_3)^{3/2}} \frac{\lambda \alpha^2 2M_{\text{Pl}}^2 \epsilon_{\text{sr}}}{\mu^4 H_{\text{sr}}^2} \\ & \quad \times \int_{t_*}^{\infty} dt a^3 e^{-3H_{\text{sr}}(t-t_*)} \cos^2[m(t-t_*)] \dot{\varphi}_2^2 m^3 u_{k_1}^* u_{k_2}^* u_{k_3}^*, \end{aligned} \quad (4.50)$$

where we used $\dot{\varphi}_2 \simeq \alpha \dot{\phi}_{\text{sr}} e^{-\frac{3}{2}H_{\text{sr}}(t-t_*)} \cos[m(t-t_*)]$. We first notice that $\cos^2[m(t-t_*)] \dot{\varphi}_2^2$ in the integrand of (4.50) contains oscillating components with the frequencies $2m$ and $4m$,

$$\cos^2[m(t-t_*)] \dot{\varphi}_2^2 = \frac{1}{8} \alpha^2 \dot{\phi}_{\text{sr}}^2 e^{-3H_{\text{sr}}(t-t_*)} \left(\cos[4m(t-t_*)] + 4 \cos[2m(t-t_*)] + 3 \right), \quad (4.51)$$

which induce the resonances around $k_t \gtrsim 2\mu k_*$ and $k_t \gtrsim 4\mu k_*$. The size of resonances can be also estimated by comparing the Hubble deformation effects. Since the integral in (4.50) has the same mass-dependence as the integrals in (4.44) and (4.46), its size can be estimated as $\sim \alpha^2 \mu^{5/2}$. Then, the resonances in the shape function can be estimated as

$$\sim \frac{\lambda \alpha^2 2M_{\text{Pl}}^2 \epsilon_{\text{sr}}}{\mu^4 H_{\text{sr}}^2} \alpha^2 \mu^{5/2} \lesssim \alpha^2 \mu^{5/2}, \quad (4.52)$$

where we used the perturbativity condition $\frac{\lambda \alpha^2 2M_{\text{Pl}}^2 \epsilon_{\text{sr}}}{\mu^4 H_{\text{sr}}^2} \lesssim 1$. This estimation well explains our numerical calculations in Fig 17.

We next discuss the peak around the turning scale. The shape function $S_{\text{conv}2}$ can be written using the expression (2.75) as

$$\begin{aligned} S_{\text{conv}2}(k_1, k_2, k_3) &= -\frac{1}{2} \frac{k_t^3}{k_1 k_2 k_3} \frac{\lambda M_{\text{Pl}}^2 \epsilon_{\text{sr}}}{H_{\text{sr}}^2} \\ & \quad \times \text{Im} \left[\int_0^{x_*} dx \frac{i\alpha}{2\mu} \left((x/x_*)^{\frac{3}{2}+i\mu} - (x/x_*)^{\frac{3}{2}-i\mu} \right) \frac{1}{x^4} \tilde{\mathcal{F}}_1(x_1) \tilde{\mathcal{F}}_2(x_2) \tilde{\mathcal{F}}_3(x_3) \right], \end{aligned} \quad (4.53)$$

and $\tilde{\mathcal{F}}_i(x_i)$ around the turning scale oscillates with high frequency $\sim x^{\pm i\mu}$ as given in (4.37). Therefore, the integrand in (4.53) can be seen as a product of four oscillating functions $\sim x^{\pm i\mu}$. Since products of two $x^{i\mu}$'s and two $x^{-i\mu}$'s lead to non-oscillating components, the leading contribution to (4.53) comes from these non-oscillating components. Using the previous order estimate $\tilde{\mathcal{F}}_i \sim \alpha$, the integral is $\sim \alpha^4 \mu^{-1}$ so that the shape function $S_{\text{conv}2}$ around the turning scale can be order estimated as

$$S_{\text{conv}2} \sim \frac{\lambda M_{\text{Pl}}^2 \epsilon_{\text{sr}}}{H_{\text{sr}}^2} \alpha^4 \mu^{-1} \sim \frac{\lambda \alpha^2 2M_{\text{Pl}}^2 \epsilon_{\text{sr}}}{\mu^4 H_{\text{sr}}^2} \alpha^2 \mu^3 \lesssim \alpha^2 \mu^3, \quad (4.54)$$

where the last inequality follows from the perturbativity condition $\frac{\lambda \alpha^2 M_{\text{Pl}}^2 \epsilon_{\text{sr}}}{\mu^4 H_{\text{sr}}^2} \lesssim 1$. This estimation well explains our numerical calculations in Fig. 17. The shape of $S_{\text{conv}2}$ around the

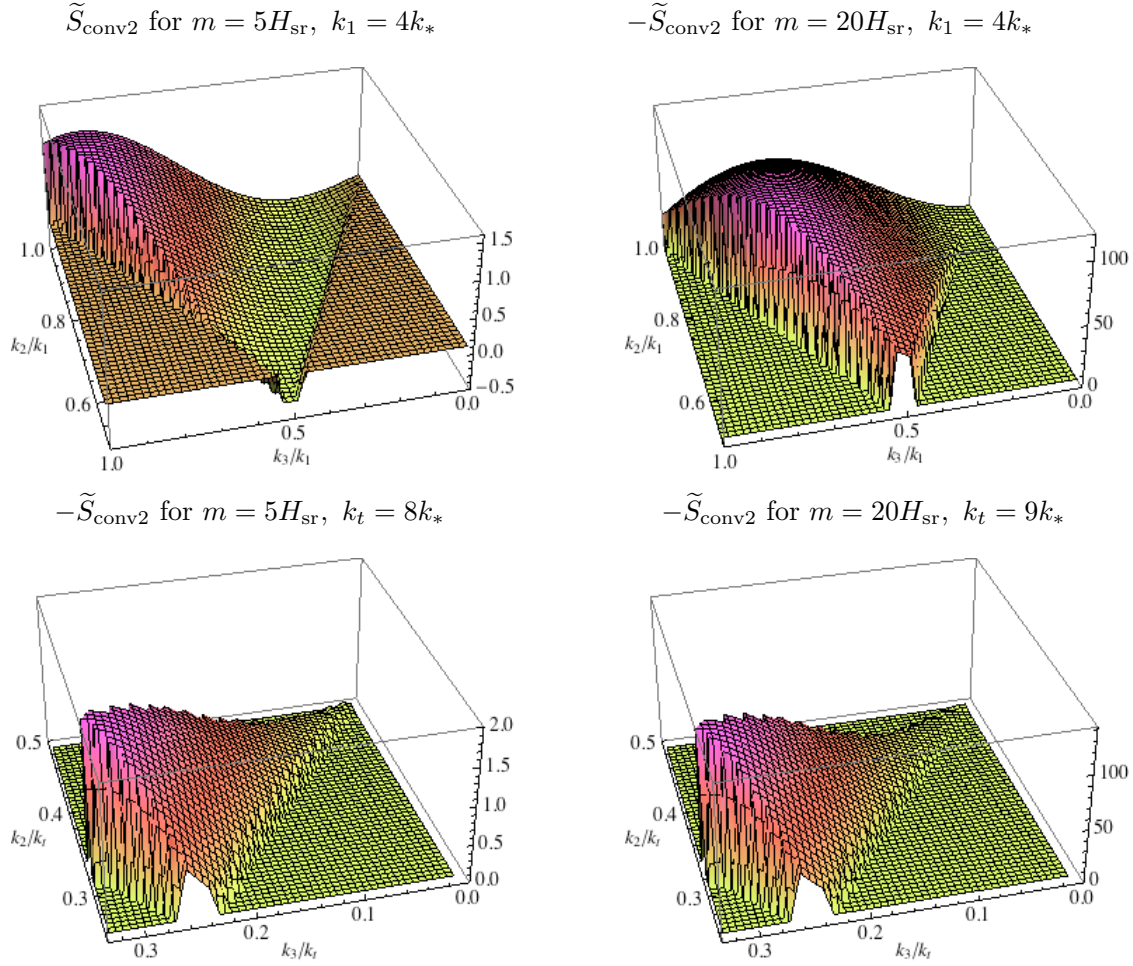


Figure 18: Shape of $S_{\text{conv}2}$. In the upper/lower figures, $\tilde{S}_{\text{conv}2}$ is plotted with maximum/total momenta being fixed. We observe that the shape function $S_{\text{conv}2}$ around the peak scale vanishes at the squeezed configuration.

tuning scale can be also discussed in a similar way. As in Sec. 4.2.1, $\tilde{\mathcal{F}}_3$ behaves as $\sim \alpha_3^2$ in the squeezed limit $\alpha_3 \rightarrow 0$ so that $S_{\text{conv}2}$ vanishes in this limit. This feature can be confirmed by our numerical calculations in Fig. 18.

4.3 Total bispectrum

At the end of this section, let us summarize features in the bispectrum.

$\mathcal{O}(\alpha^2)$ contributions As we have discussed, the Hubble deformation effects $S_{\delta H}$ and the first type of conversion effects $S_{\text{conv}1}$ are the second order in α and both of them have resonances at the scale $k_t \gtrsim 2\mu k_*$. In contrast to the power spectrum, resonances from the two effects do not cancel each other out and the size of total resonances are estimated as $\mathcal{O}(\alpha^2 \mu^{5/2})$. Around the

turning scale, the shape functions have a peak at the squeezed momentum configuration and the peak becomes sharp as the mass μ increases. Using the results of numerical calculations, the f_{NL} parameter can be read off as $f_{NL} \sim \alpha^2 \mu^{5/2} \times \mathcal{O}(1)$.

$\mathcal{O}(\lambda\alpha^4)$ contributions On the other hand, the second type of conversion effects $S_{\text{conv}2}$ are the fourth order in α and the first order in λ . Similarly to the other two contributions $S_{\delta H}$ and $S_{\text{conv}1}$, $S_{\text{conv}2}$ also contains resonances. In this case, resonances appear around the scale $k \gtrsim 4\mu k_*$ as well as $k \gtrsim 2\mu k_*$ and their size can be estimated as $\mathcal{O}\left(\frac{\lambda\alpha^2}{\mu^4} \frac{2M_{\text{Pl}}^2 \epsilon_{\text{sr}}}{H_{\text{sr}}^2} \times \alpha^2 \mu^{5/2}\right)$. In addition to the resonances, $S_{\text{conv}2}$ has a peak around the scale $k \simeq 9k_*$ and its size is estimated as $\mathcal{O}\left(\frac{\lambda\alpha^2}{\mu^4} \frac{2M_{\text{Pl}}^2 \epsilon_{\text{sr}}}{H_{\text{sr}}^2} \times \alpha^2 \mu^3\right)$. Also discussed that the shape function $S_{\text{conv}2}$ around the peak scale vanishes in the squeezed limit. The f_{NL} parameter around the resonance scale and at the peak can be read off from the numerical results as

$$f_{NL} \sim \frac{\lambda\alpha^2}{\mu^4} \frac{2M_{\text{Pl}}^2 \epsilon_{\text{sr}}}{H_{\text{sr}}^2} \times \alpha^2 \mu^{5/2} \times \mathcal{O}(0.1) \quad \text{around the resonance scale,} \quad (4.55)$$

$$f_{NL} \sim \frac{\lambda\alpha^2}{\mu^4} \frac{2M_{\text{Pl}}^2 \epsilon_{\text{sr}}}{H_{\text{sr}}^2} \times \alpha^2 \mu^3 \times \mathcal{O}(0.1) \quad \text{at the peak.} \quad (4.56)$$

Using the perturbativity condition $\frac{\lambda\alpha^2}{\mu^4} \frac{2M_{\text{Pl}}^2 \epsilon_{\text{sr}}}{H_{\text{sr}}^2} \lesssim 1$, we have

$$f_{NL} \lesssim \alpha^2 \mu^{5/2} \times \mathcal{O}(0.1) \quad \text{around the resonance scale,} \quad (4.57)$$

$$f_{NL} \lesssim \alpha^2 \mu^3 \times \mathcal{O}(0.1) \quad \text{at the peak.} \quad (4.58)$$

To summarize, the bispectrum in our model has two features: resonances at $k \gtrsim 2\mu k_*$ and a peak at $k \simeq 9k_*$. Because of the perturbativity condition, the leading contribution to the resonances are from the Hubble deformation effects $S_{\delta H}$ and the first type of conversion effects $S_{\text{conv}1}$. On the other hand, the peak arises from the cubic interaction σ^3 of massive isocurvatures. Although a dominant feature changes depending on the parameter region, our models are characterized by these two features.

5 Summary and discussion

In this paper, we discussed effects of heavy fields on primordial spectra in inflationary models with sudden turning potentials. The deviation from single field slow-roll inflation arises from the deformation of the Hubble parameter and the conversion interaction between the adiabatic and the massive isocurvature perturbations, and those effects on the power spectrum and the bispectrum are evaluated.

As discussed in Sec. 3, resonance features in the power spectrum arise from both of the two effects and their size can be estimated as $\sim \alpha^2 \mu^{1/2}$. Interestingly, resonance effects from the two effects have negative correlations generically and, in particular, it was explicitly shown that such resonance effects cancel each other out for the case with the canonical kinetic terms. This resonance cancellation is an important feature in models with canonical kinetic terms, and therefore, it can be a useful probe to distinguish models with canonical kinetic terms from those with non-canonical ones. To investigate this possibility, it would be interesting to extend our discussions to more general setups such as those with non-canonical kinetic terms or derivative interactions [18, 25]. We will discuss this subject elsewhere [33]. The power spectrum also has a peak at the turning scale. This feature originates from the conversion effect and its size can be estimated as $\sim \alpha^2 \mu$. In the case with the canonical kinetic terms, this peak feature becomes clear because of the resonance cancellation. In particular, the total deviation factor $\mathcal{C} = \frac{\Delta \mathcal{P}_\zeta}{\mathcal{P}_\zeta}$ from single field slow-roll inflation can be estimated using the heavy mass approximation as

$$\mathcal{C} \simeq \mathcal{C}_{\text{conv}} \simeq \mu \alpha^2 \frac{(\sin x_* - x_* \cos x_*)^2}{x_*^3}, \quad (5.1)$$

which takes the maximum value $\mathcal{C} \sim 0.43 \mu \alpha^2$ at the scale $x_* = k/k_* \sim 2.46$. It is important that we can extract the scale heavy field oscillations occurred from the peak position. In general, it is known that spiky features in primordial power spectra can induce wavy features on the CMB power spectra (see e.g. [37, 38]). It would be interesting to investigate the imprint of this peak feature on the CMB power spectrum for example: the remnant of primordial peak features will tell us when heavy field oscillations occurred during inflation.

As discussed in Sec. 4, the bispectrum has resonance and peak features. In contrast to the case of power spectra, the resonance cancellation does not occur in the bispectrum and both of the resonance and peak features characterize this class of models with heavy field oscillations. The size of the resonance and the peak can be estimated as $\lesssim \alpha^2 \mu^{5/2} \times \mathcal{O}(1)$ and $\lesssim \alpha^2 \mu^3 \times \mathcal{O}(0.1)$, respectively. Although the size of bispectra is not necessarily large in the perturbative regime, it would be interesting to search for this kind of scale-dependent non-Gaussianities in the observational data. An important point is that resonance features in primordial bispectra generically appear in models with heavy field oscillations (even in the case of canonical kinetic terms). Therefore, if the remnant of primordial resonance features is observed in the bispectra, it will suggest the existence of heavy field oscillations during inflation and, in particular, we can extract the mass of heavy fields from the scale of primordial resonances. Since resonance features do not appear in the power spectra for the case with canonical kinetic terms, we will further obtain details of kinetic terms by combining the analysis of primordial resonance features in the power spectra and the bispectra.

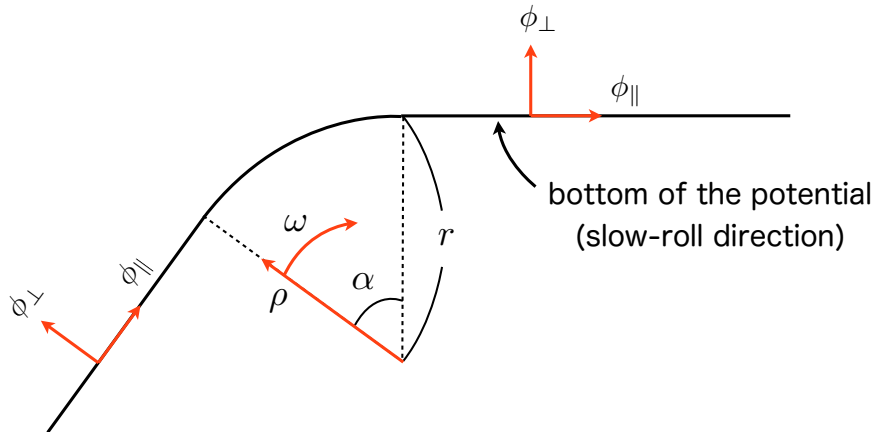


Figure 19: Turning potential with turning radius r and turning angle α .

Acknowledgments

We would like to thank Xian Gao, David Langlois, and Shuntaro Mizuno for the correspondence and valuable discussions. We are also grateful to Thorsten Battefeld, Daniel Baumann, and Shi Pi for useful discussions. The work of T.N. is supported in part by Special Postdoctoral Researchers Program at RIKEN. The work of M.Y. is supported in part by the Grant-in-Aid for Scientific Research on Innovative Areas No. 24111706 and the Grant-in-Aid for Scientific Research No. 25287054.

A Sudden limit of turning potentials

In this appendix we introduce a class of turning potentials and discuss its sudden turning limit. Suppose that the potential has a slow-roll direction and its orthogonal direction is massive. When the slow-roll direction is along a smooth curve, we can take a local coordinate $(\phi_{\parallel}, \phi_{\perp})$ of the field space such that ϕ_{\parallel} is along the slow-roll direction and ϕ_{\perp} is orthogonal to it. In such a case, it is also possible to define a separable potential at least locally:

$$V(\phi_i) = V_{\text{sr}}(\phi_{\parallel}) + V_{\perp}(\phi_{\perp}), \quad (\text{A.1})$$

where V_{sr} and V_{\perp} are the slow-roll potential and the massive potential and $\phi_{\perp} = 0$ is the bottom of the massive potential. However, when the slow-roll direction is not smooth as in the case of sudden turning potentials, it is not possible to define such a local coordinate frame and to introduce a separable potential. This is nothing but the origin of the discontinuity in the coordinate frame in Sec. 2.

To clarify this subtlety and justify our discussion, let us consider a class of smoothly turning potentials and discuss its sudden limit. As depicted in Fig. 19, we introduce a class of potentials whose slow-roll direction turns with a radius r and an angular α . We also assume that the slow-roll direction is straight before and after the turn. When the background trajectory turns along the slow-roll direction with a velocity $\dot{\phi}_{\text{sr}}$, the duration Δt of the turn is given by

$$\Delta t = \frac{r\alpha}{\dot{\phi}_{\text{sr}}}. \quad (\text{A.2})$$

We therefore would like to define the sudden turning potential by taking the limit $\Delta t \rightarrow 0$ with the turning angle α fixed. For careful treatments of this limit, let us introduce the polar coordinate system (ρ, ω) of the field space in the turning regime such that $(\rho, \omega) = (0, \omega)$ coincides with the center of the turn. In this coordinate system, the massive direction coincides with the radial direction and we can define the massive potential V_{\perp} as a function of r in the region $r > 0$. Following the setup in Sec. 2, let us define the massive potential as

$$V_{\perp} = \frac{m^2}{2}(\rho - r)^2 + \frac{\lambda}{4!}(\rho - r)^4. \quad (\text{A.3})$$

In terms of the coordinate $(\phi_{\parallel}, \phi_{\perp})$, the potential (A.3) can be written as

$$V_{\perp} = \frac{m^2}{2}\phi_{\perp}^2 + \frac{\lambda}{4!}\phi_{\perp}^4, \quad (\text{A.4})$$

which reproduces the massive potential in Sec. 2. An important point is that the description (A.4) is valid only in the region $\phi_{\perp} < r$. Since quantum fluctuations of massive fields during inflation can be estimated as $\sim \frac{H_{\text{sr}}^2}{m}$, it is necessary to assume $\frac{H_{\text{sr}}^2}{m} \lesssim r$ for the use of the expression (A.4). Therefore, to define the sudden limit of the turning potential, we require both of the following two conditions:

$$\frac{H_{\text{sr}}^2}{m} \lesssim r, \quad \Delta t \ll \frac{1}{H_{\text{sr}}}. \quad (\text{A.5})$$

Using the definition (A.2) of Δt , these conditions can be rephrased as

$$\frac{H_{\text{sr}}^2}{m} \lesssim r \ll \frac{\dot{\phi}_{\text{sr}}}{\alpha H_{\text{sr}}} = \frac{\sqrt{2}M_{\text{Pl}}\epsilon_{\text{sr}}^{1/2}}{\alpha} \sim 10^4 \times \frac{H_{\text{sr}}}{\alpha}, \quad (\text{A.6})$$

which can be naturally realized in our setup. We then define the sudden turning potential by taking the limit $\Delta t \rightarrow 0$ with α fixed and $\frac{H_{\text{sr}}^2}{m} \lesssim r$ satisfied. Based on this definition, the use of the massive potential (A.4) can be validated and our discussions in Sec. 2 can be also justified.

B Properties of the function $\mathcal{I}(\delta, n, x)$

As discussed in Sec. 3.1 and Sec. 4.1, the Hubble deformation effects $\mathcal{C}_{\delta H}$ and $S_{\delta H}$ on primordial spectra contain the function $\mathcal{I}(\delta, n, x)$:

$$\begin{aligned} \mathcal{I}(\delta, n, x) &= \int_0^x d\tilde{x} (\tilde{x}/x)^{3+\delta} \tilde{x}^n e^{-i\tilde{x}} \\ &= i^{-1-n} \left(\frac{1}{ix}\right)^{3+\delta} \left[\Gamma(4+n+\delta) - \Gamma(4+n+\delta, ix) \right]. \end{aligned} \quad (\text{B.1})$$

In this appendix its asymptotic behavior in the limits $x \rightarrow 0$ and $x \rightarrow \infty$, and its properties relevant to the resonance effects are discussed.

B.1 Asymptotic behavior of $\mathcal{I}(\delta, n, x)$

Let us start from the asymptotic behavior in the limits $x \rightarrow 0$ and $x \rightarrow \infty$. Using the asymptotic expansions of the incomplete gamma function,

$$\Gamma(\alpha, z) = \Gamma(\alpha) - z^\alpha \sum_{k=0}^{\infty} \frac{(-z)^k}{(\alpha+k)k!}, \quad (\text{B.2})$$

the asymptotic behavior of $\mathcal{I}(\delta, n, x)$ in the limit $x \rightarrow 0$ can be obtained as

$$\mathcal{I}(\delta, n, x) = x^{n+1} \sum_{k=0}^{\infty} \frac{(-ix)^k}{(4+n+\delta+k)k!} \quad (\text{B.3})$$

$$= \begin{cases} 0 & \text{for } n = 0, 1, \\ \frac{1}{3+\delta} & \text{for } n = -1, \\ \frac{1}{(2+\delta)x} - \frac{i}{3+\delta} & \text{for } n = -2. \end{cases} \quad (\text{B.4})$$

As discussed in Sec. 3.1 and Sec. 4.1, $\mathcal{C}_{\delta H}$ and $S_{\delta H}$ contain $\mathcal{I}(\delta, n, 2x_*)$ with $n = 0, -1, -2$ and $\mathcal{I}(\delta, n, x_*)$ with $n = 1, 0, -1, -2$, respectively. It may be therefore wondered that they diverge in the limit $x_* \rightarrow 0$. However, using the expression (B.4), we can show that they vanish in this limit so that they are IR-safe:

$$\lim_{x_* \rightarrow 0} \mathcal{C}_{\delta H}(x_*) = 0, \quad \lim_{x_* \rightarrow 0} S_{\delta H}(x_*) = 0. \quad (\text{B.5})$$

Let us next consider the asymptotic behavior in the limit $x \rightarrow \infty$. For this purpose, it is convenient to note the following asymptotic expansions:

$$\Gamma(\alpha, z) = e^{-z} z^{\alpha-1} \left(1 - \frac{1-\alpha}{z} + \mathcal{O}(z^{-2}) \right). \quad (\text{B.6})$$

Using this expansions, it follows that

$$\begin{aligned} \mathcal{I}(\delta, n, x) &= -i^{-1-n} e^{-ix} (ix)^n \left(1 + \frac{3+n+\delta}{ix} + \mathcal{O}(x^{-2}) \right) \\ &= \begin{cases} e^{-ix} (ix + 4 + \delta) & \text{for } n = 1, \\ ie^{-ix} & \text{for } n = 0, \\ 0 & \text{for } n = -1, -2, \end{cases} \end{aligned} \quad (\text{B.7})$$

which oscillates and diverges for $n = 0, 1$ in the large x region. As in the case of the $x \rightarrow 0$ limit, it follows from (B.7) that these singular behaviors cancel out in $\mathcal{C}_{\delta H}(x_*)$ and it vanishes in the $x_* \rightarrow \infty$ limit: $\lim_{x_* \rightarrow \infty} \mathcal{C}_{\delta H}(x_*) = 0$. On the other hand, however, such cancellation does not occur in $\mathcal{S}_{\delta H}$ and it turns out that the bispectrum $\mathcal{S}_{\delta H}$ is singular in this limit: $\lim_{x_* \rightarrow \infty} \mathcal{S}_{\delta H} \propto x_* e^{-ix_*}$. Note that the mode $k = -x/\tau$ is deep inside the horizon in the region $x \gg 1$. This kind of oscillating singular behaviors are common in the interacting theory and they are usually eliminated by the $i\epsilon$ -prescription, which is based on the assumption that the Bunch-Davies vacuum is realized deep inside the horizon. Following this physical assumptions, we would like to eliminate such oscillating parts from $\mathcal{S}_{\delta H}$ and introduce the following regularized functions $\mathcal{I}_{\text{reg}}(\delta, 1, x)$ and $\mathcal{I}_{\text{reg}}(\delta, 0, x)$:

$$\mathcal{I}_{\text{reg}}(\delta, 1, x) = \mathcal{I}(\delta, 1, x) - e^{-ix} (ix + 4 + \delta), \quad (\text{B.8})$$

$$\mathcal{I}_{\text{reg}}(\delta, 0, x) = \mathcal{I}(\delta, 0, x) - ie^{-ix}, \quad (\text{B.9})$$

which vanish in the $x \rightarrow \infty$ limit. Note that the resonance features in \mathcal{I} are well reproduced by \mathcal{I}_{reg} as in Fig. 20. In the bispectrum calculation of this paper, we use the original function \mathcal{I} for $x \lesssim 2\mu$ and the regularized function \mathcal{I}_{reg} for $x \gtrsim 2\mu$. Physically speaking, this interpolation procedure corresponds to assume that the Bunch-Davies vacuum is realized before the resonance era, where the mode is deep inside the horizon. In the following subsections, we discuss the relation between our procedure and the stationary phase approximation, which is often used to evaluate integrals of oscillating functions.

B.2 Stationary phase approximation for $\mathcal{I}(\delta, n, x)$

Let us then apply the stationary phase approximation to the function $\mathcal{I}(\delta, n, x)$:

$$\begin{aligned} \mathcal{I}(\delta, n, x) &= \int_0^x d\tilde{x} (\tilde{x}/x)^{3+\delta} \tilde{x}^n e^{-i\tilde{x}} \\ &= x^{1+n} \int_0^1 dy y^{3+n} e^{i\Omega(y)} \quad \text{with} \quad \Omega(y) = -i\delta \ln y - xy. \end{aligned} \quad (\text{B.10})$$

It is obvious from this expression that the phase factor $e^{i\Omega}$ highly oscillates for large x and the integral is suppressed by its frequency unless the phase function $\Omega(y)$ has a stationary point

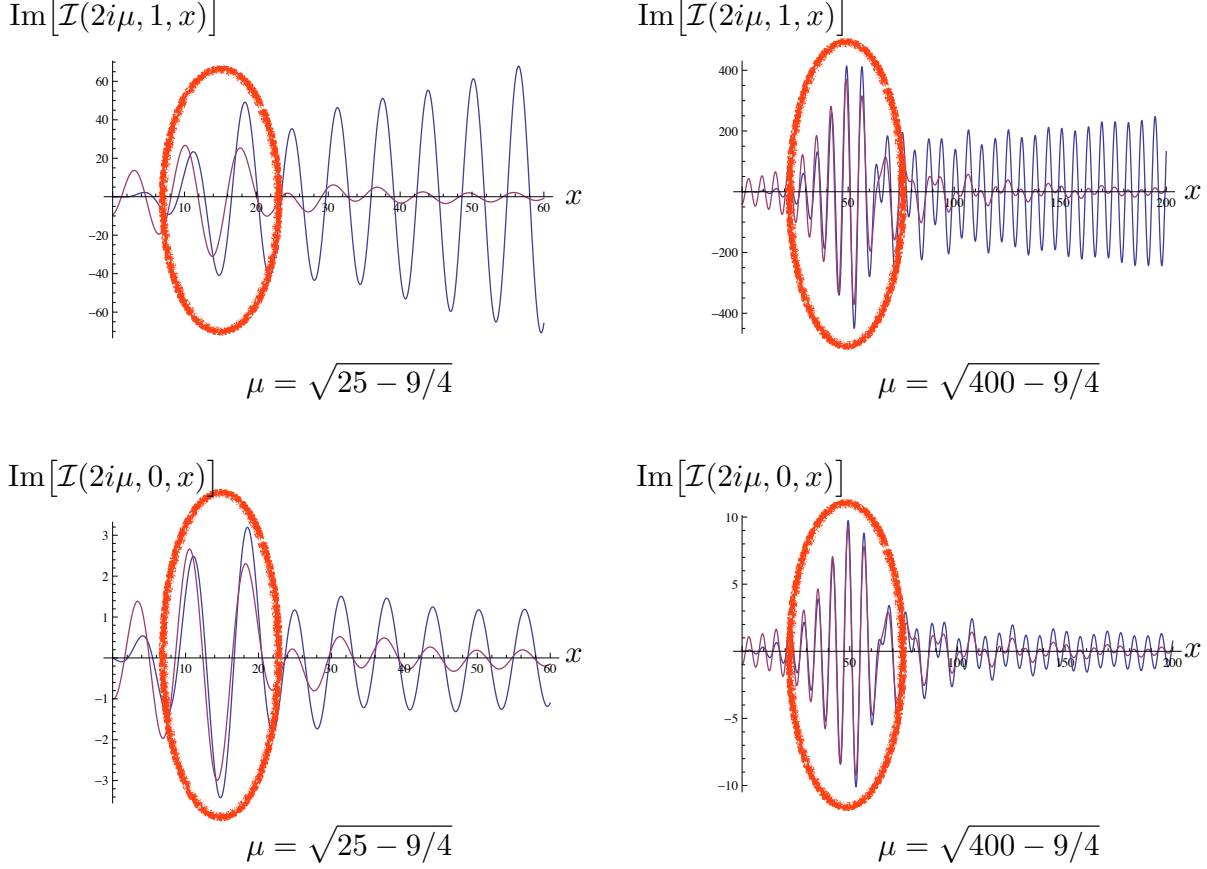


Figure 20: Comparison of \mathcal{I}_{reg} (red) and \mathcal{I} (blue). The regularized function \mathcal{I}_{reg} well reproduces the resonance features circled with thick red curves of the original function \mathcal{I} while singular behaviors deep inside the horizon are removed appropriately.

$\Omega' = 0$. While it has no stationary points for $\delta = 0, -2i\mu$, there is a stationary point for the case $\delta = 2i\mu$:

$$\Omega'(y_*) = 0 \quad \leftrightarrow \quad y_* = \frac{2\mu}{x}. \quad (\text{B.11})$$

The integral has a non-negligible contribution around this stationary point, which can be observed as the resonance. Let us then evaluate $\mathcal{I}(2i\mu, n, x)$ using the following Gaussian approximation:

$$\begin{aligned} \mathcal{I}(2i\mu, n, x) &\simeq x^{1+n} (y_*)^{3+n} e^{i\Omega(y_*)} \int_0^1 dy \exp \left[\frac{i}{2} \Omega''(y_*) (y - y_*)^2 \right] \\ &= x^{1+n} \left(\frac{2\mu}{x} \right)^{3+n+2i\mu} e^{-2i\mu} \sqrt{\frac{4\mu}{x^2}} \int_{-\sqrt{\mu}}^{\frac{x}{\sqrt{4\mu}} - \sqrt{\mu}} d\tilde{y} \exp[-i\tilde{y}^2]. \end{aligned} \quad (\text{B.12})$$

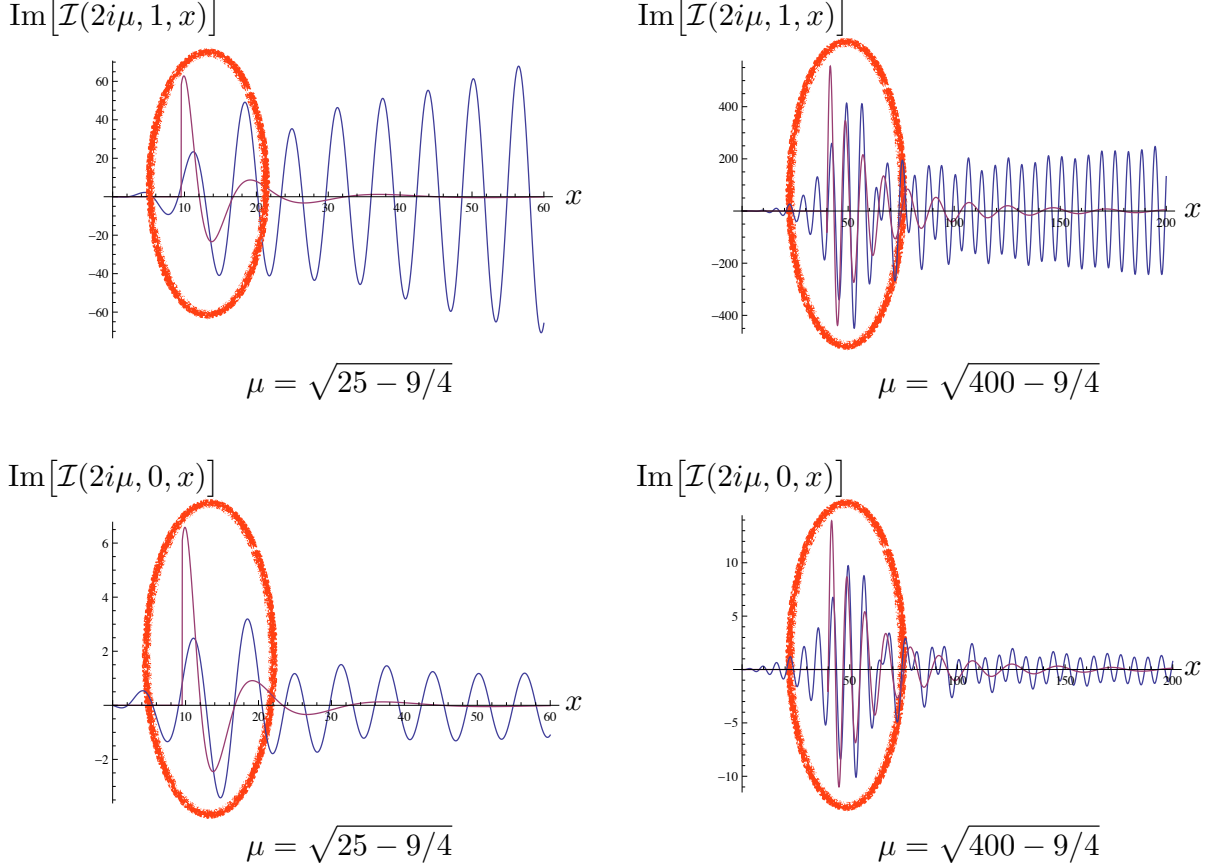


Figure 21: Stationary phase approximation for \mathcal{I} . The red curves are results of the stationary phase approximation and the blue ones are the original function \mathcal{I} . Resonance features of the original function are well reproduced except for $x \sim 2\mu$, where the approximation breaks down. Also notice that singular behaviors deep inside the horizon are removed in this approximation.

For $x \gtrsim 2\mu \gg 1$, we further approximate it as

$$\int_{-\sqrt{\mu}}^{\frac{x}{\sqrt{4\mu}} - \sqrt{\mu}} d\tilde{y} \exp[-i\tilde{y}^2] \simeq \int_{-\infty}^{\infty} d\tilde{y} \exp[-i\tilde{y}^2] = \sqrt{\frac{\pi}{i}}. \quad (\text{B.13})$$

Note that the approximation becomes worse for $x \sim 2\mu$ because the upper limit of the integral becomes zero for $x = 2\mu$: $\frac{x}{\sqrt{4\mu}} - \sqrt{\mu} = 0$ (see Fig. 21). Also note that the integral (B.12) vanishes in the limit $\mu \rightarrow \infty$ for $x < 2\mu$. By contour deformations of the integral (B.13), we obtain the following expression of $\mathcal{I}(2i\mu, n, x)$ in the stationary phase approximation:

$$\mathcal{I}(2i\mu, n, x) \simeq \left(\frac{2\mu}{x}\right)^{3+2i\mu} (2\mu)^{n+\frac{1}{2}} \sqrt{2\pi} e^{-2i\mu - \frac{i}{4}\pi}. \quad (\text{B.14})$$

As depicted in Fig. 21, the resonance effects in $\mathcal{I}(2i\mu, n, x)$ are well reproduced by the stationary phase approximation except for $x \sim 2\mu$, where the approximation breaks down as discussed

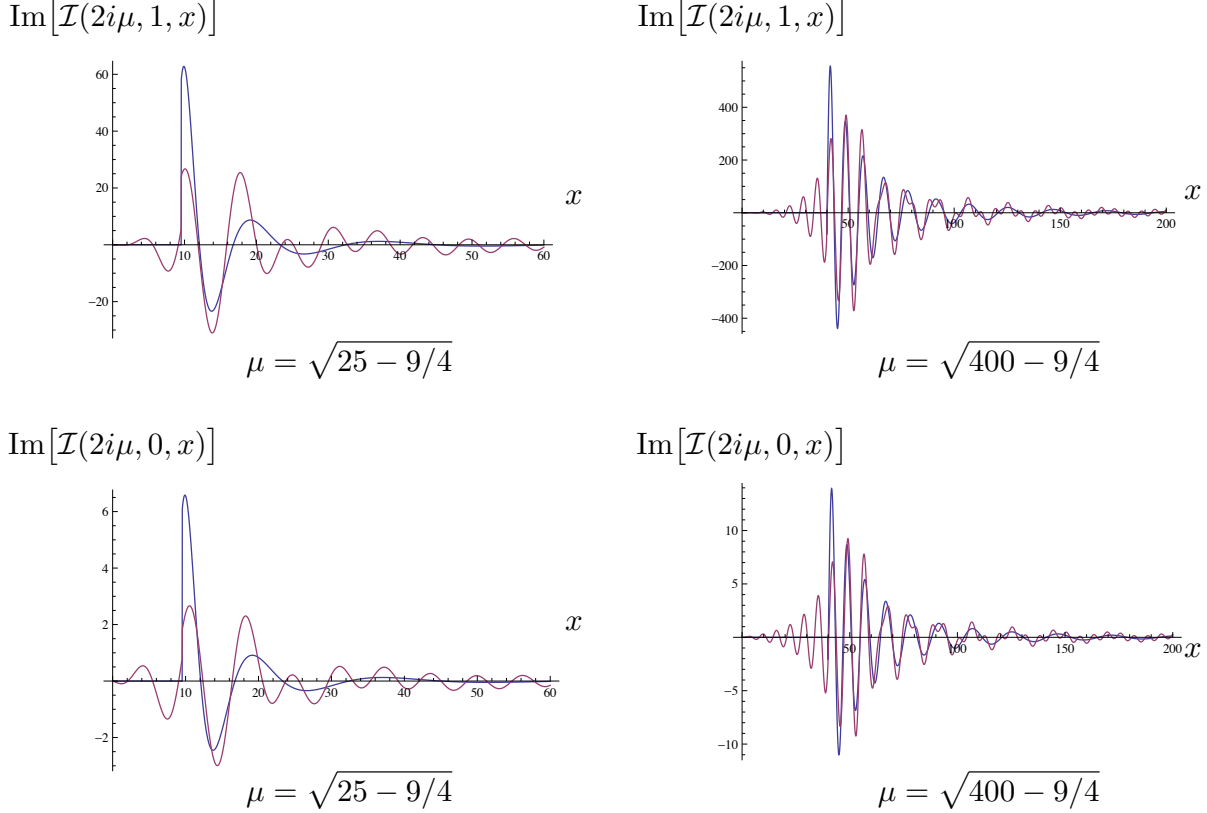


Figure 22: Comparison of our interpolation procedure (red) and the stationary phase approximation (blue). Both results well agree except for $x \sim 2\mu$, where the latter does not provide a good approximation. The agreement for $\mu = \sqrt{400 - 9/4}$ is better than that for $\mu = \sqrt{25 - 9/4}$ because the use of these procedures is justified in the large μ region.

above. Also notice that singular behaviors deep inside the horizon are regularized and removed in this approximation.

B.3 Interpolation procedure vs stationary phase approximation

Finally, we compare our interpolation procedure and the stationary phase approximation. As we have discussed, both the procedures extract the resonance features in the integral by removing singular behaviors deep inside the horizon. Our procedure is therefore considered to be essentially the same as the stationary phase approximation. In fact, as depicted in Fig. 22, their results well agree except for $x \sim 2\mu$, where the stationary phase approximation becomes worse. It should be noticed, however, the use of these procedures is not necessarily justified in the small μ region: First, the stationary phase approximation does not provides a good approximation in such a region because higher order terms in $1/\mu$ -expansions are dropped. Second, our procedure is based on the assumption that the Bunch-Davies vacuum is realized

deep inside the horizon. For small μ , however, the mode is not so deep inside the horizon at the resonance era. Therefore, in order to justify the use of our procedure, it should be specified how deep inside the horizon the Bunch-Davies vacuum is realized. In this sense, our procedure depends on the details of the assumption in the small mass region. Reflecting these subtleties, the agreement between both the procedures in the small μ region is not so well compared to the large μ region.

To summarize, our interpolation procedure is essentially the same as the stationary phase approximation and its use would be justified at least in the heavy mass region $\mu \gtrsim 10$. For small μ , however, it may be not suitable for quantitative discussions because of the subtleties in removing singular behaviors deep inside the horizon although it should be useful for qualitative discussions even in the small μ region.

References

- [1] C. L. Bennett *et al.* [WMAP Collaboration], “Nine-Year Wilkinson Microwave Anisotropy Probe (WMAP) Observations: Final Maps and Results,” arXiv:1212.5225 [astro-ph.CO]; G. Hinshaw *et al.* [WMAP Collaboration], “Nine-Year Wilkinson Microwave Anisotropy Probe (WMAP) Observations: Cosmological Parameter Results,” arXiv:1212.5226 [astro-ph.CO].
- [2] P. A. R. Ade *et al.* [Planck Collaboration], “Planck 2013 results. I. Overview of products and scientific results,” arXiv:1303.5062 [astro-ph.CO]; P. A. R. Ade *et al.* [Planck Collaboration], “Planck 2013 results. XXII. Constraints on inflation,” arXiv:1303.5082 [astro-ph.CO].
- [3] M. Yamaguchi and J. ’i. Yokoyama, “Density fluctuations in one-field inflation,” Phys. Rev. D **74**, 043523 (2006) [hep-ph/0512318].
- [4] A. J. Tolley and M. Wyman, “The Gelaton Scenario: Equilateral non-Gaussianity from multi-field dynamics,” Phys. Rev. D **81**, 043502 (2010) [arXiv:0910.1853 [hep-th]].
- [5] A. Achucarro, J. -O. Gong, S. Hardeman, G. A. Palma and S. P. Patil, “Mass hierarchies and non-decoupling in multi-scalar field dynamics,” Phys. Rev. D **84**, 043502 (2011) [arXiv:1005.3848 [hep-th]].
- [6] M. G. Jackson and K. Schalm, “Model Independent Signatures of New Physics in the Inflationary Power Spectrum,” Phys. Rev. Lett. **108**, 111301 (2012) [arXiv:1007.0185 [hep-th]].
- [7] S. Cremonini, Z. Lalak and K. Turzynski, “Strongly Coupled Perturbations in Two-Field Inflationary Models,” JCAP **1103**, 016 (2011) [arXiv:1010.3021 [hep-th]].
- [8] X. Chen, “Primordial Features as Evidence for Inflation,” JCAP **1201**, 038 (2012) [arXiv:1104.1323 [hep-th]].
- [9] X. Chen, “Fingerprints of Primordial Universe Paradigms as Features in Density Perturbations,” Phys. Lett. B **706**, 111 (2011) [arXiv:1106.1635 [astro-ph.CO]].

- [10] G. Shiu and J. Xu, “Effective Field Theory and Decoupling in Multi-field Inflation: An Illustrative Case Study,” *Phys. Rev. D* **84**, 103509 (2011) [arXiv:1108.0981 [hep-th]].
- [11] S. Cespedes, V. Atal and G. A. Palma, “On the importance of heavy fields during inflation,” *JCAP* **1205**, 008 (2012) [arXiv:1201.4848 [hep-th]].
- [12] A. Achucarro, J. -O. Gong, S. Hardeman, G. A. Palma and S. P. Patil, “Effective theories of single field inflation when heavy fields matter,” *JHEP* **1205**, 066 (2012) [arXiv:1201.6342 [hep-th]].
- [13] A. Avgoustidis, S. Cremonini, A. -C. Davis, R. H. Ribeiro, K. Turzynski and S. Watson, “Decoupling Survives Inflation: A Critical Look at Effective Field Theory Violations During Inflation,” *JCAP* **1206**, 025 (2012) [arXiv:1203.0016 [hep-th]].
- [14] X. Chen and Y. Wang, “Quasi-Single Field Inflation with Large Mass,” *JCAP* **1209**, 021 (2012) [arXiv:1205.0160 [hep-th]].
- [15] S. Pi and M. Sasaki, “Curvature Perturbation Spectrum in Two-field Inflation with a Turning Trajectory,” *JCAP* **1210**, 051 (2012) [arXiv:1205.0161 [hep-th]].
- [16] A. Achucarro, V. Atal, S. Cespedes, J. -O. Gong, G. A. Palma and S. P. Patil, “Heavy fields, reduced speeds of sound and decoupling during inflation,” *Phys. Rev. D* **86**, 121301 (2012) [arXiv:1205.0710 [hep-th]].
- [17] X. Gao, D. Langlois and S. Mizuno, “Influence of heavy modes on perturbations in multiple field inflation,” *JCAP* **1210** (2012) 040 [arXiv:1205.5275 [hep-th]].
- [18] R. Saito, M. Nakashima, Y. -i. Takamizu and J. 'i. Yokoyama, “Resonant Signatures of Heavy Scalar Fields in the Cosmic Microwave Background,” *JCAP* **1211**, 036 (2012) [arXiv:1206.2164 [astro-ph.CO]].
- [19] C. P. Burgess, M. W. Horbatsch and S. .P. Patil, “Inflating in a Trough: Single-Field Effective Theory from Multiple-Field Curved Valleys,” *JHEP* **1301**, 133 (2013) [arXiv:1209.5701 [hep-th]].
- [20] R. Gwyn, G. A. Palma, M. Sakellariadou and S. Sypsas, “Effective field theory of weakly coupled inflationary models,” *JCAP* **1304**, 004 (2013) [arXiv:1210.3020 [hep-th]].
- [21] T. Kobayashi and J. 'i. Yokoyama, “Primordial Spikes from Wrapped Brane Inflation,” *JCAP* **1302**, 005 (2013) [arXiv:1210.4427 [astro-ph.CO]].
- [22] T. Noumi, M. Yamaguchi and D. Yokoyama, “Effective field theory approach to quasi-single field inflation,” *JHEP* **1306**, 051 (2013) [arXiv:1211.1624 [hep-th]].
- [23] A. Achucarro, J. -O. Gong, G. A. Palma and S. P. Patil, “Correlating features in the primordial spectra,” arXiv:1211.5619 [astro-ph.CO].
- [24] T. Battfeld, J. C. Niemeyer and D. Vlaykov, “Probing Two-Field Open Inflation by Resonant Signals in Correlation Functions,” *JCAP* **1305**, 006 (2013) [arXiv:1302.3877 [astro-ph.CO]].
- [25] R. Saito and Y. -i. Takamizu, “Localized Features in Non-Gaussianity from Heavy Physics,” arXiv:1303.3839 [astro-ph.CO].

- [26] S. Cespedes and G. A. Palma, “Cosmic inflation in a landscape of heavy-fields,” arXiv:1303.4703 [hep-th].
- [27] V. Assassi, D. Baumann, D. Green and L. McAllister, “Planck-Suppressed Operators,” arXiv:1304.5226 [hep-th].
- [28] J. -O. Gong, S. Pi and M. Sasaki, “Equilateral non-Gaussianity from heavy fields,” arXiv:1306.3691 [hep-th].
- [29] X. Gao, D. Langlois and S. Mizuno, “Oscillatory features in the curvature power spectrum after a sudden turn of the inflationary trajectory,” arXiv:1306.5680 [hep-th].
- [30] C. Cheung, P. Creminelli, A. L. Fitzpatrick, J. Kaplan and L. Senatore, “The Effective Field Theory of Inflation,” JHEP **0803**, 014 (2008) [arXiv:0709.0293 [hep-th]];
- [31] A. Ashoorioon, A. Krause and K. Turzynski, “Energy Transfer in Multi Field Inflation and Cosmological Perturbations,” JCAP **0902** (2009) 014 [arXiv:0810.4660 [hep-th]].
- [32] X. Gao and P. Shukla, “On Non-Gaussianities in Two-Field Poly-Instanton Inflation,” JHEP **1303** (2013) 061 [arXiv:1301.6076 [hep-th]].
- [33] T. Noumi and M. Yamaguchi, in preparation.
- [34] L. Senatore and M. Zaldarriaga, “The Effective Field Theory of Multifield Inflation,” JHEP **1204**, 024 (2012) [arXiv:1009.2093 [hep-th]].
- [35] X. Gao, “Coupling structure of multi-field primordial perturbations,” arXiv:1307.2564 [hep-th].
- [36] J. M. Maldacena, “Non-Gaussian features of primordial fluctuations in single field inflationary models,” JHEP **0305** (2003) 013 [astro-ph/0210603].
- [37] A. A. Starobinsky, “Spectrum of adiabatic perturbations in the universe when there are singularities in the inflation potential,” JETP Lett. **55** (1992) 489 [Pisma Zh. Eksp. Teor. Fiz. **55** (1992) 477].
- [38] M. Kawasaki, F. Takahashi and T. Takahashi, “Making waves on CMB power spectrum and inflaton dynamics,” Phys. Lett. B **605** (2005) 223 [astro-ph/0407631].